DETECTION OF THE NUMBER OF SIGNALS IN ARRAY SIGNAL PROCESSING

By

WEI-GUO CHEN, B.Sc.(Eng.), and M.Eng.
(Beijing University of Science and Technology)

A Thesis
Submitted to the School of Graduate Studies
in Partial Fulfilment of the Requirements
for the Degree
Doctor of Philosophy

McMaster University
June 1991

DETECTION OF THE NUMBER OF SIGNALS IN ARRAY SIGNAL PROCESSING

DOCTOR OF PHILOSOPHY (1991) McMASTER UNIVERSITY

(Electrical and Computer Engineering) Hamilton, Ontario

TITLE: **Detection of the Number of Signals in Array Signal Processing**

AUTHOR: Wei-Guo Chen

B.Sc.(Eng.), and M.Eng.

(Beijing University of Science and Technology)

SUPERVISOR(S): Dr. Kon Max Wong

Professor, Chairman of Department of Electrical and Computer Engineering

B.Sc.(Eng.), Ph.D., (University of London)

D.I.C. (University of London)

Fellow, I.E.E.

Fellow, Royal Statistical Society

Fellow, Institute of Physics

Dr. James P. Reilly

Professor of Department of Electrical and Computer Engineering

B.A.Sc. (University of Waterloo)

M.Eng., Ph.D. (McMaster University)

NUMBER OF PAGES: xv, 138

To my parents

whose encouragement and love

have always been with me,

and my wife, Xianjun

whose love and understanding have made

this work complete with harmonic echos.

Abstract

This thesis addresses the detection problem in array signal processing in two aspects: (a) detection problems in white noise environments; (b) detection problems in unknown coloured (spatially correlated) noise environments. New criteria for determining the number of signals in both these kinds of noise environments are developed. The performance of the new methods is analyzed theoretically and is confirmed by computer simulations using Monte Carlo method.

The status of the existing methods for detection in array processing are reviewed. For the white noise environment, some unfavourable characteristics of existing methods are discussed, for example, the subjective threshold setting required by the traditional threshold methods, and the rigid performance of the information theoretic criteria. A new method, namely Eigen-Threshold (ET) method is proposed and analyzed theoretically and checked by computer simulations. The new method demonstrates superiority over the existing methods by: (a) not requiring a subjective threshold setting as required by the traditional threshold methods; (b) possessing a flexible performance which can be easily controlled by a single parameter, in contrast to the rigid performance given by the information theoretic criteria. By properly choosing the control parameter, the new method gives better performance than both AIC and MDL. Because of these advantages, the new ET method is more applicable in practice than other existing methods. Besides enjoying the same merit of not requiring a subjective threshold setting, the ET method gives a quantitative controllable performance which is useful in practice, because although the asymptotic consistency argument used in information theoretic criteria and some other methods has important theoretical significants but: (a) in any practical application the sample size can only be

a limited number; (b) when the sample size N is given, and a quantitative performance is desired, the asymptotic consistency argument may not make too much sense since such arguments could not give even an approximate error level except predicting whether the error rate will go to zero when N goes to infinity.

For the more difficult detection problem in the case of spatially correlated noise, there has not been any satisfactory method developed so far. By assuming a banded structure for the noise covariance matrix, which is true for many engineering applications, and applying a bi-array structure combined with canonical correlation analysis, a new elegant method is developed in this thesis. The new method, called Canonical Correlation Test (CCT) method, gives a reliable, simple, theoretically sound solution to the detection problem in unknown coloured noise environments. Massive simulations have shown that the new method is extremely robust to changes in the noise spectrum. Again, the new method is characterized by a quantitatively controllable performance.

To compare the new methods with the existing methods, the widely accepted AIC and MDL criteria are used for comparison purpose through out this thesis.

Acknowledgement

The author wishes to express his appreciation to Dr. K. M. Wong and Dr. J. P. Reilly for their encouragement, continued assistance, expert guidance and supervision throughout the course of this work. He also thanks Drs. P. C. Yip, T. Z. Luo, and C. R. Carter, the members of his Supervisory Committee, for their continuing interest and useful suggestions.

The author is grateful to Dr. Q. T. Zhang of the Communications Research Laboratiry, McMaster University, for useful discussions on detection problems, and for his inputs into the probability distribution function of the eigenvalues involved in this work. Discussions with Drs. M. L. Tiku and N. Balakrishnan, Department of Mathematics & Statistics, McMaster University, enhanced the author's understanding of multivariate analysis. The visiting of Dr. M. Kaveh, Department of Electrical engineering, University of Minnesota, Minneapolis, USA and the technical discussion with him enriched the author's knowledge on array processing. The suggestion from Dr. Q. Wu motivated the application of the bi-array structure to the canonical correlation testing (CCT) method.

It is author's pleasure to acknowledge the assistance from A. Ukrainec, and T. Greenley in computer software and equipment support.

The financial assistance provided in part by the Canadian International Development Agency through a CIDA scholarship, the Graduate School of McMaster University through a Clifton W. Sherman Graduate Scholarship, the Telecommunications Research Institute of Ontario through research funding for the Robust Array Processing project, are all gratefully acknowledged.

Finally, I extend sincere and special thanks to my entire family. It is the consistent

encouragement and love always received from my parents, during both happy and difficult times, from my earliest childhood until today, that has helped me understand, and be able to discover more and more of the natural world. The smiles, the love, and the understanding of my wife, Xianjun, and my daughter, Yuhan, have made this work complete with harmonic echos.

Contents

List of Tables

List of Figures

Chapter 1

Introduction

1.1 What is array processing?

Applications of array techniques in various engineering fields have already had a long history. In underwater sound engineering, for example, application of sensor arrays in sonar systems can be found as early as 1910's [31] for detection of submarines. For radar systems, the first electronically scanned antenna array was designed and built in 1959 [21] to obtain a antenna with high resolution and rapid scan ability. Such an ability is important for resolving the modes of propagation arriving from different directions within a short time interval.

In an array system, the received signals are obtained by means of a group of sensors at different known spatial locations in the field of interest. The function of the array can be understood as spatially sampling the propagating wave phenomenon of interest. Depending on the sensor characters and the medium of propagation, the traveling waveforms undergo deterministic and/or random modifications. Besides these modifications, the sensor outputs are further polluted by additive noise such as measurement and thermal noise. To extract information of interest from these modified and polluted samples, the array outputs are further processed by various techniques and these procedures are called *array signal processing*. The function of array signal processing is to refine the outputs of the sensor array and to extract required information (number of targets, positions, speeds and other properties of the targets). In some circumstances, array processing also supplies

control messages for system operations such as *beamforming* and *system adaptation.* The applications of array processing are quite broad, ranging from communications, radar, and sonar systems, to fields such as radio astronomy, telephony, seismology, and ultrasonics [1]. However, this thesis will mainly address the detection problem (the problem of determining number of sources[1]), specifically in radar and sonar systems. Extending the methods developed in this thesis to other array processing problems should not be difficult if similar mathematical models are applied.

1.2 Why use an array structure?

The motivation of the development of array techniques comes from special requirements in engineering practice.

As we all know, sensing elements play a very important part in the engineering world. They serve as the eyes of the respective systems. In different applications the term *sensor* has different meanings. In radar, telecommunications, and radio astronomy, a sensor usually means an *antenna.* In sonar system, a sensor means a *hydrophone* for *passive, listening-only sonar* or a *transducer* for *active sonar.* In *exploration seismology*, a sensor usually means a *geophone.*

A single sensor is very limited in its performance capabilities. But, by combining individual sensors into an array, the designer can achieve better, more flexible characteristics such as *high gain* (or *sensitivity*), *higher and more flexible directivity*, and the capability for *multiple source handling* than from a single sensor.

Take *radar* and other antenna-related systems as an example. In these systems, antennas are devices ordinarily used for transmitting and receiving electromagnetic energy. For some systems, these purposes may well be served by an antenna consisting of a single element. Depending on the operating frequency, range, environment, economy, and many other factors, this element may be as simple as a dipole or loop antenna or as complex

[1] In array processing, the term *targets*, *sources*, and *spatial signals* (or simply *signals*) usually refer to the same physical concept; therefore, we will treat these terms synonymously in this thesis.

as a parabolic reflector antenna. To obtain *high directivity, narrow beams, low side lobes, steerable beams, and particular pattern characteristics* with relatively simple sensor elements, systems composed of a group of antenna elements, called an *antenna array* or simply *array*, are introduced.

Similarly, in *sonar* systems, array structures are also applied to achieve lower side lobes, to provide beam steering over wide angular sectors, and to achieve multi-target handling capability.

In *radio astronomy*, an array structure is used to increase the *antenna aperture* to receive emissions from remote celestial sources. The arrays used for this purpose may have tens of elements and may extend from hundreds of meters to nearly the diameter of the earth.

For more details on various applications of array techniques, one may consult Haykin [33].

1.3 Functions of array processing in sonar and radar systems

Before we discuss the basic problems studied in array processing, we now look at two examples which illustrate the functions of array processing in radar and sonar systems.

A simplified block diagram of the receiver part of a typical radar system is given in Figure 1.1 [28, Monzingo, p.13, Fig.1-3]. The major blocks and their corresponding functions are described in Table 1.1 [11]. The system is composed of five major functional blocks; they are the array antenna, transmitter, receiver, signal processing, and display sections. The RF waveforms emitted by the antenna are generated by the local oscillator and transmitter. The reflected spatial waves of interest are received by the array antenna. In the receiver section, amplitude adjustment and frequency conversion is carried out. The major concern of the receiver is to achieve the highest possible signal-to-noise-ratio (SNR). Having maximized the SNR in the receiver section, target detection and target parameter estimation are performed in the signal processing section. The output from the signal

processing section may serve several purposes; i.e., to drive the display devices as shown in Figure 1.1 for example, and/or to provide the control section the necessary information for adaptation operation of the system, or beamforming of the antenna pattern.

The second example is a typical sonar receiver. The block diagram of the principal elements of this receiver is shown in Figure 1.2. In the so-called *wet end*, the transducer array receives signals from the underwater medium. The array processing section includes the spatial and temporal operations. In this section, outputs from the sensor array are processed by spectral analysis, correlation, etc., which are followed by the detection and estimation operations.

As we can see from these two examples, the coverage of array processing applications is very broad. But modern array processing as a research direction is more concentrated on developing high performance algorithms for the two most basic problems: detection and estimation.

The term *detection* in array processing is used to refer to the process of determining whether or not a target exists. If there are any, the number of targets needs to be determined. The term *estimation* refers to the process of extracting information concerning the targets, or in other words, obtaining estimates of target parameters such as position (angles of arrival and distance), strengths and cross correlations among the target waveforms, the sizes and velocities of the targets, etc. Sometimes, the noise and interference parameters also need to be estimated.

1.4 The signal model used in array processing

1.4.1 Waveform and array geometry assumptions

As we mentioned in section 1.1, array processing deals with the signals carried by propagating wave phenomena. The spatially separated array elements serve as spatial sample points of the propagating waves. Generally speaking, the waves may have any shape, but in most theoretical analysis the waves are assumed to be *plane waves*; in other words, the

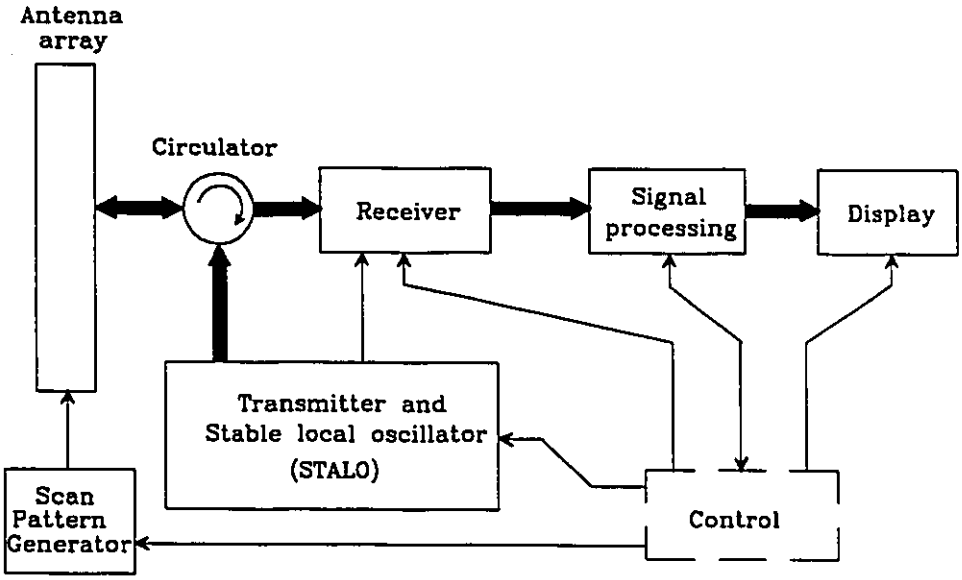

Figure 1.1: Block diagram of a typical radar system

Table 1.1: Founctions of blocks in Figure 1.1

Block	Function
Transmitter	generates high power R.F. waveform
Antenna	determines direction and shape of transmit and receive beam
Receiver	provides frequency conversion and low noise amplification
Signal processing	provides target detections, target and clutter tracking, and target trajectory estimates.
Display	converts processed signals into meaningful tactical information

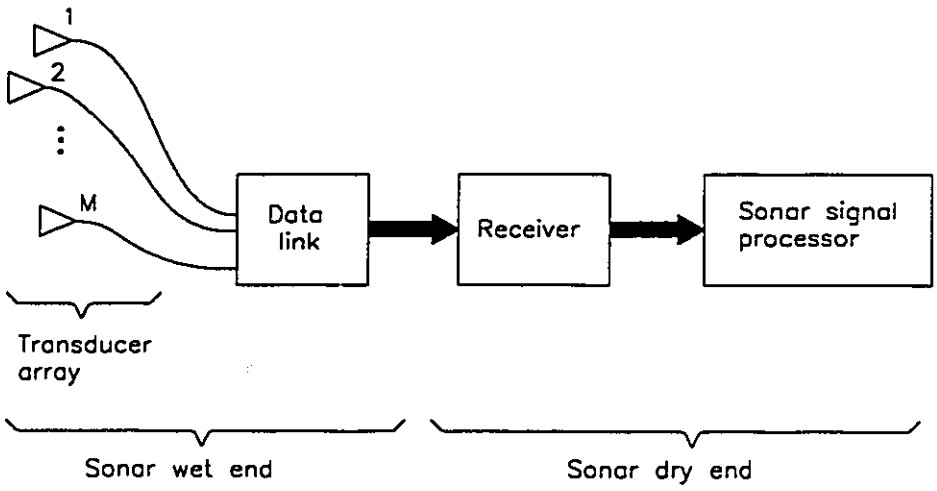

Figure 1.2: Block diagram of a sonar receiver

waves are assumed from *far field sources*. The array elements can also be arranged in a three dimensional space in various configurations. Indeed, many different kinds of array configurations applying different shapes and spacings can be found. However, there are certain limitations which restrict the way the elements are located. For example, a spatial analogy of Nyquist's sampling theorem indicates that the minimum sensor spacing must be less than or equal to a half of the wavelength in the propagating medium. Also, the array must be amenable to theoretic analysis and design, and must also abide by various manufacturing and implementation restrictions. As a result of these limitations, the most commonly used array geometric structures are those with regular shapes such as linear, circular, and planar arrays with regular spacings. Among these array configurations, the *linear array* with *equally spaced identical elements* is the dominant one, due to its simplicity.

In this thesis we also adopt the plane wave assumption and concentrate our discussion on linear arrays with equally spaced identical elements. The details of the array terminology used in this thesis can be found in Figure 1.3.

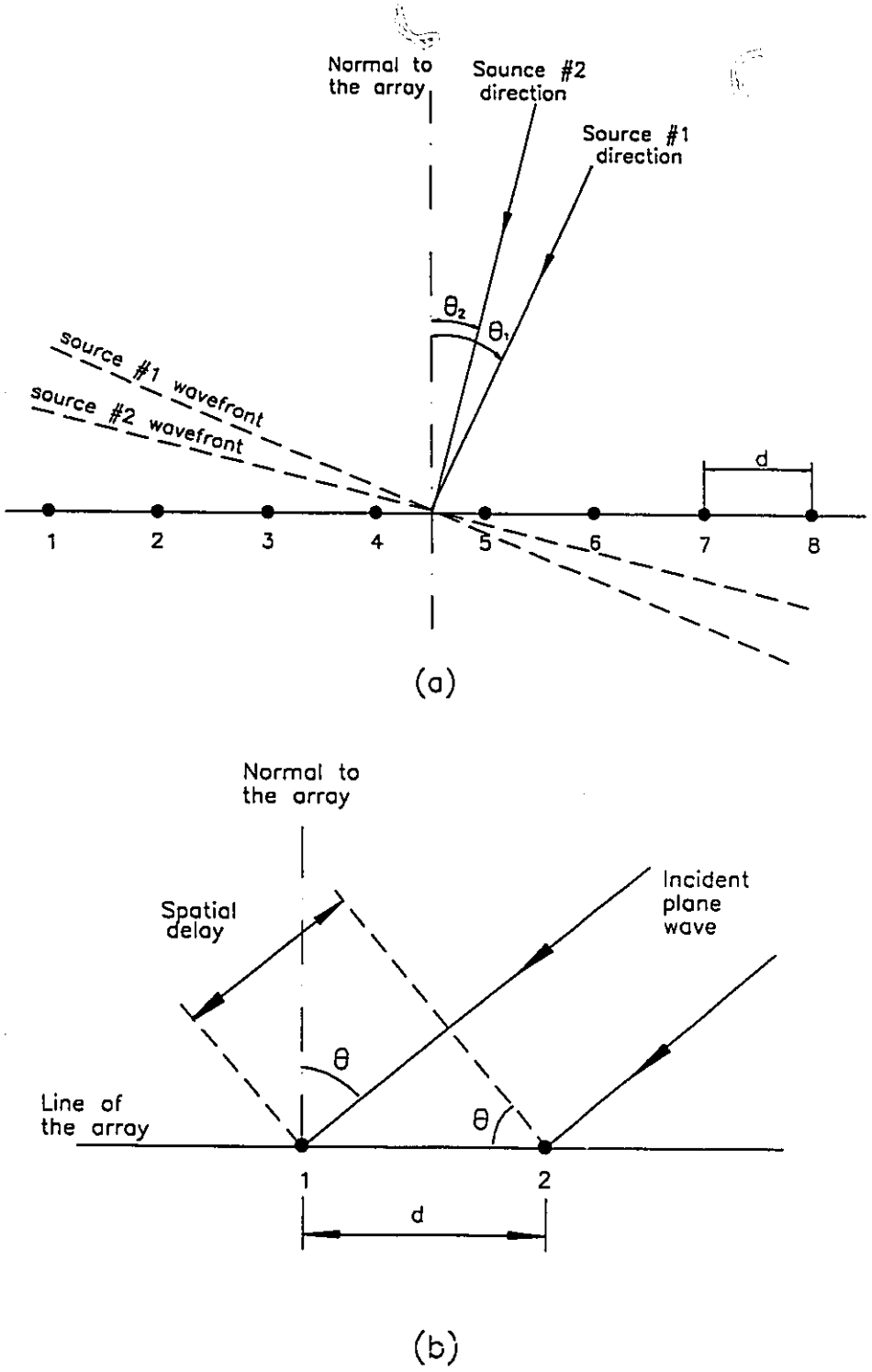

Figure 1.3: (a) The wave fronts of plane waves and linear array geometry, (b) The spatial delay incurred between adjacent elements when a plane wave impinges on a linear array.

1.4.2 Spatial sampling model

Assume the array of interest has p equally spaced elements, and there are k sources impinging on the array. As we pointed out before, the array elements serve as spatial sample points in the field of interest. The output of each element is a function of time t which describes the state of the corresponding spatial point. For p array elements, these functions form a p-dimensional vector which can be written as

$$\tilde{x}(t) = [\ \tilde{x}_1(t),\ ...,\ \tilde{x}_p(t)\ ]^T \tag{1.1}$$

where $\tilde{x}_i(t),\ \ i = 1, ..., p$ are the outputs of the p array elements.

Alternatively the outputs of the array may be expressed as a function of frequency by using temporal Fourier transform [2]

$$x(\omega) = F\{\tilde{x}(t)\} = [\ x_1(\omega),\ ...,\ x_p(\omega)]^T \tag{1.2}$$

where $F\{\cdot\}$ denotes the temporal Fourier transform operator.

The range of frequency in Equation (1.2) is problem dependent. It depends on the frequency range of the sources of interest and the purpose of the system. For some systems, the frequency range may be a very narrow band centered on a frequency ω_o. For other systems, the useful information may be embedded in a relatively broad range of frequencies. For each frequency, we can express the output of the m-th array element by

$$x_m(\omega) = \sum_{i=1}^{k} s_i(\omega) e^{j\omega\alpha_i(m-1)d} + v_m(\omega) \qquad m = 1, 2, ..., p \tag{1.3}$$

where ω is the temporal frequency, $s_i(\omega),\ i = 1, 2, ..., k$ are the temporal Fourier transform coefficients of the i-th source, α_i is defined by $\alpha_i = \sin(\theta_i)/c$. The quantity θ_i is the spatial angle of arrival of the i-th source, c is the propagation speed of the wave, d is the spatial separation of adjacent sensors, and $v_m(\omega)$ is the noise component.

[2] In array processing, both temporal and spatial operations are involved. The term temporal Fourier transform refers to the Fourier transform with respect to the time variable t.

1.4.3 Narrow band spatial-temporal sampling model

In practice, array outputs are digitized by temporal sampling and A/D conversions. For radar and active sonar systems, the temporal sampling is done after demodulating the array outputs to baseband. For passive sonar systems, the frequency range of the received signal is already in baseband form, and therefore can be directly sampled. There are various schemes for the implementation of the temporal sampling procedure. One of the schemes is first to sample the baseband signal and then to apply the temporal FFT. This procedure is described in Figure 1.4.

In Figure 1.4, the baseband outputs of the array are sampled and $n_s = n_p \times N$ samples are taken, where both n_p and N are integers. The samples are sectioned to N segments each with length n_p, so the sample data matrix has the form

$$\tilde{\boldsymbol{X}} = \left[\begin{array}{ccc|ccc|c|ccc} \tilde{x}_1(1) & \dots & \tilde{x}_1(n_p) & \tilde{x}_1(n_p+1) & \dots & \tilde{x}_1(2n_p) & \dots & \dots & \tilde{x}_1(n_s) \\ \tilde{x}_2(1) & \dots & \tilde{x}_2(n_p) & \tilde{x}_2(n_p+1) & \dots & \tilde{x}_2(2n_p) & \dots & \dots & \tilde{x}_2(n_s) \\ \dots & \dots & \dots & \dots & \dots & \dots & \dots & \dots & \dots \\ \tilde{x}_p(1) & \dots & \tilde{x}_p(n_p) & \tilde{x}_p(n_p+1) & \dots & \tilde{x}_p(2n_p) & \dots & \dots & \tilde{x}_p(n_s) \end{array}\right]$$

$$= \left[\tilde{\boldsymbol{X}}_1 \ \tilde{\boldsymbol{X}}_2 \ \dots \ \tilde{\boldsymbol{X}}_N\right] \tag{1.4}$$

Then, for each section of samples, the temporal FFT is carried out and the result is called a *snapshot*. At this stage, each snapshot is a $p \times n_p$ matrix. Let us denote these matrices by $\boldsymbol{X}_n$, $n = 1, 2, ..., N$. The (m, i)th element of $\boldsymbol{X}_n$ is the FFT of the m-th row of the n-th segment $\tilde{\boldsymbol{X}}_n$ evaluated at $\omega = 2\pi(i-1)/n_p$.

For multi-frequency or wide band array processing, more than one column of each $\boldsymbol{X}_n$ may be used. There have been several methods for solving array processing problems for wide band signals [64][38][13]. These methods use more information than methods using the narrow band assumption; therefore, they usually give better performance but require a more complicated algorithm and more computational intensity. In this thesis, we will use the narrow band assumption in the derivation of our new criteria. Readers interested

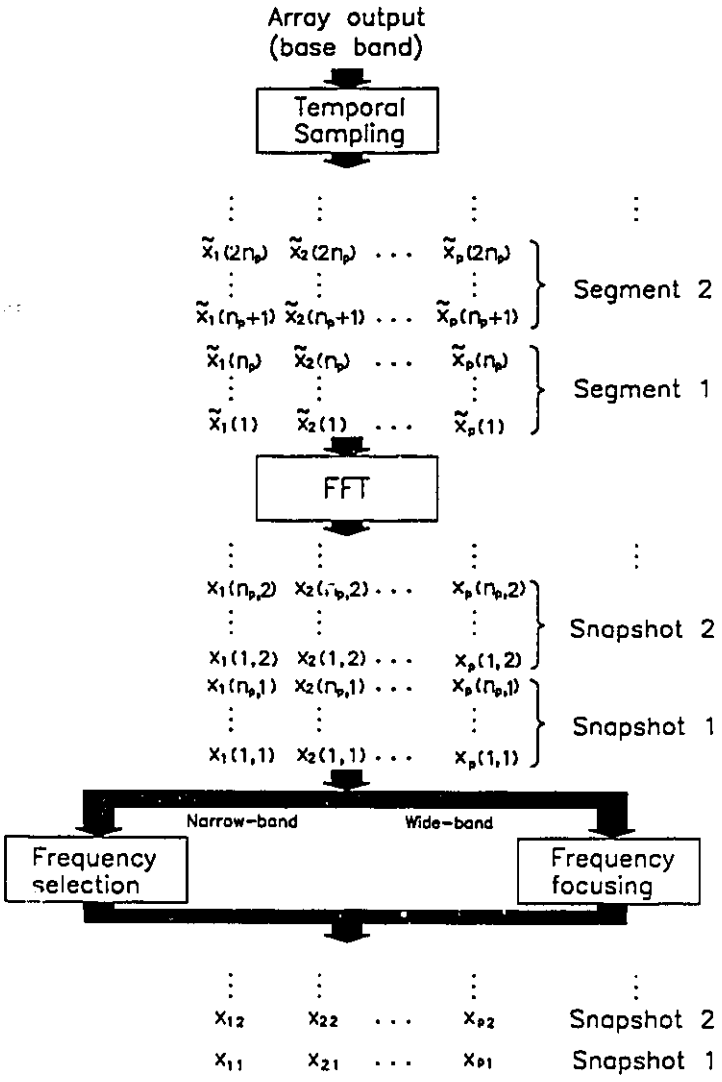

Figure 1.4: An example of a scheme for signal pre-processing in array processing

in wide band processing may refer the papers mentioned above. It should be pointed out that most wide band methods usually apply certain techniques such as *focusing* to convert the wide band problem to an equivalent narrow band problem. After such conversions, the methods developed in this thesis may still be used.

Under the narrow band assumption, after frequency selection, each snapshot matrix X_n has only one column. In other words, each snapshot becomes a vector. A very simple signal model can then be obtained, and is written as

$$x_m(n) = \sum_{i=1}^{k} s_i(n) e^{j\phi_i(m-1)} + v_m(n) \tag{1.5}$$

where $x_m(n)$ stands for the m-th element of the n-th snapshot. The quantity $\phi_i = \omega_0 d \sin(\theta_i)/c$, is the electrical angle of i-th signal, ω_0 is the centre frequency of the narrow band, d is the spatial separation of the elements of the array, and c is the propagation speed. When the separation d is selected as $\lambda_0/2$, where λ_0 is the wavelength, then $\lambda_0 = 2\pi c/\omega_0$, and the angle ϕ_i becomes $2\pi d \sin(\theta_i)/\lambda_0 = \pi \sin(\theta_i)$. The quantity s_i is the complex amplitude of the i-th source, which has a complex Gaussian distribution in most situations, and $v_m(n)$ is the noise component of the m-th element, assumed to be complex Gaussian with zero mean and covariance matrix Σ_v.

After sampling and FFT, the N snapshots of the p-dimensional vector form a data matrix,

$$X = \begin{bmatrix} x_{11} & x_{12} & \cdots & x_{1N} \\ x_{21} & x_{22} & \cdots & x_{2N} \\ \cdots & \cdots & \cdots & \cdots \\ x_{p1} & x_{p2} & \cdots & x_{pN} \end{bmatrix} . \tag{1.6}$$

This data matrix and the signal model given by Equation (1.5) are the starting point of most algorithms for detection and estimation of narrow band signals in array processing. Using the data matrix defined by Equation (1.6), the signal model given by Equation (1.5) can be expressed more compactly as

$$x_n = A(\phi) s_n + v_n, \quad n = 1, ..., N \tag{1.7}$$

where x_n is the n-th column of the data matrix given by Equation (1.6). The vector s_n is the n-th snapshot of the complex amplitudes of the signals. The $p \times k$ matrix A is called *direction matrix* whose (m, i)-th element is $\exp\{j\phi_i(m-1)\}$.

Notice that x_n is a sample of a random process, from Equation (1.7) the covariance matrix of this random process can be obtained as

$$\Sigma = A(\phi)\Sigma_s A(\phi)^H + \Sigma_v \tag{1.8}$$

where Σ_s is the covariance matrix of signals, and Σ_v is the covariance matrix of noise. If the noise covariance matrix has a diagonal form with equal entries, the noise is called *white noise* because such spatially uncorrelated noise has a flat spectrum. For the white noise situation, the signal model can be written as

$$\Sigma = A(\phi)\Sigma_s A(\phi)^H + \sigma^2 I \tag{1.9}$$

where σ^2 is the power of the noise, usually unknown. For this specific structure, it is easy to verify that the rank of matrix Σ equals k, the number of signals when noise is absent. This is because both $A(\phi)$ and Σ_s are rank k matrices. When the power of the white noise takes a non-zero value, it can be shown that the eigenvalues of matrix Σ has a special structure. Arranging the eigenvalues in descending order, the first k eigenvalues are larger than the $p-k$ smaller eigenvalues, and the $p-k$ smaller eigenvalues are all equal to σ^2. This special eigenvalue structure (or equivalently, the residual structure in model matching) is the basic fact on which most detection methods are based.

1.5 Summary of basic problems and development in array processing

The basic problems studied in array processing can be briefly summarized as

1. Detection of number of targets
2. Estimation of target parameters
3. Adaptive beamforming

The major difficulties in detection and estimation usually arise from the following phenomena:

1. The limitation of the array aperture,
2. The noise and interference in the environment and receiver system,
3. Non-ideal signal characters, such as non-planar wavefronts, correlation between different incident signal components, etc.,
4. Calibration errors of the array elements.

Let us discuss the influence of array aperture first. An array with individual elements can be considered as a spatially sampled version of spatially continuous aperture antenna. The aperture is measured in wavelengths. The beamwidth of an array system is inversely proportional to the aperture of the array. Generally speaking, the larger the aperture, the narrower the beamwidth; therefore, the higher the resolution the array system can achieve. This is especially true when the conventional spatial FFT method is used for array processing, because conventional methods cannot distinguish targets falling within one beamwidth [36]. Another troublesome phenomenon of FFT processing is the side lobes inherent in the spatial spectrum. These side lobes are caused by the finite size of the array, and they may cause confusion and may conceal some smaller targets located in the range of the side lobes.

In an attempt to alleviate the inherent limitations of the FFT approach, many alternative methods have been proposed in the last two decades. Among them, methods based on parametric models give the best resolution. The Multiple Signal Classification (MUSIC) algorithm [57], for example, in principle can achieve infinite resolution for finite array aperture under noiseless conditions. Methods belonging to the parametric type are numerous, Autoregressive Moving Average (ARMA) Estimation [32], Maximum Entropy Estimation(MEE) [14][56], Prony Spectral Density Estimation [12], Maximum Likelihood Estimation (MLE) [52], and Maximum A Posterior Probability Estimation (MAP) [53], to mention a few. A very important fact we should mention here is that all these parametric methods require knowledge of the number of signals to start the estimation procedure, and

usually the correctness of this knowledge is crucial in the estimation process. However, in most practical situations, the number of signals is unknown, and systems can only obtain this information by determining the number of signals from the sampled data, or in other words, by applying a *detection procedure*. For this reason, detection is a very important aspect in modern array processing.

Methods for detection in array processing can be classified according to the principles they use and the problems for which they are developed. The earliest detection criteria are based on testing the significance of the residuals after fitting a model to the data [10][4]. The problem with this approach is that the residual is also a function of the noise level. Without knowledge concerning the noise level, the threshold for testing must be set subjectively. This causes difficulty in engineering applications because in most practical situations, the noise level is a unknown variable.

To avoid this subjective threshold problem, several new methods have been developed using different approaches, which all fall into the same framework. Detection techniques in this class are called information theoretic criteria. The Akaike Information Criterion (AIC) [2] and the Minimum Description Length criterion (MDL) [58][54] are two typical examples. Information theoretic criteria assume white noise in the candidate models [66][73][69]; therefore they belong to the class of methods for white noise environments.

Spatially correlated noise is also called coloured noise because the spectrum of this type of noise is not flat. For unknown coloured noise, the information theoretic criteria can not be used directly. However, if the covariance matrix of the coloured noise is known, the noise components in the array outputs can be transformed to white noise by a so-called *whitening* technique [74]. After whitening, all the methods applicable for the white noise environment can then be applied.

The more difficult situations arise in the presence of spatially correlated noise with unknown covariance matrix. For detecting number of signals in such environments, few methods are proposed. Le Cadre proposed a parametric method for carrying out the detection-estimation procedure jointly. In Le Cadre's method, noise is modelled by an ARMA model,

and maximum likelihood estimation is used to estimate an enlarged parameter set in which the noise ARMA parameters are included. The problem with this method is that more uncertainty is added to the estimates as the result of expanding the parameter set.

Correlated signals such as multipath propagation and "smart" jammers can severely damage the performance of the parametric methods, especially for those methods using spatial projection techniques and principal component analysis. The reason is that when the correlation of the signals increases and approaches unity, the amplitudes of the principal components of the signals are dispersed over a larger range; the amplitude of the smallest principal component will decrease and will approach zero. This will cause difficulty, or even make it impossible to separate the noise subspace from the signal subspace. One of the solutions for processing correlated signals is the so called *spatial smoothing* technique [23][59][51]. The price paid in spatial smoothing is a reduced actual array aperture. Another method which can work for correlated signals is maximum likelihood estimation, without using principle decompositions.

The calibration problem arises when the characteristics of the response of the array sensors differ from each other or differ from the assumed values. The difference is called calibration error, which may include both amplitude error and phase error. Calibration errors can also be induced by mutual coupling between the sensor elements or by differences in the electrical or mechanical characteristics of the channel associated with each sensor. The existence of calibration error usually deteriorates the performance of the array system.

Another obvious difficulty associated with array processing is the hardware requirements and computational "horsepower" required to execute the array processing algorithms. Although an array system usually can give superior performance over that of a single sensor (antenna or sonar transducer), an array system does require increased hardware and computer power to perform the data processing. Therefore, the development of array processing methodology is closely coupled with the development of electronics, fast algorithms (the FFT, being a good example), and computer technology. As a result of the rapid development of solid state electronics and new computer architectures, modern computers can now carry out real-time data processing on the array outputs. The development of parallel

computing techniques such as systolic arrays, gives modern array systems the means to implement far more complicated algorithms, such as eigen-analysis based algorithms. With this support from quickly expanding available computer power, one trend in array processing research is the development of new criteria and algorithms which are more amenable to implementation on massively parallel architectures.

The main theme of this thesis concerns the *detection problem in array processing.* The contributions of this thesis to detection methods in array processing are:

1. A new attractive alternative method referred to as the Eigen-Threshold(ET) method, for the white noise environment [16][17].
2. A new method based on canonical correlation analysis for detection in the presence of spatially correlated noise [18][19]. This method is referred to as the Canonical Correlation Testing (CCT) method.

Chapter 2

Methods for detection in array processing

2.1 Definition of probability of detection and errors

In array signal processing, the term *detection* means determining the number of sources based on received data which are usually noise polluted. There is always a chance of making a wrong decision when one tries to determine the number of signals from noise polluted data. Let us denote the true number of signals by k, and the estimated number of signals by $\hat{k}$. We say the signals are correctly detected if $k = \hat{k}$. Otherwise, we say a detection error has occurred. According to whether $\hat{k} > k$ or $\hat{k} < k$, the detection errors are classified into two kinds. Whenever $\hat{k} > k$, we say a *false alarm error* has occurred. Whenever $\hat{k} < k$, we say a *missing error*, or simply a *miss*, has occurred. These definitions of errors and their probabilities are summarized in Table 2.1.

2.2 Hypothesis testing

The problem of detection (determining the number of signals) can be viewed as a special case of model identification. As one of the basic problems occurring in science and engineering practice, model identification has been studied from different approaches for

Table 2.1: Definition of errors and probabilities

Value of $\hat{k}$	$\hat{k} = k$	$\hat{k} > k$	$\hat{k} < k$
Name of event	Signals are detected correctly	False alarm has occurred	A "miss" has occurred
Probability of the event	$P_D = \mathrm{P}(\hat{k} = k)$	$P_F = \mathrm{P}(\hat{k} > k)$	$P_M = \mathrm{P}(\hat{k} < k)$

several decades. The earliest method developed for this purpose is the method of *Hypothesis Testing*. The development of the general theory of hypothesis testing is due originally to Neyman and Pearson (1933)[46], who proposed seeking tests that minimize the chances of error. The notion of cost and risk were introduced by Wald (1939)[63], who is responsible for much of the development of the theory in analogy to the theory of games. For the development of hypothesis testing theory for *multivariate analysis* (a statistical field which may be applied directly to array processing), we should mention the names of M. S. Bartlett, and D. N. Lawley. In the two papers by Bartlett (1951)[6](1954)[7], the χ^2 approximations of the analysis of multiplying factor yielded the fundamentals of the χ^2 based multivariate hypothesis test. In the paper by Lawley (1956)[40] the χ^2 approximation problem is further examined for testing the equality of the remaining eigenvalues of the covariance matrix, where the effects of the k largest eigenvalues have been removed.

In this section, we shall use the procedure given by Lawley [40] to illustrate the idea of the hypothesis test, as it applies to array processing.

2.2.1 Hypothesis testing using Bartlett and Lawley's χ^2 tests

Consider the signal model given by Equation (1.7) in Section 1.4. Using the sample data matrix defined in Equation (1.6), a matrix $\boldsymbol{S}$ is defined as

$$\boldsymbol{S} = \boldsymbol{X}\boldsymbol{X}^H \tag{2.1}$$

where $\boldsymbol{X}$ is the $p \times N$ sample data matrix defined in Equation (1.6), p being the dimension of the sensor array from which the data is sampled, and N being the number of snapshots. The matrix $\boldsymbol{S}$ is related to the sample covariance matrix $\hat{\boldsymbol{\Sigma}}$ by

$$\hat{\boldsymbol{\Sigma}} = \frac{1}{N}\boldsymbol{X}\boldsymbol{X}^H = \frac{1}{N}\boldsymbol{S} \,. \tag{2.2}$$

Denote the eigen decomposition of the matrix $\boldsymbol{S}$ by

$$\boldsymbol{S} = \boldsymbol{Q}\boldsymbol{L}\boldsymbol{Q}^H \tag{2.3}$$

where $\boldsymbol{L}$ is a diagonal matrix,

$$\boldsymbol{L} = \mathrm{diag}[l_1,\ l_2,\ ...,\ l_p] \,, \tag{2.4}$$

where $l_1 > l_2 > ... > l_p$ are the eigenvalues of $\boldsymbol{S}$, and $\boldsymbol{Q}$ is a unitary matrix whose columns are the eigenvectors of $\boldsymbol{S}$.

Assuming that there are k signals and the noise is white, as we have mentioned in section 1.4, the eigenvalues of the true covariance matrix will have the following relations.

$$\lambda_1 > \lambda_2 > ... > \lambda_k > \lambda_{k+1} = ... = \lambda_p = \lambda \tag{2.5}$$

where λ is *unknown* in our discussion.

According to the case IIIc discussed in Bartlett's paper [7], the criterion used for testing the hypothesis

$$\begin{cases} H_0: & \lambda_{k+1} = ... = \lambda_p = \lambda \\ H_1: & \lambda_i,\ \ i = k+1, ..., p \ \text{ are not all equal} \end{cases} \tag{2.6}$$

is

$$C_N[-\log_e(l_{k+1}l_{k+2}...l_p) + (p-k)\log_e((l_{k+1} + l_{k+2} + ... + l_p)/(p-k))] \underset{H_0}{\overset{H_1}{\gtrless}} \gamma \tag{2.7}$$

where C_N is the Bartlett's correction factor. For this case [1],

$$C_N = N - \frac{1}{6}\left(2p + 1 + \frac{2}{p}\right) \tag{2.8}$$

[1]This coefficient and the corresponding degrees of freedom of the χ^2 approximate given by Bartlett is for real data

and this criterion follows approximately the χ^2 distribution with $(p-k-1)(p-k+2)/2$ degrees of freedom when the hypothesis H_0 is true. By setting a threshold γ corresponding to a specified false alarm rate, the number of equal eigenvalues can be determined through hypothesis testing. Then the number of signals can be obtained because the number of equal eigenvalues is $p-k$, where p is the number of sensors of the array, and k is the number of signals.

2.2.2 Problem with the χ^2 test

The problem with the method of hypothesis testing is the *uncertainty* over the degrees of freedom of the criterion.

In 1956 Lawley published his result on this topic [40]. He pointed out that the criterion given by Equation (2.7) does not, even asymptotically, follow a χ^2 distribution, though it will approximately do so if the eigenvalues of the true covariance matrix Σ, λ_1, λ_2, ... λ_k as given in Equation (2.5), are large and λ is small. Even then the effective number of degrees of freedom depends on the amount of variance removed from each variate by the first k principle components.

To correct such an uncertainty, T. W. Anderson suggested the use of the form $c\chi^2_d$ to describe the distribution of the criterion, where c and d are constants and where χ^2_d denotes a χ^2 variable with d degrees of freedom. However, in most practical situations, the knowledge required in determining these two constants is not available. Therefore, such further corrections may only be done subjectively.

The requirement that the χ^2-test thresholds must be set subjectively limited the applicability of the above hypothesis testing methods in array processing. As an effort to avoid this subjectivity, information theoretic criteria are introduced.

2.3 Information theoretic criteria

We use the term *information theoretic criteria* to refer a class of detection criteria which are derived from different approaches but fall into the same framework. The information theoretic criteria framework can be expressed as follows:

Consider a family of k_M models $\mathcal{M} = \{M_i\}$,

$$M_i = \{f(\boldsymbol{x}|\theta_i) \mid \theta_i \in \Theta\}, \quad i = 1, ..., k_M \tag{2.9}$$

where $f(\boldsymbol{x}|\theta_i)$ is the density function of $\boldsymbol{x}$ with parameter θ_i, and Θ is the parameter space of the model family. The information criteria are given by the form

$$\text{IC}(i) = -2L_N(\hat{\theta}_i) + c_N q_i, \quad i = 1, ..., k_M \tag{2.10}$$

where i is the index of the candidate model, $\hat{\theta}_i$, $L_N(\theta_i)$, q_i are respectively the quasi maximum likelihood estimates (QMLE), the quasi log-likelihood, and the number of free adjusted parameters under the model M_i. The model minimizing the criterion given by Equation (2.10) will be regarded as the best model in the family. The coefficient c_N is the weighting factor of the second term, called the *penalty term*, and makes the criteria different from each other. Akaike [2] proposed $c_N = 2$ in his AIC, Schwartz [58] and Rissanen [54] proposed $c_N = \log_e N$ in the MDL (BIC), and Hannan and Quinn [30] proposed $c_N = C \log_e \log_e N \quad (C > 0)$ in their Φ criterion. To give reader some more detail, and to facilitate the discussion later on, we now give a brief discussion on each criterion's penalty term.

2.3.1 Akaike's information theoretic criterion (AIC)

The reason this technique is called an *information theoretic criterion* is because it is derived on the basis of the *Kullback-Leibler mean information measure.*

Let $\boldsymbol{x}$ be a random vector with a probability density function (pdf) $g(\cdot)$. Consider a family of pdf's defined by

$$\mathcal{F} = \{f(\boldsymbol{x}|\theta)\ \theta \in \Theta\} \tag{2.11}$$

where Θ is the space of the parameters. The true distribution $g(x)$ is assumed to be an element in this family with true parameters θ_t. That is

$$g(x) = f(x|\theta_t) \tag{2.12}$$

The Kullback-Leibler mean information is defined as

$$\begin{aligned} I(g; f, \theta) &= E_{\theta_t}[\log_e g(x)] - E_{\theta_t}[\log_e f(x|\theta)] \\ &= \int g(x) \log_e g(x) dx - \int g(x) \log_e f(x|\theta) dx \\ &= \int g(x) \log\{g(x)/f(x|\theta)\} dx \\ &= \int f(x|\theta_t) \log\{f(x|\theta_t)/f(x|\theta)\} dx \end{aligned} \tag{2.13}$$

where E_{θ_t} denotes the expectation operator with respect to $g(x)$, the pdf with true parameters θ_t.

The K-L mean information has the following properties:

a. $I(g; f, \theta) = 0$ if and only if $f(x|\theta) = g(x)$

b. $I(g; f, \theta) \geq 0$

Therefore, it can be used as a measure for discrimination between $g(\cdot)$ and $f(\cdot|\theta)$. Thus, the model identification problem becomes the problem of finding the model which minimizes the Kullback-Leibler mean information among the family.

Let $x_1, \cdots, x_N$ be some i.i.d. samples of x. Define the quasi-likelihood and the quasi maximum likelihood estimate (QMLE) based on N independent observations as

$$L_N(\theta) = \sum_{i=1}^{N} \log_e f(x_i|\theta) \tag{2.14}$$

$$L_N(\hat{\theta}) = \max_{\theta \in \Theta} L_N(\theta) \tag{2.15}$$

The modifier "quasi" means the likelihood function is maximized for the model under test and this model is not necessarily of the true order. By applying a Taylor expansion about the quasi true parameter θ_0, and using the relation

$$(\hat{\theta} - \theta_0)^T J_N(\theta_0)(\hat{\theta} - \theta_0) \sim \chi^2_q, \tag{2.16}$$

where

$$J_N(\theta) = E_\theta \left[\frac{\partial \log_e g(\boldsymbol{x}_N|\theta)}{\partial \theta} \cdot \frac{\partial \log_e g(\boldsymbol{x}_N|\theta)}{\partial \theta^H} \right] \tag{2.17}$$

is the Fisher's information matrix, χ^2_q is the χ^2 distribution of q degrees of freedom, q being the number of free adjusted parameters of the true model, Akaike showed that minimizing the Kullback-Leibler mean information $I(g; f, \theta)$ is equivalent to minimizing the criterion

$$\mathrm{IC}_{AIC} = -2L_N(\hat{\theta}) + 2q \,. \tag{2.18}$$

2.3.2 Minimum description length criterion (MDL)

The criterion AIC developed by Akaike attracted broad attention because of its elegant theoretical formulation and its striking difference from the traditional hypothesis testing methods. But before long, a problem with the AIC was noticed. Firstly, the AIC is given in a fixed formulation; therefore, the performance is not flexible. Secondly, this rigid performance is not quite satisfactory. When used for detection in array processing, the AIC yields a certain residual probability of error which persists even at high signal to noise ratios and/or when the number of samples (snapshots) goes to infinity. In statistical terms, the AIC is not *consistent.*

Consistency, as a statistical concept, is defined as follows: An estimator t_n, using a sample of n values, will be said to be a consistent estimator of θ if, for any positive ϵ and η, however small, there is some N such that the probability that

$$|t_n - \theta| < \epsilon \tag{2.19}$$

is greater than $1 - \eta$ for all $n > N$. In notation of the theory of probability

$$\mathrm{P}\{|t_n - \theta| < \epsilon\} > 1 - \eta, \quad for \;\; n > N \tag{2.20}$$

An equivalent statement for t_n being a consistent estimator of θ is that t_n converges to θ in probability.

Inspired by Akaike's pioneering work, and with a view to improve the AIC in terms of consistency, a new criterion was derived independently by Schwartz [58] and Rissanen [54]

from quite different points of view. Schwartz's approach, namely BIC, is based on Bayesian arguments. He assumed that each competing model in the candidate model family can be assigned a prior probability, and proposed to select the model that yields the maximum posterior probability. Rissanen's approach is based on information theoretic arguments. Since parametric modeling can also be considered as encoding the observed data by parameters, Rissanen proposed to select the model that gives the minimum code length. The new criterion is known as *Minimum Descriptive Length (MDL) Criterion.* For large N, the MDL and the BIC have the same form, given by

$$\mathrm{IC}_{MDL} = -2L_N(\hat{\theta}) + q_i \log_e N \,. \tag{2.21}$$

Compared with the AIC, the only change offered by the MDL is that the coefficient $c_N = 2$ in the penalty term is replaced by $\log_e N$. This factor adjusts the penalty term according to the sample size N to ensure consistency of the MDL criterion. The proof of the consistency of the MDL can be found in [73][75].

2.3.3 Formulation of the AIC and the MDL with eigenvalues

In 1985, Wax and Kailath [66] published forms of the AIC and MDL criteria expressed in terms of the eigenvalues of $\hat{\Sigma}$ (or S). Criteria in this form can be very conveniently used in high resolution array processing for detection of the number of signals.

Let $\{l_i\}$, $i = 1, 2, ..., p$ be the eigenvalues of the sample covariance matrix of $p \times p$ dimensions formed from N samples of array output. The array outputs are assumed to be p dimensional complex processes. The eigenvalues are assumed to be arranged in descending order. According to [66], the AIC and MDL can then be expressed as

$$\mathrm{AIC}(k) = -2\log_e \left(\frac{\prod_{i=k+1}^{p} l_i^{1/(p-k)}}{\frac{1}{p-k}\sum_{i=k+1}^{p} l_i} \right)^{(p-k)N} + 2k(2p-k) \tag{2.22}$$

$$\mathrm{MDL}(k) = -\log_e \left(\frac{\prod_{i=k+1}^{p} l_i^{1/(p-k)}}{\frac{1}{p-k}\sum_{i=k+1}^{p} l_i} \right)^{(p-k)N} + \frac{1}{2}k(p-k)\log_e N \tag{2.23}$$

where k is the number of signals under test. The estimated number of signals will be the k which minimizes the criterion. The criteria given by Equations (2.22) and (2.23) will be repeatedly referred to in this thesis so that comparisons can be made with the new criteria developed in the ensuing chapters.

2.3.4 Other information theoretic criteria

Besides the well-known AIC and MDL criteria, there are numerous other criteria which fit into the information theoretic criteria framework. Among them, we mention the works of Hannan, and Zhao and Krishnaiah etc.

Hannan, in 1979, proposed a so-called Φ-criterion for selecting the best order of an AR models [30]. His argument is based on the law of the iterated logarithm. It has the form

$$\mathrm{IC}_\Phi = -2\log_e L_N(\hat{\theta}) + q_i C \log_e \log_e N \tag{2.24}$$

where $C > 2$.

Zhao, Krishnaiah and Bai [73] further generalized the results of Akaike, Hannan, Schwartz, and Rissanen by proposing a criterion called *Efficient Detection Criterion* (EDC)

$$\mathrm{IC}_{EDC} = -2\log_e L_N(\hat{\theta}) + C(N)q_i \tag{2.25}$$

where $C(N)$ is not given in a specific form, but for consistency, it must satisfy the following two conditions:

$$\lim_{N\to\infty} C(N)/N = 0 \tag{2.26}$$

$$\lim_{N\to\infty} C(N)/\log_e \log_e N = \infty \tag{2.27}$$

Hence, we see the MDL is a special case, and the Φ-criterion a boundary case, of the EDC.

Yin and Krishnaiah proposed a detection criterion which has a more general form. With certain r-regular conditions satisfied, a real function $f(\cdot)$ replaces the log-likelihood function in the EDC:

$$\mathrm{IC}_{GDC} = f(l_{k+1}^{(n)}, \cdots, l_p^{(n)}) + q_k C_n \tag{2.28}$$

where $l_i^{(n)}$ is an estimate of λ_i, where $\lambda_1 \geq \lambda_2 \geq ...\lambda_k > \lambda_{k+1} = ... = \lambda_p$ are nonrandom constants which are not necessarily eigenvalues, and satisfy $|l_i^{(n)} - \lambda_i| = 0(\alpha_n)$, as $n \to \infty$ a.s., for $i = 1, \cdots, p$, the $\alpha_n > 0$ are nonrandom, $\alpha_n \to 0$. The quantity $C_n > 0$ is a nonrandom function of n, it should satisfy: $C_n \to 0$, and $\alpha_n^{r+1}/C_n \to 0$, r being the level of regularity of the function $f(\cdot)$. The quantity q_k is the number of free adjusted parameters of the model assuming k signals. Details of this method can be found in [69].

2.4 Comparison of the hypothesis testing method and the information theoretic criteria

As we mentioned before, the hypothesis testing methodology proposed by Bartlett and Lawley is the χ^2 approximation of the likelihood ratio criterion. From the performance point of view, the hypothesis testing method represents an effort to give a quantitatively controllable error performance for the detection (model selection) procedure. By introducing the correction factor, this effort succeeds in giving a fairly good approximation when the noise level is low (the noise eigenvalue is small). But when the noise level is relatively high, the accuracy of the approximation becomes a function of the signal to noise ratio. When the signal to noise ratio diminishes, the accuracy of the approximation becomes poor. This means if we do not correct this influence, the actual performance of the method may differ from the theoretically predicted one. To correct this influence, knowledge of the true SNR is required. In most practical problems the SNR is unknown. Therefore, a certain subjective judgment is required in the application of the hypothesis testing method of Bartlett and Lawley.

In contrast to this, the information theoretic criteria are developed from totally different bases. By using Kullback-Leibler mean information and other information measures for

model selecting, the information theoretic criteria do not need a subjectively set threshold. Another characteristic of this class of criteria is that consistency is emphasized in these methods developed after the AIC. The consistency of these criteria is brought in by introducing a weighting factor, which is a function of the sample size N, into the penalty term of the criteria. By selecting the weighting function properly (which means the function should satisfy the conditions given in Equations (2.26) and (2.27)), the consistency of the criteria is ensured. However, for limited N, quantitative error performance is not directly obtainable for the information criteria, although fairly complex procedures [65][70] do exist for this purpose.

Comparing these two approaches, the common and contrasting characteristics can be summarized as

1. The common characteristic — the core of the criteria: The central part of the hypothesis testing method and most information theoretic criteria can be shown to be a likelihood ratio. From Equations (2.7), (2.22), and (2.23), we see that the likelihood terms are invariant to multiplication of the eigenvalues by a common factor. Since the noise variance is such a common factor in the noise eigenvalues, its influence may be removed from the criteria. This property enables the likelihood ratio criterion based criteria to effectively deal with the situations in which the noise variance is unknown.

2. The contrasting characteristic — the threshold/penalty term: the hypothesis testing method uses the χ^2 approximation to quantitatively control the false alarm performance, but essentially fails because of the requirement of a subjective threshold. The information theoretic criteria avoid such subjectivity by introducing a penalty term which is determined using asymptotic consistency arguments.

Obviously, the major advantage of the information criteria is that it eliminates the subjective threshold required by the hypothesis testing method. Therefore, the information theoretic criteria are more useful for solving practical problems. However, information theoretic criteria are based on consistency arguments. No straightforward quantitative performance analysis is directly available for these criteria, although the performance can

be derived through somewhat complex procedures[65][70]. We notice that although the consistency argument has important theoretical impact, in practice, the sample size N can only be finite. When N is fixed, and quantitative performance is desired, consistency arguments may not make too much sense. Hence, in this thesis, although we use mainly asymptotic theory for our theoretic analysis, our arguments are more concentrated on the development of new methods which can give a *quantitative theoretical prediction* of their error performance. As a result of such an emphasis, our new methods presented in this thesis are characterized by *quantitatively controllable performances*, i.e., the false alarm rate may be controlled to within any reasonable level. Hence, the performance of the methods may always approach near-optimum levels, regardless of the operational SNR.

Chapter 3

A new method for detection in the white noise environment

This chapter addresses two main issues:

Firstly, a discussion on the asymptotic distributions of the eigenvalues of the sample covariance matrix under the white noise assumption is presented. This discussion provides the statistical theoretical support for our new method. The distributions involved are for complex data, and are given in several different forms. These asymptotic distributions are valuable not only because the literature on this topic is limited, but also because they are useful for giving the reader a clearer, deeper view of the behavior of the sample eigenvalues, which are widely used in various modern array processing techniques in direct or indirect manners. Furthermore, if the reader compares these distribution functions with their real data counterparts, interesting correspondences are revealled.

Secondly, based on the distribution of the normalized sample eigenvalues, a new method, namely the Eigen-Threshold (ET) [16][17] method for detecting the number of signals in the white noise environment is proposed. This new method is based on one step predictions of the upper threshold of the estimates of the smallest multi-fold eigenvalue of the covariance matrix. The probability of the predicted threshold being exceeded can be controlled by a parameter t. For a given probability of error P_e, the new method yields lower value of SNR threshold than that of the MDL, and has a lower error rate than that

of the AIC at high SNR. In contrast to the hypothesis testing methods based on Bartlett and Lawley's χ^2 tests, or T. W. Anderson's confidence interval approach, subjectively set thresholds are not required in this new method. This is because the thresholds used in the ET method are generated in a one-step prediction manner which therefore, enables the threshold values to be adjusted adaptively under different noise levels. Before a detailed discussion of the new method, let us first introduce the eigen-threshold concept.

The performance analysis of the new method is given in the next chapter.

3.1 Eigen-decomposition of the covariance matrix

Consider a linear array of p sensors. The array output can be expressed as a complex vector $\boldsymbol{x}(t)$, where,

$$\boldsymbol{x}(t) = \boldsymbol{A}(\theta)\boldsymbol{s}(t) + \boldsymbol{n}(t) \tag{3.1}$$

where $\boldsymbol{s}(t)$ is a $k \times 1$ vector which denotes the complex envelopes of the k narrow-band signals. The elements of $\boldsymbol{s}(t)$ are assumed to be independent Gaussian distributed random variables with zero mean. $\boldsymbol{A}(\theta)$ is a $p \times k$ matrix whose columns are the direction vectors with parameters θ denoting the angles of arrival of the k signals. With each signal incident from a different direction, $\boldsymbol{A}(\theta)$ is a full column rank matrix. The vector $\boldsymbol{n}(t)$ is a $p \times 1$ vector representing the receiver noise of the p sensors. It is assumed to be a complex, zero mean, Gaussian white process.

Let $\boldsymbol{\Sigma}$ be defined as the covariance matrix of $\boldsymbol{x}$, then

$$\boldsymbol{\Sigma} = \boldsymbol{A}(\theta)\boldsymbol{\Sigma}_s\boldsymbol{A}(\theta)^H + \sigma_n^2\boldsymbol{I} \tag{3.2}$$

where $\boldsymbol{\Sigma}_s = \mathrm{E}\{\boldsymbol{s}(t)\boldsymbol{s}(t)^H\}$ is the covariance matrix of $\boldsymbol{s}(t)$, where $\mathrm{rank}(\boldsymbol{\Sigma}_s) = k$ for non-coherent signals, and σ_n^2 is an unknown constant representing the noise power of each sensor.

Because $\boldsymbol{\Sigma}$ is a nonnegative definite Hermitian matrix, it can always be decomposed to a diagonal form as follows:

$$\boldsymbol{\Sigma} = \boldsymbol{Q}\boldsymbol{\Lambda}\boldsymbol{Q}^H \tag{3.3}$$

where Q is a unitary matrix whose columns are the eigenvectors of Σ, and Λ is a diagonal matrix whose diagonal elements are the eigenvalues of Σ assumed to be arranged in descending order such that

$$\Lambda = \text{diag}(\lambda_1, \lambda_2, ..., \lambda_k, \lambda, \ ..., \ \lambda) \tag{3.4}$$

and

$$\lambda_1 > \lambda_2 > \ ... \ > \lambda_k > \lambda = \sigma_n^2 \ . \tag{3.5}$$

If the covariance matrix Σ were available, one might determine the number of signals simply by counting the multiplicity of the smallest eigenvalues of Σ . In practice however, since Σ must be estimated from the samples of the array output $x(t)$, the last $p - k$ eigenvalues are no longer equal. Now assume $x(t_1)$, $x(t_2)$, ... $x(t_N)$ are a group of samples of $x(t)$, which may be simply denoted by x_1, x_2, ... x_N, then the estimate of Σ is given as

$$\hat{\Sigma} = \frac{1}{N} S \tag{3.6}$$

where

$$S = \sum_{i=1}^{N} x_i x_i^H \tag{3.7}$$

which follows the complex Wishart distribution $W_p(N, \Sigma)$. Therefore, the probability density function of S can be expressed as

$$f(S) = \frac{|S|^{N-p}}{\tilde{\Gamma}_p(N)|\Sigma|^N} \exp[-\text{tr}(\Sigma^{-1}S)] \tag{3.8}$$

where $|\Sigma| = det(\Sigma)$,

$$\tilde{\Gamma}_p(N) = \pi^{p(p-1)/2} \prod_{i=1}^{p} \Gamma(N - i + 1) \tag{3.9}$$

and the eigen decomposition of $\hat{\Sigma}$ has the form

$$\hat{\Sigma} = \hat{Q} D \hat{Q}^H \tag{3.10}$$

where $\hat{Q}$ is a unitary matrix of dimension $p \times p$, and is an estimate of Q. The matrix D is diagonal of dimension $p \times p$, and is an estimate of Λ, which is given as

$$D = \text{diag}(d_1, \ d_2, \ ..., \ d_p) \tag{3.11}$$

where $d_1 > d_2 > \ ... \ > d_p$ with probability one for finite N. It is known that the exact distribution of $\boldsymbol{D}$ is [35]

$$\begin{aligned} & f(d_1, d_2, ..., d_p | \lambda_1, \lambda_2, ..., \lambda_k, \lambda) \\ = \ & \frac{\pi^{p(p-1)} |\boldsymbol{S}|^{N-p}}{\tilde{\Gamma}_p(N)\tilde{\Gamma}_p(p)|\boldsymbol{\Sigma}|^N} \cdot {}_0\mathrm{F}_0(-\boldsymbol{\Sigma}^{-1}, \boldsymbol{D}) \prod_{i=1}^{p-1} \prod_{j=i+1}^{p} (d_i - d_j)^2 \end{aligned} \tag{3.12}$$

where ${}_0\mathrm{F}_0(-\boldsymbol{\Sigma}^{-1}, \boldsymbol{D})$ is the hypergeometric function with matrix arguments $\boldsymbol{\Sigma}^{-1}$, and $\boldsymbol{D}$.

This special function is difficult to calculate because of the infinite integrations involved. For this reason, asymptotic distributions which are easier to apply in practical situations have been derived in a number of papers for various cases[3, 43, 15, 71, 68]. These distributions are further modified for the development and analysis of the eigen-threshold method of this thesis.

3.2 Asymptotic distributions of the residual eigenvalues

The asymptotic distribution of $d_1 > d_2 > ... > d_p$, the eigenvalues of the sample covariance matrix $\hat{\Sigma}$ can be derived by expanding the hypergeometric function. Various authors have obtained the asymptotic expansion for the joint distribution given by Equation (3.12). For the cases where the true eigenvalues $\lambda_1, \lambda_2, ..., \lambda_p$ are distinct, the asymptotic distribution has been given by G. A. Anderson [3], and Li and Pillai [43]. For the case with *multifold* eigenvalues, which is more difficult, the asymptotic distribution has been derived by Chattopadhyay [15], and Zhang and Wong [71]. The proof has also been summarized in another paper of Wong, Zhang, Reilly, and Yip [68]. Here we present the distribution derived by the authors above as a theorem. The lengthy proof is omitted.

Theorem 3.1 *Suppose $\boldsymbol{S} = N\hat{\boldsymbol{\Sigma}}$ follows the complex Wishart distribution $W_p(N, \boldsymbol{\Sigma})$, that is, the probability distribution function of $\boldsymbol{S}$ can be expressed as*

$$f(\boldsymbol{S}) = \frac{|\boldsymbol{S}|^{N-p}}{\tilde{\Gamma}_p(N)|\boldsymbol{\Sigma}|^N} \exp[-\mathrm{tr}(\boldsymbol{\Sigma}^{-1}\boldsymbol{S})] \tag{3.13}$$

where

$$\tilde{\Gamma}_p(N) = \pi^{p(p-1)/2} \prod_{i=1}^{p} \Gamma(N-i+1) \tag{3.14}$$

and the eigenvalues of $\hat{\Sigma}$ *and* Σ *are* $d_1 > d_2 > ... > d_p$ *and* $\lambda_1 > \lambda_2 > ... > \lambda_k > \lambda_{k+1} = ... = \lambda_p = \lambda$ *respectively. Then the asymptotic probability density function of* $d_1 > d_2 > ... > d_p$ *is given by*

$$f(d_1, \ d_2, \ ..., \ d_p|\lambda_1, \lambda_2, ..., \lambda_k, \lambda) = \frac{N^{pN-k(2p-k-1)/2}\pi^{p(p-1)-k(k+1)/2}\tilde{\Gamma}_k(p)}{\tilde{\Gamma}_p(N)\tilde{\Gamma}_p(p)} \cdot$$

$$\exp\left\{-N\left[\sum_{i=1}^{k}\frac{d_i}{\lambda_i} + \sum_{i=k+1}^{p}\frac{d_i}{\lambda}\right]\right\} \cdot \prod_{i=1}^{k-1}\prod_{j=i+1}^{k}\frac{\lambda_i\lambda_j}{(\lambda_i-\lambda_j)(d_i-d_j)} \cdot \prod_{i=1}^{k}\frac{d_i^{N-p}}{\lambda_i^N} \cdot$$

$$\prod_{i=k+1}^{p}\frac{d_i^{N-p}}{\lambda^N} \cdot \prod_{i=1}^{k}\prod_{j=k+1}^{p}\frac{\lambda_i\lambda}{(\lambda_i-\lambda)(d_i-d_j)} \cdot \prod_{i=1}^{p-1}\prod_{j=i+1}^{p}(d_i-d_j)^2 \tag{3.15}$$

This asymptotic distribution function is still in a relatively complicated form. To get a further simplified expression which enables us to study the behavior of the eigenvalues in a more standardized form, a set of normalized eigenvalues are defined by normalizing the difference between each sample eigenvalue and its corresponding true eigenvalue as

$$\eta_i = N^{1/2}\left(\frac{d_i}{\lambda_i} - 1\right), \quad i = 1, \ 2, \ ..., \ p \tag{3.16}$$

where $\lambda_i = \lambda$, for $i = k+1, \ k+2, \ ..., \ p$. To derive the asymptotic distribution of these normalized sample eigenvalues, we first rearrange the distribution function given by Equation (3.15) to a more standard form in which the influence between eigenvalues with different values is presented more clearly, and therefore can be converted to new variables more easily.

Corollary 3.1 *Suppose* $S = N\hat{\Sigma}$ *has the complex Wishart distribution* $W_p(N, \Sigma)$*, and the eigenvalues of* $\hat{\Sigma}$ *and* Σ *are* $d_1 > d_2 > ... > d_p$ *and* $\lambda_1 > \lambda_2 > ... > \lambda_k > \lambda_{k+1} = ... = \lambda_p = \lambda$ *respectively. Then the asymptotic probability density function of* $d_1 > d_2 > ... > d_p$ *given by*

Theorem 3.1 may be rearranged as

$$f(d_1, \ d_2, \ \ldots, \ d_p|\lambda_1, \lambda_2, \ldots, \lambda_k, \lambda) = \frac{N^{pN-k(2p-k-1)/2}\pi^{p(p-1)-k(k+1)/2}\tilde{\Gamma}_k(p)}{\tilde{\Gamma}_p(N)\tilde{\Gamma}_p(p)} \cdot$$

$$\prod_{i=1}^{k}\left[\frac{d_i^{N-p}}{\lambda_i^{N-p+1}} \cdot \exp(-\frac{N \cdot d_i}{\lambda_i})\right] \cdot \prod_{i=1}^{k-1}\prod_{j=i+1}^{k}\frac{d_i - d_j}{\lambda_i - \lambda_j} \cdot \prod_{i=1}^{k}\prod_{j=k+1}^{p}\frac{d_i - d_j}{\lambda_i - \lambda} \cdot$$

$$\prod_{i=k+1}^{p}\left[\frac{d_i^{N-p}}{\lambda^{N-k}} \cdot \exp(-\frac{N \cdot d_i}{\lambda})\right] \cdot \prod_{i=k+1}^{p-1}\prod_{j=i+1}^{p}(d_i - d_j)^2 \qquad (3.17)$$

In this expression, the first k distinct eigenvalues and the last $p-k$ eigenvalues with $p-k$ multifold are clearly grouped. The mutual influences between these $k+1$ groups are described by the coupling factors

$$\prod_{i=1}^{k-1}\prod_{j=i+1}^{k}\frac{d_i - d_j}{\lambda_i - \lambda_j}, \quad \prod_{i=1}^{k}\prod_{j=k+1}^{p}\frac{d_i - d_j}{\lambda_i - \lambda}, \quad \prod_{i=k+1}^{p-1}\prod_{j=i+1}^{p}(d_i - d_j)^2 \qquad (3.18)$$

The first factor in Equation (3.18) gives the mutual coupling between the first k distinct eigenvalues. The second one describes the influence of the first k eigenvalues on the $(k+1)$-th group, the last $p-k$ eigenvalues. The last factor in Equation (3.18) reflects the intra-relation of the eigenvalues among the $(k+1)$-th group. It is interesting to notice that because the last $p-k$ eigenvalues are multifold, the corresponding factor has a different form from the factor for the distinct eigenvalues.

Applying the definition of the normalized eigenvalue given by Equation (3.16) to the distribution function given in Corollary 3.1, an asymptotic distribution of the normalized eigenvalues is given by the following theorem.

Theorem 3.2 *Suppose $S = N\hat{\Sigma}$ has the complex Wishart distribution $W_p(N, \Sigma)$, and the eigenvalues of $\hat{\Sigma}$ and Σ are $d_1 > d_2 > \ldots > d_p$ and $\lambda_1 > \lambda_2 > \ldots > \lambda_k > \lambda_{k+1} = \ldots = \lambda_p = \lambda$*

respectively. Define the normalized eigenvalues as

$$\eta_i = N^{1/2}\left(\frac{d_i}{\lambda_i} - 1\right), \quad i = 1, 2, ..., p \tag{3.19}$$

where $\lambda_i = \lambda$, *for* $i = k+1, k+2, ..., p$, *the asymptotic probability density function of* $\eta_1, \eta_2, ..., \eta_p$ *is given by*

$$f(\eta_1, \eta_2, ..., \eta_p|\Sigma) = \prod_{i=1}^{k} \frac{1}{(2\pi)^{1/2}} \exp\left\{-\frac{\eta_i^2}{2}\right\} \cdot$$

$$\prod_{i=k+1}^{p} \frac{1}{(2\pi)^{1/2}\Gamma(p-i+1)} \exp\left\{-\frac{\eta_i^2}{2}\right\} \cdot \prod_{i=k+1}^{p-1} \prod_{j=i+1}^{p} (\eta_i - \eta_j)^2 \tag{3.20}$$

Proof: Apply the variable transform defined in Equation (3.16) on Equation (3.17), and notice the Jacobian for this transform is

$$|J| = \left|\frac{\partial(d_1, d_2, ..., d_p)}{\partial(\eta_1, \eta_2, ..., \eta_p)}\right| = N^{-p/2}\lambda^{p-k}\prod_{i=1}^{k}\lambda_i \,. \tag{3.21}$$

The asymptotic distribution of $\eta_1, ..., \eta_p$ can be written as

$$f(\eta_1, \eta_2, ..., \eta_p|\lambda_1, \lambda_2, ..., \lambda_k, \lambda) = \frac{N^{pN-p^2/2}\pi^{p(p-1)-k(k+1)/2}\tilde{\Gamma}_k(p)\exp(-pN)}{\tilde{\Gamma}_p(N)\tilde{\Gamma}_p(p)} \cdot$$

$$\prod_{i=1}^{k}\left[(1+N^{-1/2}\eta_i)^{N-p}\exp(-N^{1/2}\eta_i)\right] \cdot \prod_{i=1}^{k-1}\prod_{j=i+1}^{k}\left[\frac{N^{-1/2}(\eta_i\lambda_i - \eta_j\lambda_j)}{\lambda_i - \lambda_j} + 1\right] \cdot$$

$$\prod_{i=1}^{k}\prod_{j=k+1}^{p}\left[\frac{N^{-1/2}(\eta_i\lambda_i - \eta_j\lambda)}{\lambda_i - \lambda} + 1\right] \cdot \prod_{i=k+1}^{p}\left[(1+N^{-1/2}\eta_i)^{N-p}\exp(-N^{1/2}\eta_i)\right] \cdot$$

$$\prod_{i=k+1}^{p-1}\prod_{j=i+1}^{p}(\eta_i - \eta_j)^2 \tag{3.22}$$

In Equation (3.22), the coupling factors corresponding to distinct eigenvalues converge to unity at a rate of $O(N^{-1/2})$. By expanding $(1+N^{-1/2}\eta)^N$ and $\exp(-N^{1/2}\eta)$ respectively it can be shown that for large N,

$$(1+N^{-1/2}\eta)^N \exp(-N^{1/2}\eta) = \exp(-\eta^2/2) + O(N^{-1/2}) \tag{3.23}$$

By using the Stirling's formula

$$n! \approx (2\pi n)^{1/2} n^n \exp\{-n\} \tag{3.24}$$

it can be shown that when N is large,

$$\frac{N^{pN-p^2/2}}{\prod_{i=1}^{p}\Gamma(N-i+1)} \exp(-pN) \approx (2\pi)^{-p/2} \tag{3.25}$$

Combining these results and applying them to Equation (3.22), we have the asymptotic distribution of the normalized sample eigenvalues, which completes our proof. □

Note that in the distribution function given by Theorem 3.2, if λ_i is a distinct population eigenvalue then η_i is asymptotically independent of η_j for $j \neq i$ at a rate of $O(N^{-1/2})$, and the limiting distribution of η_i, $i = 1, \ldots, k$ are standard normal. For real variables, this result was first observed by Girshick [25] using the asymptotic theory of maximum likelihood estimates. For the case where Σ has multiple eigenvalues the result was presented by T. W. Anderson [4]. The same conclusion as in Theorem 3.2 can be reached for complex data.

According to this asymptotic independence, the joint distribution of the last $p-k$ normalized eigenvalues can be obtained simply by partitioning the joint distribution function of $\eta_1, \cdots, \eta_p$ and is given by following corollary.

Corollary 3.2 *Suppose $S = N\hat{\Sigma}$ has the complex Wishart distribution $W_p(N, \Sigma)$, and the eigenvalues of $\hat{\Sigma}$ and Σ are $d_1 > d_2 > \ldots > d_p$ and $\lambda_1 > \lambda_2 > \ldots > \lambda_k > \lambda_{k+1} = \ldots = \lambda_p = \lambda$ respectively. Define normalized eigenvalues as*

$$\eta_i = N^{1/2}\left(\frac{d_i}{\lambda_i} - 1\right), \quad i = 1, 2, \ldots, p \tag{3.26}$$

where $\lambda_i = \lambda$, for $i = k+1,\ k+2,\ ...,\ p$, the asymptotic probability density function of the $p-k$ smallest normalized eigenvalues $\eta_{k+1},\ \eta_{k+2},\ ...,\ \eta_p$ is given by

$$f(\eta_{k+1},,...,\eta_p|\Sigma) = \prod_{i=k+1}^{p} \frac{1}{(2\pi)^{1/2}\Gamma(p-i+1)} \exp\left\{-\frac{\eta_i^2}{2}\right\} \cdot \prod_{i=k+1}^{p-1} \prod_{j=i+1}^{p} (\eta_i - \eta_j)^2 \quad (3.27)$$

Obviously, when the number of signals k equals zero, this distribution is the distribution function of the normalized eigenvalues given all population eigenvalues are equal. On the other hand, because this distribution does not depend on the first k eigenvalues, it can also be considered as the distribution function of the normalized eigenvalues of a sample covariance matrix of order $q = p - k$ whose corresponding population eigenvalues are equal. According to this characteristic, we can further write the limiting distribution of the average of the last $p-k$ normalized eigenvalues in a very simple form.

Theorem 3.3 *Suppose $S = N\hat{\Sigma}$ has the complex Wishart distribution $W_p(N, \Sigma)$, and the eigenvalues of $\hat{\Sigma}$ and Σ are $d_1 > d_2 > ... > d_p$ and $\lambda_1 > \lambda_2 > ... > \lambda_k > \lambda_{k+1} = ... = \lambda_p = \lambda$ respectively. Define average eigenvalue of the last $p-k$ eigenvalues as*

$$l = \frac{1}{p-k} \sum_{i=k+1}^{p} d_i \quad (3.28)$$

then the limiting distribution of l is

$$(N(p-k))^{1/2}(l-\lambda)/\lambda \sim G(0,1) \quad (3.29)$$

where $G(0,1)$ stands for the Gaussian distribution with zero mean and unity variance.

The proof of this theorem is enclosed as an appendix to this chapter. The similar result for real data has been given by T. W. Anderson [4]. What we have given here is the extension to complex data.

3.3 The Eigen-threshold (ET) concept

According to Theorem 3.2, the distribution of the last $p-k$ normalized eigenvalues is asymptotically independent of the first k normalized eigenvalues when the last population eigenvalues are equal. The asymptotic joint distribution for the last $p-k$ normalized eigenvalues is given in Corollary 3.2. The marginal distribution functions of each of the normalized eigenvalues can be evaluated from the joint distribution by the following integrations:

$$f(\eta_i) = \int_{-\infty}^{+\infty} \int_{-\infty}^{\eta_{k+1}} \cdots \int_{-\infty}^{\eta_{p-1}} f(\eta_{k+1}, ..., \eta_p|\Sigma) d\eta_p d\eta_{p-1} ... d\eta_{i-1} d\eta_{i+1} ... d\eta_{k+1}$$
$$i = k+1, k+2, ..., p. \qquad (3.30)$$

where $f(\eta_{k+1}, ..., \eta_p|\Sigma)$ is given by Equation (3.27). An example of the marginal distribution functions evaluated by these integrations for the case of $p = 8$, $k = 3$, $N = 100$ is shown in Figure 3.1. It is quite obvious that the distribution of each eigenvalue η_i (and therefore d_i) is well concentrated in a certain region. Using this fact, we may specify this region by an upper threshold and a lower threshold in a symmetric way such that the probability of the eigenvalue falling into the region equals a given value, say, $1-\alpha$. We denote the upper threshold of the i-th eigenvalue η_i by $\eta_i^u(\alpha)$. The eigenvalue will exceed this threshold with probability $\alpha/2$. We call this threshold *upper eigen-threshold* or just *eigen-threshold.* This threshold is distinct from most eigenvalue thresholds used by other authors in that it is not a fixed value, but a function of the eigenvalue index. Therefore, it has the advantage of being adaptable to the measured noise subspace eigenvalues. For the case of $p = 8$, $k = 3$, $N = 100$, $\alpha = 0.10$, the values $\eta_i^u(0.10)$ versus the index i are shown in Figure 3.2.

The eigen-threshold has the following characteristics:

- For normalized eigenvalues $\{\eta_i\}$, the eigen-threshold can be pre-evaluated when N, p, and k are given. It does not depend on the multifold eigenvalue λ.
- For sample eigenvalue $\{d_i\}$, the eigen-threshold can be determined using the definition of $\{\eta_i\}$. However, in the conversion, the multifold eigenvalue λ is required.

Once the eigen-threshold is determined, it can be used for determining the number

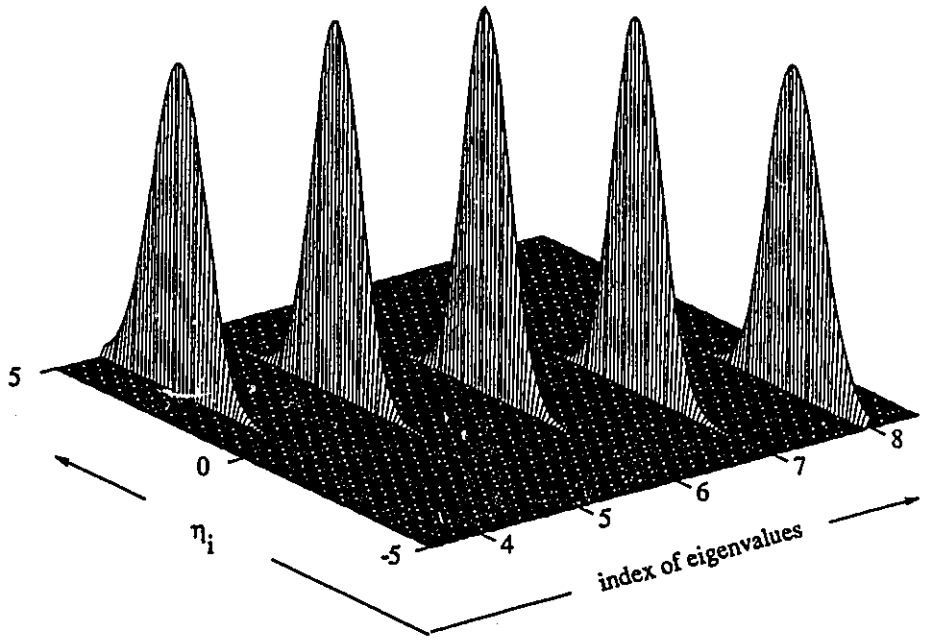

Figure 3.1: Illustration of the distribution of the normalized eigenvalues.

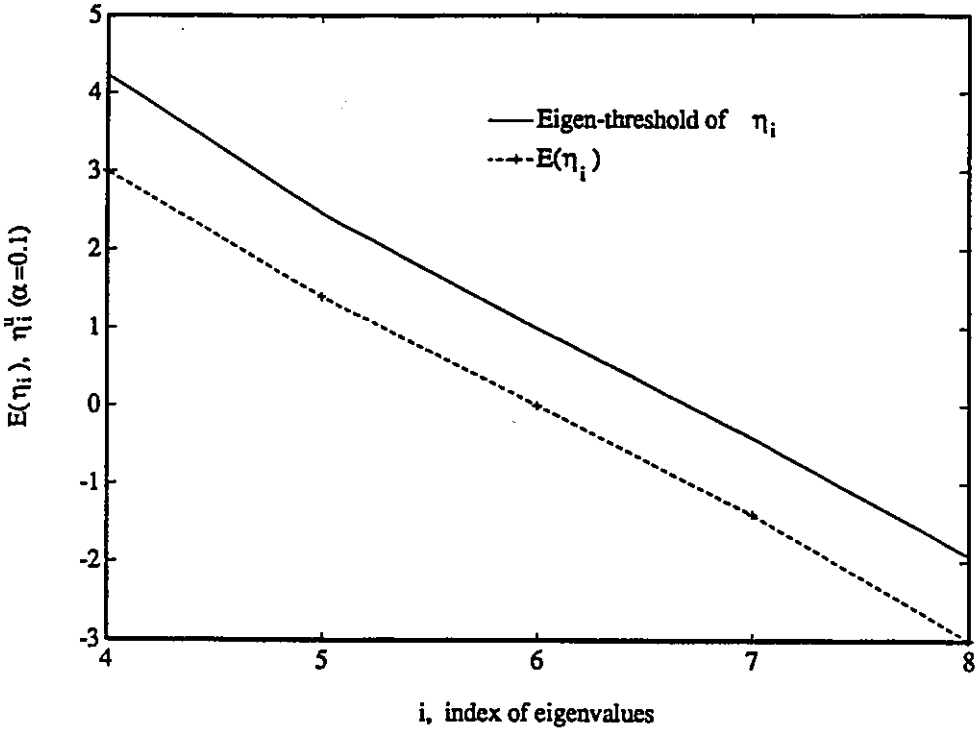

Figure 3.2: Eigen-threshold of the normalized noise eigenvalues.

of signals by hypothesis testing; i.e., by observing whether or not the eigenvalue exceeds its threshold.

3.4 Approximation of the Eigen-threshold

From Equation (3.16), the definition of the normalized eigenvalues $\{\eta_i\}$, we know that the conversion from $\{\eta_i^u\}$ to $\{d_i^u\}$, the upper thresholds of sample eigenvalues $\{d_i\}$, the true multifold eigenvalue λ is required. In practice, the value of the multifold eigenvalue (the noise power in the detection problem) is unknown. Therefore, the eigen-thresholds of the sample eigenvalues $\{d_i\}$ cannot be easily determined from the eigen-thresholds of the normalized versions. In this section, we will discuss a method to approximate the eigen-threshold without knowing the value of the true noise power. A one-step prediction formula is derived.

Let the averaged observed noise-subspace eigenvalues l_i be defined as

$$l_i = \frac{1}{p-i+1}\sum_{j=i}^{p} d_j, \qquad i = k+1...,p \tag{3.31}$$

When $i = k+1$ Equation (3.31) gives l_{k+1}, the maximum likelihood estimate of λ.

From Theorem 3.3 we know that

$$(N(p-k))^{1/2}(l_{k+1}-\lambda)/\lambda \sim G(0,1). \tag{3.32}$$

Define t as the two-direction threshold such that

$$\int_{-t}^{t}(2\pi)^{-1/2}\exp(-u^2/2)du = 1-\alpha. \tag{3.33}$$

From Equations (3.32) and (3.33) we have, with confidence level $1-\alpha$, the confidence interval of the averaged eigenvalue as

$$-t \le (N(p-k))^{1/2}(l_{k+1}-\lambda)/\lambda \le t \tag{3.34}$$

or

$$1 - t(N(p-k))^{-1/2} \le l_{k+1}/\lambda \le 1 + t(N(p-k))^{-1/2}. \tag{3.35}$$

Since we are using the asymptotic distribution of the eigenvalues here, the size of the sample N is assumed to be large enough such that

$$t/N^{1/2} < 1. \tag{3.36}$$

If we assume that the multiplicity of the multifold eigenvalue λ is m, from Equation (3.35) we have

$$1 - t(N \cdot m)^{-1/2} \leq l_{p-m+1}/\lambda \leq 1 + t(N \cdot m)^{-1/2} \tag{3.37}$$

and if we assume the multiplicity of λ is $m+1$, we have,

$$1 - t(N(m+1))^{-1/2} \leq l_{p-m}/\lambda \leq 1 + t(N(m+1))^{-1/2} \tag{3.38}$$

To derive the upper-threshold for the $(p-m)$th observed eigenvalue d_{p-m}, we divide Equation (3.37) by Equation (3.38) and take the right half of the quotient, hence

$$\frac{l_{p-m}}{l_{p-m+1}} \leq \frac{1 + t(N(m+1))^{-1/2}}{1 - t(N \cdot m)^{-1/2}} \ . \tag{3.39}$$

The condition $t/N^{1/2} < 1$ given in Equation (3.36) ensures that the ratio in the right hand side of Equation (3.39) is positive. Notice that l_{p-m} can be expressed in terms of l_{p-m+1} and d_{p-m} as

$$l_{p-m} = \frac{1}{m+1} \sum_{i=p-m}^{p} d_i = \frac{1}{m+1} \left[\sum_{i=p-m+1}^{p} d_i + d_{p-m} \right] = \frac{m}{m+1} l_{p-m+1} + \frac{d_{p-m}}{m+1} \tag{3.40}$$

In Equation (3.40), we have used the fact

$$l_{p-m+1} = \frac{1}{m} \sum_{i=p-m+1}^{p} d_i \ . \tag{3.41}$$

Now, substituting Equation (3.40) into Equation (3.39), we obtain

$$d_{p-m} \leq d^u_{p-m} = \left[(m+1) \frac{1 + t(N(m+1))^{1/2}}{1 - t(N \cdot m)^{-1/2}} - m \right] l_{p-m+1} \tag{3.42}$$

where d^u_{p-m} defined above is the predicted upper threshold value for d_{p-m}.

The usage of this formula is discussed in the following section.

3.5 Hypothesis testing for determining the number of signals

Now we are in a position to introduce a hypothesis testing procedure for k, the number of signals. Our procedure tests q, the multiplicity of the noise eigenvalue. The number of signals is related to q by the relation,

$$k = p - q \ . \tag{3.43}$$

The eigen-threshold concept is applied to this hypothesis testing procedure with the following understanding. If there are k signals and our assumption of the multiplicity of λ is correct, then the $q = (p - k)$ observed noise eigenvalues d_{k+1}, ..., d_p should be below the threshold. As the result of the existence of the signal component, the smallest observed signal eigenvalue $d_k = d_{p-q}$ should exceed the predicted threshold. To determine q (or k) from p possible values requires a multiple hypothesis test. This multiple hypothesis test may be decomposed into a sequence of binary hypothesis tests. In our case we establish a testing procedure as follows:

Define a set of binary hypotheses $\{\mathrm{H}_m\}$, $m = 1, 2, ..., p$ as

$$\bar{\mathrm{H}}_m : \quad k < p - m \tag{3.44}$$

$$\mathrm{H}_m : \quad k = p - m \tag{3.45}$$

The test procedure starts with $m = 1$, where m is the assumed multiplicity of the noise eigenvalue λ. For each m, we accept H_m or $\bar{\mathrm{H}}_m$ according to

$$d_{p-m} \underset{\bar{\mathrm{H}}_m}{\overset{\mathrm{H}_m}{\gtrless}} d^u_{p-m} \tag{3.46}$$

where d^u_{p-m} is the threshold of the $(p - m)$-th observed eigenvalue given by Equation (3.42).

If H_m is accepted, stop testing, and assign $\hat{k} = p - m$. If $\bar{\mathrm{H}}_m$ is accepted, put $m = m + 1$, continue testing until either H_1 is accepted or $m = p$.

The application of this procedure is simple. However, as a detection method there are two points which require further discussion. The first is the choice of t in Equation (3.42). The second is the error performance of this hypothesis testing procedure which is based on the prediction formula (3.42). In the next chapter, the answers for both these questions are given.

3.6 Appendix

This section is for the proof of the Theorem 3.3.

From Corollary 3.2 we know that:

1. the last $p-k$ normalized eigenvalues η_{k+1}, η_{k+2}, ..., η_p are asymptotically independent of the first k distinct eigenvalues and,
2. the marginal joint distribution of these $p-k$ normalized eigenvalues is the same as that of the eigenvalues of a $p-k$ variate process which has all its population eigenvalues equal.

Therefore, we can change our proof to the asymptotic distribution of the equivalent $p-k$ variate process.

Consider a q variate complex Gaussian process $\boldsymbol{x}$, where $q = p-k$, with zero means and a covariance matrix whose eigenvalues are equal. Without losing generality we assume the true covariance matrix equals $\lambda \boldsymbol{I}$.

Define the sample covariance matrix of this process formed from a set of N samples $\boldsymbol{x}_1$, $\boldsymbol{x}_2$, ... $\boldsymbol{x}_N$ of $\boldsymbol{x}$ by,

$$\hat{\boldsymbol{\Sigma}} = \frac{1}{N}\sum_{i=1}^{N} \boldsymbol{x}_i \boldsymbol{x}_i^H \tag{3.47}$$

and denote the eigenvalues of this matrix by d_i, $i = 1, ..., q$. What we need to prove is for large N

$$\frac{\sqrt{qN}}{\lambda}\left(\frac{1}{q}\sum_{i=1}^{q} d_i - \lambda\right) \sim \mathrm{G}(0, 1) \tag{3.48}$$

where G(0, 1) stands for the normal distribution. From matrix theory we know that

$$\sum_{i=1}^{q} d_i = \mathrm{tr}(\hat{\Sigma}) \tag{3.49}$$

where tr(·) indicates the trace operation of the matrix argument, that is, the sum of the diagonal elements which are denoted by $\hat{\sigma}_{ii}$, $i = 1, ..., q$. The quantities $\hat{\sigma}_{ii}$ can be expressed in terms of the sampled data as

$$\hat{\sigma}_{ii} = \sum_{j=1}^{N} \mathrm{Re}(x_{ij})^2 + \sum_{j=1}^{N} \mathrm{Im}(x_{ij})^2 \tag{3.50}$$

where $\mathrm{Re}(x_{ij})$ and $\mathrm{Im}(x_{ij})$ are the real and imaginary part of x_{ij}, the j-th sample of the i-th element of the random process. From the definition of the complex Gaussian distribution we know that $\mathrm{Re}(x_{ij})$ and $\mathrm{Im}(x_{ij})$ are i.i.d. random processes which follow real Gaussian distribution $\mathrm{G}(0, \lambda/2)$. Therefore the sum of these diagonal elements can be written as

$$L = \sum_{i=1}^{q} \sum_{j=1}^{2N} y_j^2 = \sum_{i=1}^{2qN} y_i^2 \tag{3.51}$$

where y_i follows distribution $\mathrm{G}(0, \lambda/2)$. So we can write

$$2L/\lambda \sim \chi^2_{2qN} \tag{3.52}$$

where χ^2_{2qN} denotes the χ^2-distribution with $2qN$ degrees of freedom. The first and second moments of this χ^2 distribution are known to be

$$\mu_1 = 2qN \tag{3.53}$$

$$\mu_2 = 4qN \tag{3.54}$$

It is well known that the characteristic function of χ^2_υ-distribution is [37]

$$\phi(t) = (1 - 2it)^{-\upsilon/2} \tag{3.55}$$

Shifting the χ^2_υ by its mean value υ and scaling it by the square root of its variance 2υ , the c.f. becomes

$$\phi(t) = \exp\left\{-\frac{\upsilon it}{\sqrt{2\upsilon}}\right\} \cdot \left(1 - \frac{2it}{\sqrt{2\upsilon}}\right)^{-\upsilon/2} \tag{3.56}$$

and

$$\begin{aligned}\log \phi(t) &= \frac{-vit}{\sqrt{2v}} - \frac{v}{2}\left[\frac{-2it}{\sqrt{2v}} - \frac{1}{2}\left(\frac{2it}{\sqrt{2v}}\right)^2 - \frac{1}{3}\left(\frac{2it}{\sqrt{2v}}\right)^3 - \frac{1}{4}\left(\frac{2it}{\sqrt{2v}}\right)^4 - \dots\right] \\ &= -\frac{1}{2}t^2 + O((2v)^{-1/2}) \end{aligned} \tag{3.57}$$

This means that when v goes to infinity, the c.f. approaches $\exp\{-t^2/2\}$. Recognizing that this is the c.f. of the normal distribution with zero mean, we arrive at the conclusion that the limiting distribution of χ^2_v is normal distribution $\mathrm{G}(v,\, 2v)$.

That is, when N goes to infinity, using Equations (3.52) (3.53)(3.54) we have

$$2L/\lambda \;\sim\; \mathrm{G}(2qN,\, 4qN) \tag{3.58}$$

Define the average of the sample eigenvalues (or the diagonal elements) of $\hat{\Sigma}$ as

$$l = \frac{L}{qN} \tag{3.59}$$

From Equation (3.58), we can write

$$l \;\sim\; \mathrm{G}\left(\lambda,\, \frac{\lambda^2}{qN}\right) \tag{3.60}$$

By shifting and scaling this distribution, we have

$$\sqrt{qN}\left(\frac{l-\lambda}{\lambda}\right) \;\sim\; \mathrm{G}(0,\, 1) \tag{3.61}$$

That completes our proof. □

Chapter 4

Performance analysis of the ET method

4.1 Composition of the total detection error

According to the definitions of a correct detection and a detection error given in Chapter 2, the performance of a detection criterion can be characterized by the probability of correct detection P_D, or by the probability of error P_e. The probabilities P_D and P_e are related by

$$P_D = 1 - P_e \ . \tag{4.1}$$

The probability of error can be further decomposed to the probability of false alarm P_F and the probability of missing P_M. This decomposition can be expressed as

$$P_e = P_M + P_F \ . \tag{4.2}$$

Consider the hypothesis testing procedure discussed in the last section. The meaning of the terms *correct detection, false alarm*, and *missing* can be defined as follows. Suppose that there are k signals impinging upon the array, and at the m-th step, the hypothesis H_m, or equivalently $\hat{k} = p - m$, is accepted. We say the signals are correctly detected if $\hat{k} = k$. Otherwise, we say a detection error has occurred. This error is classified as a false alarm or a miss according to whether $\hat{k} > k$ or $\hat{k} < k$. Whenever $\hat{k} > k$, we say a false alarm error has occurred. Whenever $\hat{k} < k$, we say a miss has occurred.

We examine the hypothesis testing procedure to obtain an expression for the probability of error. At the m-th stage of testing for $m = 1, 2, ..., p-1$, we apply the test expressed by Equation (3.46). There are two possible outcomes which are represented by the following events:

$$\begin{aligned} A_m &: d_{p-m} > d^u_{p-m} \\ \bar{A}_m &: d_{p-m} \leq d^u_{p-m} \, . \end{aligned}$$

We denote the probability of these two events happening at the m-th stage by $\mathrm{P}(A_m)$ and $\mathrm{P}(\bar{A}_m)$ respectively.

Now, for $1 \leq m \leq p-k-1$, if A_m happens, the test will stop and we will conclude that $p-m$ signals exist, where $p-m > k$. This constitutes a false alarm. Thus, we can formulate the probability of false alarm as

$$P_F = \mathrm{P}(A_1 \cup A_2 \cup ... \cup A_{p-k-1}) \tag{4.3}$$

Since A_m is an impossible event unless $\bar{A}_i$, for all $i < m$ happen, then we can write Equation (4.3) as

$$\begin{aligned} P_F &= \mathrm{P}(A_1) + \mathrm{P}(\bar{A}_1 \cap A_2) + \mathrm{P}(\bar{A}_1 \cap \bar{A}_2 \cap A_3) + ... \\ &\quad + \mathrm{P}(\bar{A}_1 \cap \bar{A}_2 \cap ... \cap \bar{A}_{p-k-2} \cap A_{p-k-1}) \\ &= \mathrm{P}(A_1) + \sum_{m=2}^{p-k-1} \mathrm{P}\left(A_m \cap \left(\cap_{n=1}^{m-1} \bar{A}_n\right)\right) \end{aligned} \tag{4.4}$$

Equivalently, the probability of false alarm can also be expressed by

$$P_F = 1 - \mathrm{P}\left(\cap_{n=1}^{p-k-1} \bar{A}_n\right). \tag{4.5}$$

If the test goes on until $m = p-k$, and if A_{p-k} happens, we will conclude that k signals exist, which means that we have detected the number of signals correctly. This will happen only if no false alarm occurs. Thus the probability of a correct detection happening is

$$P_D = (1 - P_F)\mathrm{P}(A_{p-k}) \tag{4.6}$$

Finally, if the test goes on until $p-k+1 \leq m \leq p$, implying that no false alarm nor correct detection has happened, then we have the situation in which $k-p+m$ signals have been missed when A_m happens. We further note that since $A_{m+1} \subset \bar{A}_m$, missing $(k-p+m)$ for $m > p-k+1$ implies $(k-p+m-1)$ signals have already been missed which further implies that at least one signal has already been missed. But missing at least one signal occurs if $\bar{A}_{p-k}$ happens; thus, the probability of missing can be written as

$$P_M = (1-P_F)\mathrm{P}(\bar{A}_{p-k}) = (1-P_F)(1-\mathrm{P}(A_{p-k})) \tag{4.7}$$

4.2 Probability of false alarm

To evaluate the probability of false alarm, as shown in Equation (4.5), we need to evaluate the probability of all A_m not happening for $m = 1, ..., p-k-1$. In other words, we need to evaluate the probability of Equation (3.42) not being violated when $m \leq p-k-1$. But Equations (3.42) and (3.39) are equivalent events; thus, we can utilize the eigenvalue ratio on the left hand side of Equation (3.39) for the calculation of P_F. Let us denote this eigenvalue ratio as

$$\rho_m = l_{p-m}/l_{p-m+1}, \qquad m = 1, ..., p-k-1 \tag{4.8}$$

This ratio is compared with a threshold γ_m given by the right hand side of Equation (3.39), i.e.,

$$\gamma_m(t) = \frac{1+t(N(m+1))^{-1/2}}{1-t(N\cdot m)^{-1/2}} \tag{4.9}$$

which, for given m and N, is a function of the parameter t. When $\rho_m \leq \gamma_m(t)$, then $\bar{A}_m$ occurs. Hence, the probability can be expressed as

$$\mathrm{P}\left(\cap_{n=1}^{m} \bar{A}_n\right) = \mathrm{P}(\rho_1 \leq \gamma_1(t), \cdots, \rho_{p-k-1} \leq \gamma_{p-k-1}(t)) \tag{4.10}$$

which can be defined by a cumulative distribution function

$$\mathrm{F}_{\rho_1 \cdots \rho_{p-k-1}}(\gamma_1(t), \cdots, \gamma_{p-k-1}(t)) = \mathrm{P}(\rho_1 \leq \gamma_1(t), \cdots, \rho_{p-k-1} \leq \gamma_{p-k-1}(t)) \tag{4.11}$$

It can be shown (in the Appendix of this chapter) this distribution function is given by

$$\begin{aligned} \mathrm{F}(t) &= \mathrm{F}_{\rho_1 \cdots \rho_{p-k-1}}(\gamma_1(t), \cdots, \gamma_{p-k-1}(t)) \\ &= \mathrm{P}(\rho_1 \le \gamma_1(t), \cdots, \rho_{p-k-1} \le \gamma_{p-k-1}(t)) \\ &= \int_{-\infty}^{\gamma_{p-k-1}(t)} \int_{-\infty}^{\gamma_{p-k-2}(t)} \cdots \int_{-\infty}^{\gamma_1(t)} \int_{-\infty}^{\infty} |y_1^{p-k-1} \rho_1^{p-k-2} \cdots \rho_{p-k-2}| \\ &\quad f_y(\rho_{p-k-1}\rho_{p-k-2}\cdots\rho_1 y_1, \rho_{p-k-2}\cdots\rho_1 y_1, \cdots, \rho_1 y_1, y_1 | \Sigma) \\ &\quad d\rho_{p-k-1} d\rho_{p-k-2} \cdots d\rho_1 dy_1 \end{aligned} \tag{4.12}$$

where f_y is given by Equation (4.31) and has non-zero values only in region R_y which is given by Equation (4.35).

It should be pointed out that both the integrand and the integration region in Equation (4.12) are quite complicated, and very difficult to evaluate analytically. However, they can still be evaluated by numerical methods. In Figure 4.1, a curve shows the results of evaluations of $P_F = 1 - \mathrm{F}(t)$ under the condition $N = 100$, for $p = 8$, $k = 3$ (therefore, the noise dimension equals $p - k = 5$). The results for $N = 500$ is also evaluated and is plotted on Figure 4.2 to show the insensitivity of the distribution to changes in number of snapshots. For different N values, we can find that P_F is almost the same.

4.3 Probability of missing

As shown in Equation (4.7) the probability of missing depends on the probability of missing at least one signal, i.e., in the $(p-k)$-th step of hypothesis testing, $d_k < d_k^u$. Now, from Equation (3.42)

$$\begin{aligned} d_k^u &= \left[(p-k+1) \frac{1 + t(N(p-k+1))^{-1/2}}{1 - t(N(p-k))^{-1/2}} - (p-k) \right] l_{k+1} \\ &= a \cdot l_{k+1} \end{aligned} \tag{4.13}$$

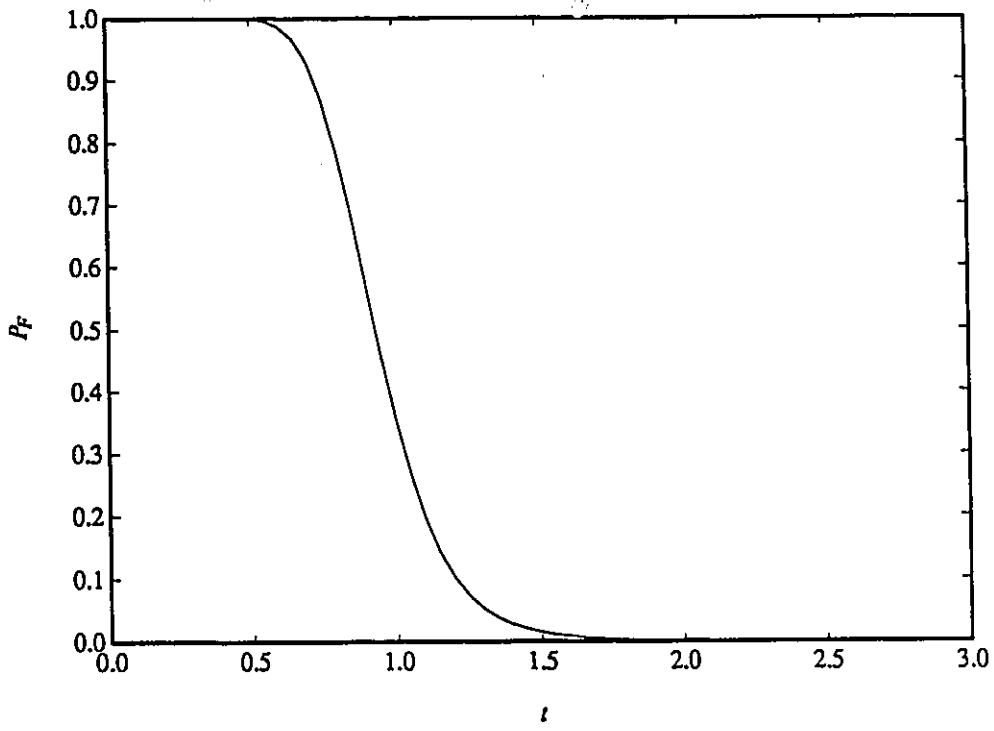

Figure 4.1: $P_F(t)$ for $N = 100$, $p = 8$, $k = 3$.

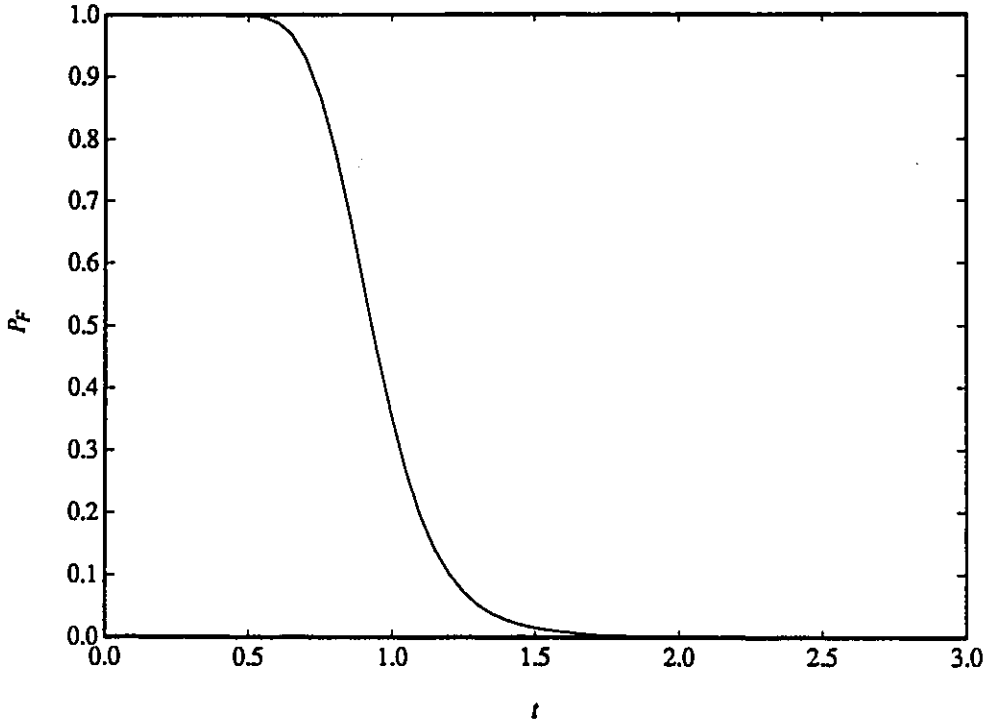

Figure 4.2: ($P_F(t)$ for $N = 500$, $p = 8$, $k = 3$.

where a is the prediction coefficient corresponding to the terms in the brackets of Equation (4.13), i.e., d_k^u is a linear function of l_{k+1}, the maximum likelihood estimate of the noise subspace eigenvalue. Also, d_k is the observed k-th eigenvalue after N snapshots. From the hypothesis testing procedure given in last chapter and from Equation (4.13), we know that the probability of missing is determined by the value of d_k relative to that of l_{k+1}. The larger is d_k compared to l_{k+1}, the smaller is the probability of missing. All the signal and noise parameters apply their influence on the probability of missing through changing the relative value of d_k when the prediction coefficient a is given. Therefore, it is reasonable to infer that the probability of missing at least one signal depends on the ratio of $\mathrm{E}[d_k]$ and $\mathrm{E}[l_{k+1}]$. Let us denote this ratio by r, i.e.,

$$r = \mathrm{E}[d_k]/\mathrm{E}[l_{k+1}] \tag{4.14}$$

The signal and noise parameters influence this ratio in different ways. The SNR changes this ratio in a straight forward manner. The lower is the value of SNR, the less significant is the signal component in d_k, and the closer to unity is the ratio r; therefore, the higher is the probability of missing. Other factors influence the ratio through variation of the signal subspace eigenvalues. Closely located signals, large differences in signal power levels, or small numbers of snapshots usually make the signal subspace eigenvalues disperse over a larger range than that with well separated, equally powered signals, or with a larger number of snapshots. When the signal subspace eigenvalues disperse over a larger range, the value of d_k becomes smaller (so does the ratio r) because d_k is the smallest among these signal subspace eigenvalues.

To evaluate $\mathrm{P}(d_k < d_k^u)$, we have to find the probability density functions (PDF) of d_k and d_k^u, or equivalently, the PDF of $d_k/\mathrm{E}[l_{k+1}]$ and $d_k^u/\mathrm{E}[l_{k+1}]$. Now, it is well-known [4][44]

$$(d_k - \lambda_k) \sim \mathrm{G}(\mu_N, \lambda_k^2/N + \sigma_N^2) \tag{4.15}$$

where, $\mu_N = O(N^{-1})$ and $\sigma_N^2 = O(N^{-2})$. Under the condition of large N, both μ_N and σ_N^2 tend to zero. Therefore, we can write the following approximate asymptotic behavior such that

$$(d_k - \mathrm{E}[d_k])/\mathrm{E}[d_k] \sim \mathrm{G}(0, 1/N) \tag{4.16}$$

Using Equations (4.14) and (4.16) we can write

$$\frac{d_k}{\mathrm{E}[l_{k+1}]} = \frac{d_k}{\mathrm{E}[d_k]} \cdot \frac{\mathrm{E}[d_k]}{\mathrm{E}[l_{k+1}]} = r \cdot \frac{d_k}{\mathrm{E}[d_k]} \sim \mathrm{G}(r, \frac{r^2}{N}) \tag{4.17}$$

Thus if we denote the random variable $d_k/\mathrm{E}[l_{k+1}]$ by z, then the PDF of z is given by

$$f_z(z) = (2\pi)^{-1/2}\sigma_z^{-1}\exp\{-(z-r)^2/(2\sigma_z^2)\} \tag{4.18}$$

where

$$\sigma_z = r/N^{1/2} \tag{4.19}$$

We now turn our attention to the random variable d_k^u, which as shown in Equation (4.13), is a linear function of l_{k+1}. The same argument leading to Equation (4.16) can be applied here by substituting $\mathrm{E}[l_{k+1}]$ for λ in Theorem 3.3 so that the approximate asymptotic behavior of l_{k+1} is

$$(N(p-k))^{1/2}(l_{k+1} - \mathrm{E}[l_{k+1}])/\mathrm{E}[l_{k+1}] \sim \mathrm{G}(0,1) \tag{4.20}$$

Using Equations (4.13) and (4.20), we have

$$d_k^u/\mathrm{E}[l_{k+1}] = a \cdot l_{k+1}/\mathrm{E}[l_{k+1}] \sim \mathrm{G}(a, a^2/(N(p-k))) \tag{4.21}$$

Thus, if we denote the random variable $d_k^u/\mathrm{E}[l_{k+1}]$ by x, then the PDF of x is

$$f_x(x) = (2\pi)^{-1/2}\sigma_x^{-1}\exp\{-(x-a)^2/(2\sigma_x^2)\} \tag{4.22}$$

where

$$\sigma_x = a/(N(p-k))^{1/2} \tag{4.23}$$

Notice that d_k is asymptotically independent to other sample eigenvalues, so z is independent to x. Therefore, the probability of missing at least one signal can be rewritten as

$$\begin{aligned} \mathrm{P}(\bar{A}_{p-k}) &= P(d_k < d_k^u) = P(z < x) \\ &= \int_0^\infty (2\pi\sigma_x\sigma_z)^{-1}\exp\{-(x-a)^2/(2\sigma_x^2)\}\int_0^x \exp\{-(z-r)^2/(2\sigma_z^2)\}dzdx \end{aligned} \tag{4.24}$$

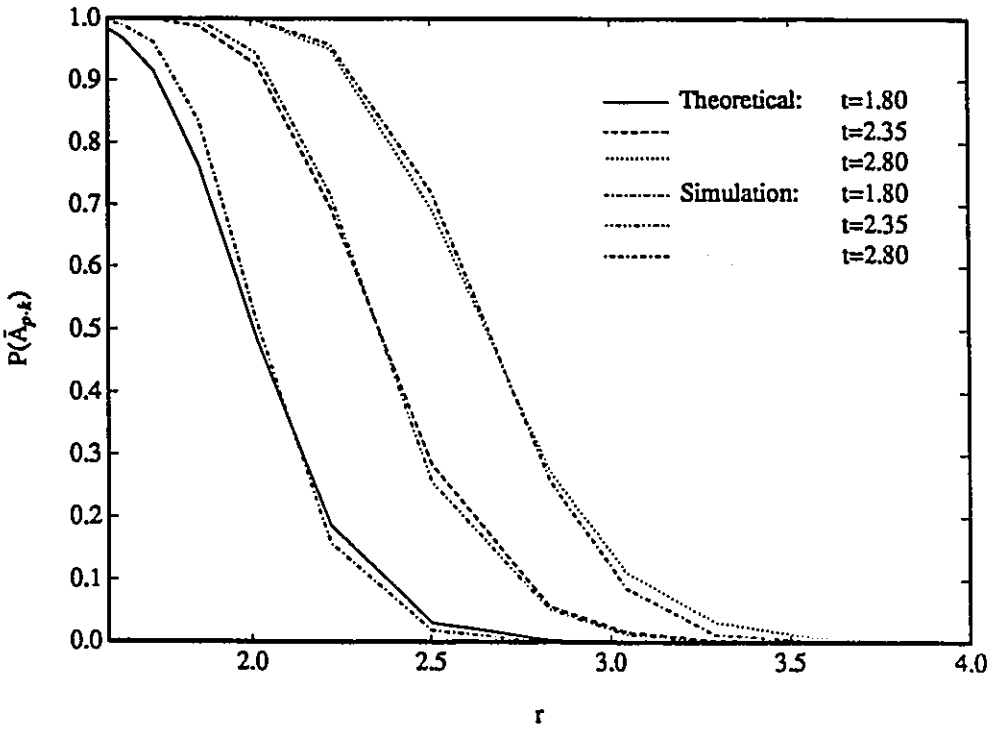

Figure 4.3: $P(\tilde{A}_{p-k})$ vs. r of the Eigen-threshold method p=8, k=3, N=100, 500 trials averaged in the simulation.

This probability is plotted against r for various values of t in Figure 4.3 in which $p = 8$, $k = 3$, $N = 100$. The values of t chosen are 1.8, 2.35, and 2.8. To verify that these theoretical curves are accurate, simulations are performed on the computer. The same parameters p, k, and N, are employed. With the same parameters and SNR, the received signal is created by simulation according to the signal model described by Equation (1.5). The observed covariance matrix $\hat{\Sigma}$ is obtained after taking 100 snapshots of the simulated received signal. The ratio r can be obtained by solving for the least signal eigenvalue of $\hat{\Sigma}$ and the average noise subspace eigenvalue. These values are then averaged over 500 trials and the ratio of their averages calculated. With the various values of t, the frequencies of the event $\bar{A}_{p-k}$ happening in 500 trials are recorded. The SNR is then varied so that the same procedure can be repeated for another value of r. The results obtained by simulation are also shown in Figure 4.3. It can be observed that the theoretical and the simulation results are in close agreement.

The total probability of missing can now be evaluated using Equation (4.7) and the total probability of error can be evaluated using Equation (4.2).

4.4 Selection of the parameter t in the ET method

The question that immediately arises is how to choose t, and whether there is an optimum value of t. We can choose t according to whether the probability of false alarm is required to satisfy a certain allowable level, or the average probability of total error is required to be minimum.

If we require the rate of false alarm to satisfy a specified level, the corresponding t can be determined from the curve of P_F against t shown in Figure 4.1 which is calculated by Equation (4.5). For example, $t(P_F = 1.5\%) \approx 1.5$, and $t(P_F = 0.85\%) \approx 1.6$.

If it is desired that the average probability of total error is minimum over a specified SNR range, we can locate the optimum value of t by minimizing quantity

$$\min_t \bar{P}_e(t; R_{SN}) = \min_t \frac{1}{R_{SN}} \int_{R_{SN}} P_e d\rho_{SN} \tag{4.25}$$

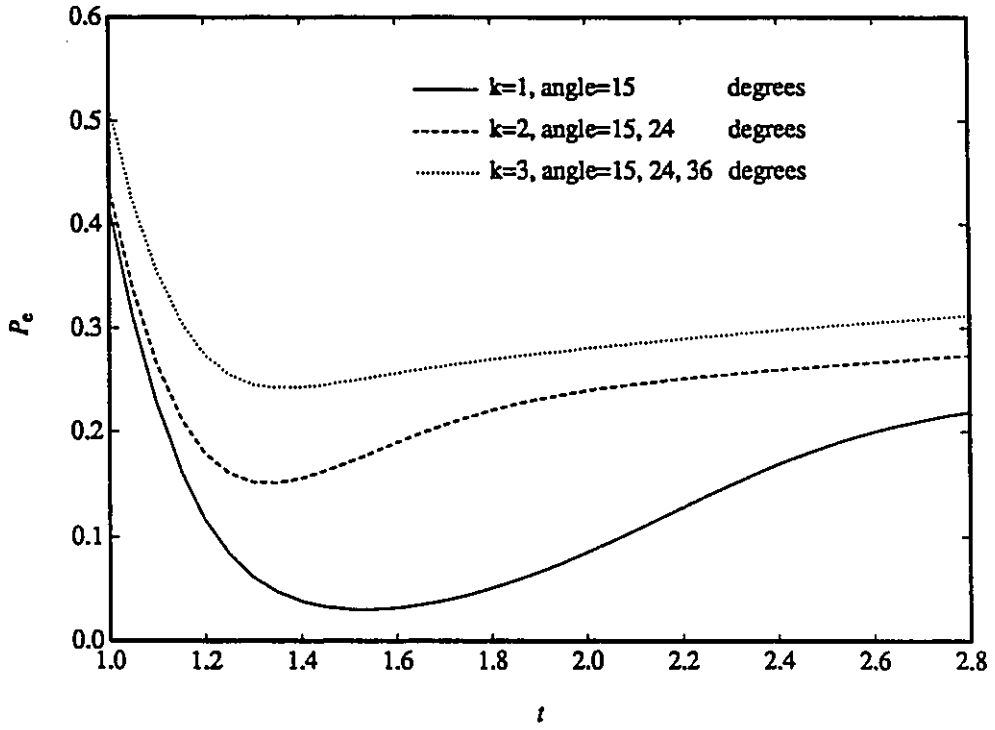

Figure 4.4: Average probability of error vs. t for the ET method. p=8, N=100. 500 trials averaged in the simulation. SNR interval = -10 dB to 20 dB.

where, ρ_{SN} is the SNR, R_{SN} is the range of SNR in which we are interested. In the following, we choose R_{SN} to be the range of SNR from -10 dB to 20 dB. To calculate P_e in the integral of Equation (4.25), according to Equations (4.7) and (4.2), $\mathrm{P}(\bar{A}_{p-k})$ and P_F need to be evaluated. Since $\mathrm{P}(\bar{A}_{p-k})$ is originally evaluated as a function of r, the ratio of $\mathrm{E}[d_k]$ to $\mathrm{E}[l_{k+1}]$, in Equation (4.25) is required to be a function of SNR; therefore, a conversion of the variables is necessary. This is done by using the same method described in Section 4.3 to estimate $\mathrm{E}[d_k]$ and $\mathrm{E}[l_{k+1}]$ with given values of SNR, p, k, N, and angles of arrival. Here, for convenience, we make use of the insensitivity of P_F to changes in N, p and k by using the same $P_F(t)$ curve shown in Figure 4.1 for different numbers of signals. By using Equation (4.7) to calculate P_M from $P_(\bar{A}_{p-k})$, and using Equation (4.2) to obtain P_e by combining P_M and P_F, then, $\bar{P}_e(t; R_{SN})$ can be evaluated by Equation (4.25). In Figure 4.4 three curves of $\bar{P}_e(t; R_{SN})$, where $R_{SN} = (-10, 20)$ dB, are shown against t for the case of $p = 8$, $N = 100$ and different numbers of signals. The numbers of signals used here are $k = 1$, 2, and 3. The angles of arrival are 15, 24, and 36 degrees. From Figure 4.4, it can be seen that for $k = 1$, as t increases from unity, P_e decreases very quickly and is minimum when $t \approx 1.5$. Further increases in t increase P_e, but at a slower rate than the initial decrease. For $k \geq 2$, the initial decrease of P_e is also very steep, but after a minimum P_e is reached, a further increase in t only increases P_e slightly. Also, for $k \geq 2$, the value of t at which the minimum P_e is achieved is lower in value than that for $k = 1$. Since in general, we do not know how many signals are there, it would be safe to choose $t \approx 1.5$, so that even if $k > 1$, the P_e with this choice of t is not much higher than the real minimum P_e.

4.5 Simulation results

Results of three simulations are given in this section to illustrate the performance of the eigen-threshold method.

4.5.1 Performance of the ET method with respect to different t values

The first simulation is for checking the error performance of the eigen-threshold method. The conditions for this simulation are listed in Table 4.1. The simulation results are plotted in Figure 4.5. The theoretical curves calculated by Equations (4.5)(4.7) and (4.2) are plotted in Figure 4.6. Signals are assumed to be of equal power, the SNR is defined as the ratio of the power of one signal to σ_n^2, the power of noise. We find that the error rates under high SNR and the position of the threshold in P_e–SNR relations in these two plots are in close agreement.

4.5.2 Comparison of the ET method with AIC and MDL

The second simulation is for comparing the performance of the eigen-threshold method under different t values. The results are plotted in Figure 4.7 and the conditions used are listed in Table 4.2. The result shows that the probability of false alarm can be quantitatively controlled by adjusting t. Such a characteristic provides the detection criterion with a valuable degree of freedom, which may be used for trading off the probability of false alarm at high SNR and the probability of missing under low SNR to make the total error probability as low as possible. It is interesting to notice that, as we expected in theoretical analysis, when t is larger than 1.5 the probability of false alarm under high SNR conditions approaches zero.

In the third simulation, the eigen-threshold method is compared with the MDL and the AIC criterion. The conditions used for this simulation are the same as those for the second simulation. The results are shown in Figure 4.8. It is well-known [70][65] that the AIC emphasizes better performance under relatively low SNR at the expense of being

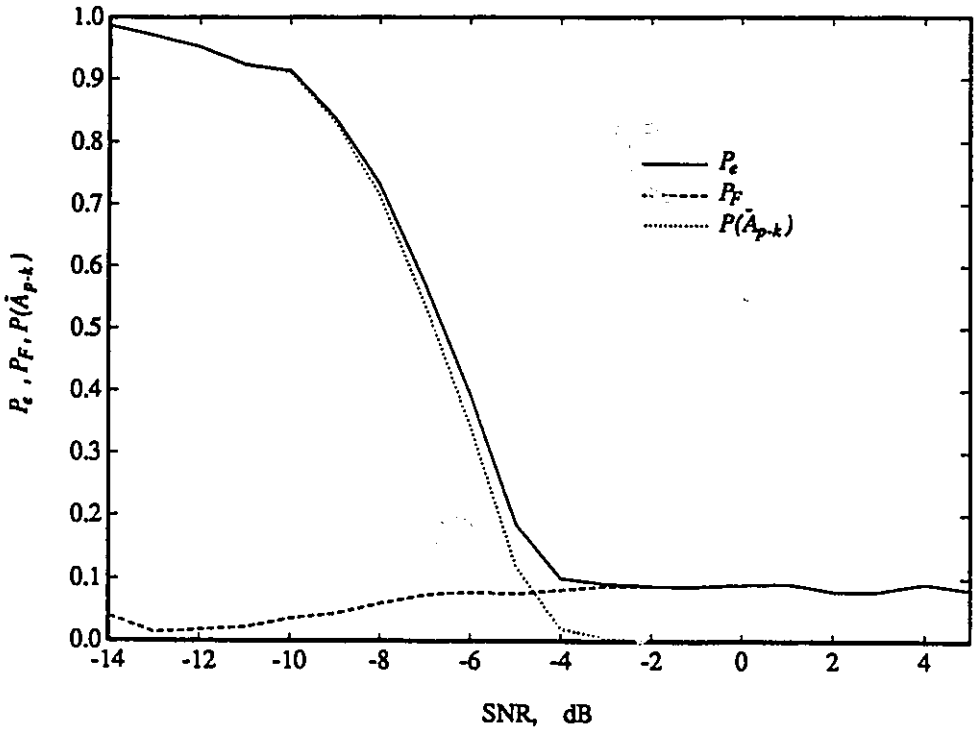

Figure 4.5: Probability of detection error vs. SNR for ET method (Simulation). $p = 8$, $k = 3$, $N = 100$, $t = 1.20$, trials=500.

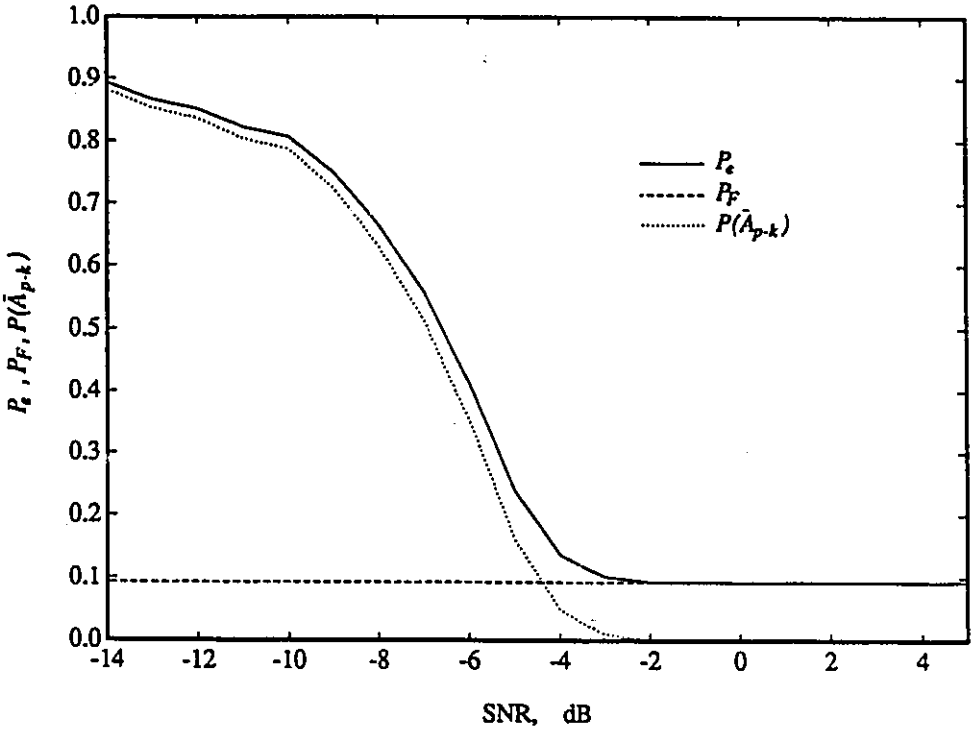

Figure 4.6: Probability of detection error vs. SNR for ET method (Theoretical). $p = 8$, $k = 3$, $N = 100$, $t = 1.20$.

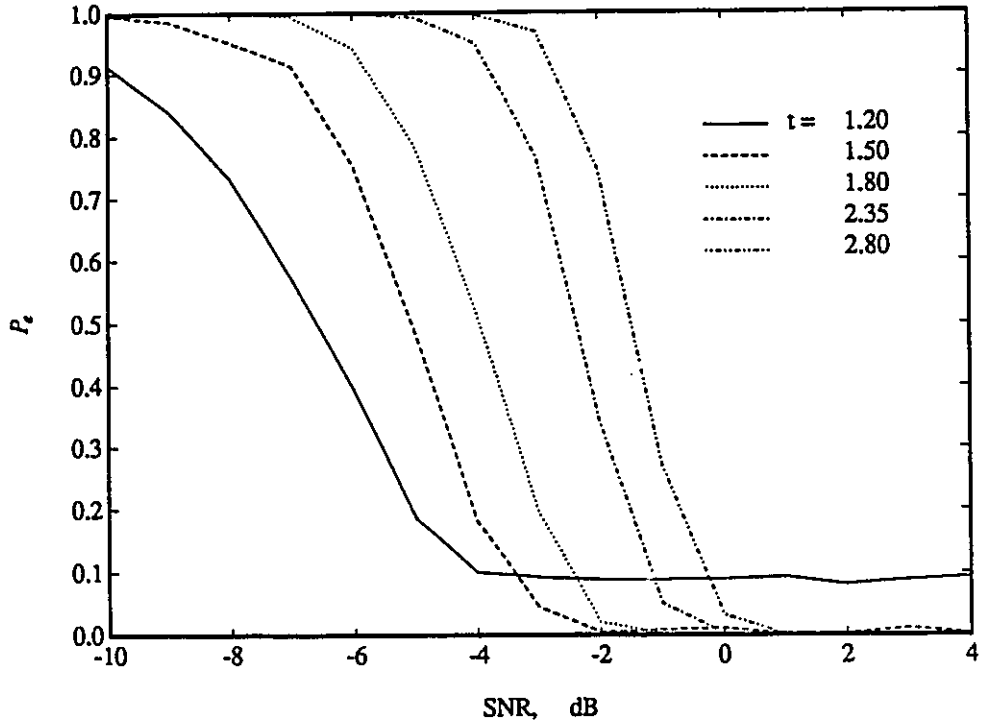

Figure 4.7: Probability of detection error vs. SNR for ET method under different t values. $p = 8$, $N = 100$, $k = 3$, Angles=15, 24, 36 degrees, trials=200.

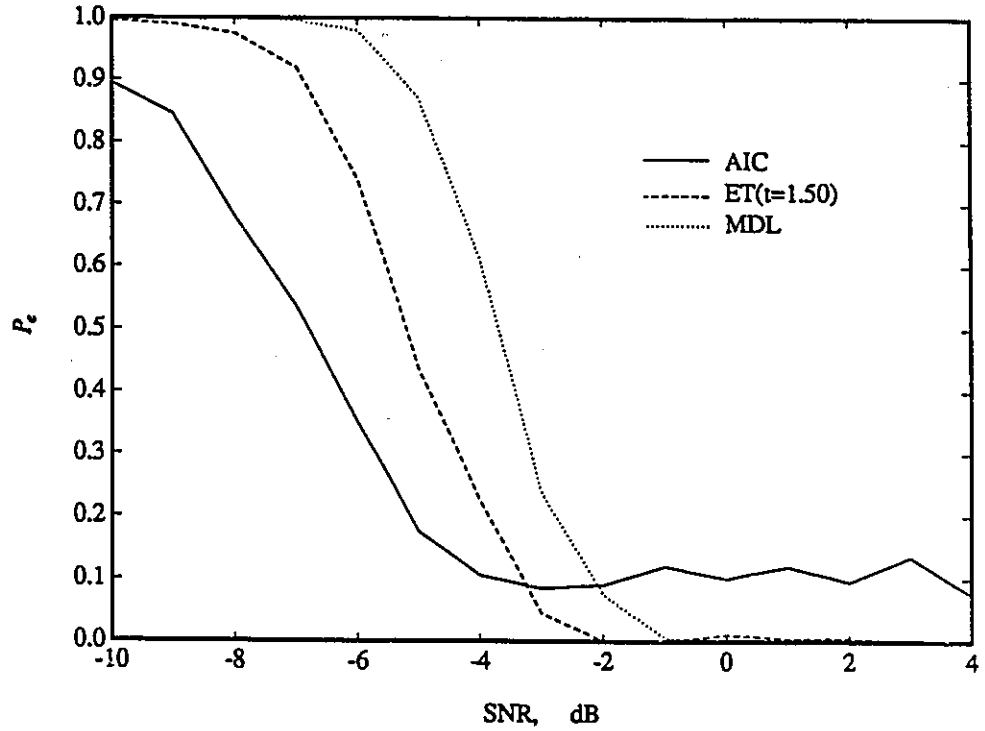

Figure 4.8: Probability of detection error vs. SNR for AIC, MDL, and ET methods. $p = 8$, $N = 100$, $k = 3$, Angles=15, 24, 36 degrees, trials=200.

Table 4.1: CONDITIONS OF SIMULATION 1

Number of sensors:	8
Number of snapshots:	100
Number of signals:	3
Signal power:	$A^2(1) = A^2(2) = A^2(3) = 1.0$
Signal angles of arrival:	15, 24, 36 degrees
Number of trials averaged:	500

Table 4.2: CONDITIONS OF SIMULATION 2 AND 3

Number of sensors:	8
Number of snapshots:	100
Number of signals:	3
Signal power:	$A^2(1) = A^2(2) = A^2(3) = 1.0$
Signal angles of arrival:	15, 24, 36 degrees
Number of trials averaged:	200

inconsistent. On the other hand, the MDL criterion eliminates this inconsistency while sacrificing the performance at relatively low SNR. Since the performance of the eigen-threshold method can be adjusted by appropriate choice of the parameter t, a suitable choice of t will yield a performance which takes advantage of both the AIC and the MDL criterion such that at relatively low SNR, the performance is superior to MDL whereas at high SNR, the inconsistency of AIC is removed. It can be observed from Figure 4.8 that for a choice of $t = 1.5$, this goal is achieved.

Many other simulations involving different signal and noise conditions have been carried out. A general discussion of the observations is presented here:

a). Effects of the variation of signal parameters

Variation of the signal parameters can be effected in various ways, viz., variation of total signal power, variation of the power of the signals relative to each other, and variation of the angles of separation between the signals. If the noise parameters remain unchanged,

these variations would affect the "effective SNR" r, which is defined in Equation (4.14) and represents the ratio of the smallest eigenvalue to the noise power. In general, if the total signal power decreases, or if the total power is constant but the the discrepancy of power between signals increases, then r decreases. Similarly, if the angles of separation between the signals decrease, r also decreases. If r decreases, the performance of the detection methods, viz., the AIC, the MDL, and the ET methods all deteriorate. However, observing the results of many simulations with different variations of the signal parameters, the relative performance of these methods remain more or less the same, i.e. the ET method maintains its superiority over the MDL method at low SNR while showing consistency in its estimates at high SNR, thereby outperforming the AIC method. Note that since the ET, the AIC, and the MDL methods use only the noise eigenvalues as a measure for the determination of the number of signals, a change of the signal parameters in general will primarily affect the missing error rate only.

b). Effects of the variation of the number of snapshots

The ET method is based on the assumption of asymptotic Gaussian distribution given by Theorem 3.3. Under finite data records, the asymptotic conditions may not be met. The question of how large should N be so that Equation (3.32) is true has not been answered analytically. However, from the results of the many simulations involving different finite numbers of snapshots N, the number of snapshots N_a for which the detection probability $P_D(N)$ of the ET method approaches sufficiently close ($|P_D - P_D(N)|/P_D < 1\%$) to the asymptotic detection probability P_D calculated by Equations (4.5), (4.6), (4.12) and (4.7) depends on the choice of the parameter t. The approximate values of N_a are shown in Table 4.5.2 which is obtained from averaging over a large number of trials under several signal and noise conditions. These results inform us that in general, for a particular value of t, one has to have a minimum number of snapshots given by Table 4.5.2 so that the asymptotic conditions are sufficiently closely approximated to ensure the validity of the method. If the minimum number of snapshots is not provided, then the error rate of the method may drastically increase. However, we note that both the AIC and the MDL methods are also asymptotic methods [21], and hence these methods will also break down

if the asymptotic conditions are not met.

Table 4.5.2

t	1.2	1.5	1.8
N_a	90	48	35

4.6 Discussion

The concept of the upper eigen-threshold of the noise subspace eigenvalues has been introduced in last chapter. This upper eigen-threshold is not a subjectively set threshold. Rather, the threshold is set by a one-step prediction method. Based on this concept, a new method for detecting the number of signals arriving at the array has been developed. Because of the way that the eigen-threshold is set, the method enables the detection to be carried out adaptively under various signal and noise conditions. The performance of this method has also been analyzed. Simulations have been carried out on the computer showing that the probability of error of this method is in close agreement with that obtained by theoretical analysis. A distinct feature of this new method of detection is that its performance is adjustable by the choice of the parameter t. For a wide range of SNR and for a range of number of incident signals, the optimum value of t falls within the range of 1.3 to 1.5. In general, the choice of $t = 1.5$ appears to be a good choice. In comparing the new method to the commonly used criteria (AIC and MDL), it is found that for a suitable choice of t, the new method eliminates the irreducible probability of error exhibited by the AIC while being superior to MDL in performance under low SNR.

The AIC and the MDL criteria have been extended to the case of detecting wide-band signals by establishing focusing matrices for various frequency components, and constructing a transformed covariance matrix $\boldsymbol{R}$ [64] so that the eigenvalues of $\boldsymbol{R}$ are utilized [64]. Since the ET method is developed based on the testing of the eigenvalues of the covariance matrix, the same method of imposing eigen-threshold tests on the eigenvalues of $\boldsymbol{R}$ may be

maintained so that the ET method can also be extended to the case of detecting wide-band signals. With its advantage over the AIC and the MDL criteria, the ET method presents an attractive alternative for the detection of the number of signals in array processing.

4.7 Appendix

To find the formulation of $\mathrm{F}(t) = \mathrm{F}_{\rho_1 \cdots \rho_{p-k-1}}(\gamma_1(t), \cdots, \gamma_{p-k-1}(t))$ in Equation (4.12), let us introduce a group of intermediate variables

$$y_i = l_i/\lambda, \qquad i = k+1,\ k+2,\ ...,\ p. \tag{4.26}$$

Then from Equation (4.8), ρ_m can be expressed by the ratio of y_{p-m} to y_{p-m+1}. Using the formula [48, pp.196–197] for obtaining the distribution function for quotient of two random variables, the distribution function of ρ_m can be calculated by

$$f_{\rho_m}(\rho_m) = \int_{R_{y_{p-m+1}}} |y_{p-m+1}| f_{y_{p-m,p-m+1}}(\rho_m y_{p-m+1}, y_{p-m+1}|\Sigma) dy_{p-m+1} \tag{4.27}$$

where $f_{y_{p-m,p-m+1}}(y_{p-m}, y_{p-m+1}|\Sigma)$ is the joint distribution function of y_{p-m} and y_{p-m+1} given Σ. $R_{y_{p-m+1}}$ is the integration region of y_{p-m+1}.

Using vector notation, we let

$$y = [y_{k+1}\ \ y_{k+2}\ \ \cdots\ \ y_p]^T \tag{4.28}$$

and

$$\eta = [\eta_{k+1}\ \ \eta_{k+2}\ \ \cdots\ \ \eta_p]^T \tag{4.29}$$

where η_i is defined in Equation (3.19). From Equations (3.19) and (3.31) the relation between y_i and η_i can be written as

$$y = N^{-1/2} I_{p-k} \begin{bmatrix} (p-k)^{-1} & \cdots & \cdots & (p-k)^{-1} \\ 0 & (p-k-1)^{-1} & \cdots & (p-k-1)^{-1} \\ \cdots & \cdots & \cdots & \cdots \\ 0 & \cdots & 0 & 1 \end{bmatrix} \eta + 1 \tag{4.30}$$

where I_{p-k} is an identity matrix and the vector $\mathbf{1} = [1\ 1\ ...\ 1]^T$, both of $(p-k)$ dimension.

The joint distribution of y_{k+1}, ..., y_p can be found by applying the variable transformation above to Equation (3.27) as

$$f_y(y|\Sigma) = \frac{|J|}{(2\pi)^{(p-k)/2}\Gamma(p-k)\cdots\Gamma(1)} \cdot \exp\left\{\frac{1}{2}\sum_{i=k+1}^{p}\eta_i^2(y)\right\} \cdot \prod_{i=k+1}^{p}\prod_{j=i+1}^{p}(\eta_i(y)-\eta_j(y))^2 \tag{4.31}$$

where, the Jacobian,

$$|J| = \Gamma(p-k+1)\cdot N^{(p-k)/2}. \tag{4.32}$$

The $\eta_i(y)'s$ are defined by the following linear transform;

$$\eta = N^{1/2}\begin{bmatrix} (p-k) & -(p-k-1) & & & \\ & (p-k-1) & . & & \\ & & . & . & \\ & & & . & -1 \\ & & & & 1 \end{bmatrix}(y-1) \tag{4.33}$$

The distribution function $F(t)$ can be evaluated by using Equation (4.31) and repeatedly applying Equation (4.27), the distribution function $F(t)$ is obtained as the following integration,

$$\begin{aligned} \mathrm{F}(t) &= \mathrm{F}_{\rho_1\cdots\rho_{p-k-1}}(\gamma_1(t),\cdots,\gamma_{p-k-1}(t)) \\ &= \mathrm{P}(\rho_1 \le \gamma_1(t),\cdots,\rho_{p-k-1} \le \gamma_{p-k-1}(t)) \\ &= \int_{-\infty}^{\gamma_{p-k-1}(t)}\int_{-\infty}^{\gamma_{p-k-2}(t)}\cdots\int_{-\infty}^{\gamma_1(t)}\int_{-\infty}^{\infty}|y_1^{p-k-1}\rho_1^{p-k-2}\cdots\rho_{p-k-2}| \\ &\quad f_y(\rho_{p-k-1}\rho_{p-k-2}\cdots\rho_1 y_1, \rho_{p-k-2}\cdots\rho_1 y_1,\cdots,\rho_1 y_1, y_1|\Sigma) \\ &\quad d\rho_{p-k-1}d\rho_{p-k-2}\cdots d\rho_1 dy_1 \end{aligned} \tag{4.34}$$

where $f_y(\cdot)$ have non-zero values only in R_y, the region of the $y_i's$ which corresponds to

$$R_\eta = (-\infty < \eta_p < \eta_{p-1} < \cdots < \eta_{k+1} < +\infty). \tag{4.35}$$

Chapter 5

Strategy for Detection in non-white noise environments

5.1 Detection difficulties arising in non-white noise environments

In the previous chapters, the noise is assumed to be spatially uncorrelated. In other words, the noise is white because uncorrelated noise has a flat spectrum. However, in engineering practice, the noise may be spatially correlated. From this chapter onwards, we consider this fact in our discussion. Detection of the number of sources in the presence of non-white noise is relatively more difficult than in white noise environments due to the complexity introduced into the detection problem from the noise part. In the white noise situation discussed in the last two Chapters, only the noise power level is unknown, so we can still make use of the spectral information, i.e. flatness, of the white noise for detection. Both the information criteria and the ET method belong to this type. When non-white noise is considered, both power level and spectral shape information (or equivalently, the parameter set which completely describes the noise characteristics) may be unknown. The structure of the noise model may vary over a large range; likewise, so do the parameters. In other words, each noise model may be represented by a point in a large parameter space, while white noise is represented by a specific point in the space. Within this large space, the chance of

appearance of pure white noise is relatively small. Because of this variation in noise spectral characteristics, methods developed under the white noise assumption may suffer significant performance degradation in the presence of coloured noise. To illustrate the influence of non-white noise, an example is given in Figure 5.1, which shows the performance of the widely accepted AIC and MDL methods when the noise changes from white to moderately coloured. It can be seen that, the more severely coloured the noise becomes, the more deterioration the AIC and the MDL suffer in their performance, leading finally to a complete failure. As will be discussed in later chapters, this failure is mainly due to a high false alarm error rate induced by the non-white noise influence.

5.2 Strategy for detection in non-white noise environment

Before considering the details of our new method, let us briefly discuss the existing methods, and possible approaches for the detection problem involving non-white noise.

5.2.1 Methods using autocovariance information

There are methods which are based on the statistics of (or closely related to) the power level or power spectrum of the noise process and signals. We call these methods *Autocovariance information* based methods. The term autocovariance is used to refer the covariance within an array. These methods can be discussed according to the cases in which they may be applied.

For the case in which the noise power is known, the detection strategy is relatively simple because a threshold can be set according to the noise power to separate signals from the noise. Furthermore, there is a strategy which is relatively less sensitive to a non-white noise environment [4]. However, in most practical situations the noise level is unknown. So the applications of this type of methods are quite limited.

If the noise level is not known but the spectral information of the noise is available in certain forms, e.g., in the form of the noise covariance matrix (white noise is a special case of

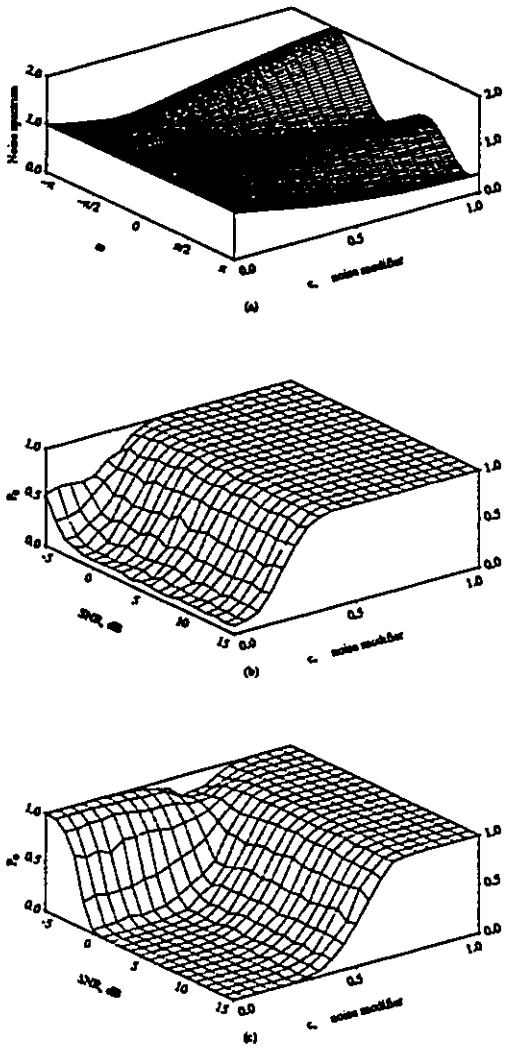

Figure 5.1: Illustration of the deterioration of the performance of the AIC and the MDL when the noise changes from white to coloured. (a) Spectrum of the environment noise, (b) The performance surface of the AIC, (c) The performance surface of the MDL.

this kind, since the noise covariance matrix is known to be diagonal with equal entries), the detection problem can always be converted to an equivalent white noise detection problem by applying the so-called *whitening technique*. After such a conversion, the methods developed for detection in white noise environments such as AIC, MDL, and our new ET method, can be applied to the transformed variates.

The most difficult situation arises when both the power level and spectral information are unknown. Such a combination renders all the existing spectral shape dependent methods unusable. One approach proposed by Le Cadre [42] to attack the detection problem in this difficult situation is to include the unknown noise parameters to the estimation procedure. In the method proposed by Le Cadre, the signals are modelled by line spectra as usual, and the noise is modelled by an ARMA model. By trying all the possible candidate models including the noise parameters in the estimation (model fitting) procedure, the residuals of the fit are checked by applying information criteria to find the best model. One problem with this approach is that the size of the parameter set which is estimated is relatively large compared with the number of signal parameters in which we are really interested. Such a large parameter set size will not only drastically increase the computational requirements, but will also introduce extra uncertainties which will worsen the estimates of the signal parameters. Also, a very basic question which has not been answered in this approach is the separability of the noise parameters from the signal parameters in the estimation using discrete data. As a result of the discrete spatial sampling by the array sensors, the signal spectrum is no longer a line spectrum. The separability of the signal spectrum from the noise spectrum can only be insured when the number of sensors are very large. The chance of mis-modeling signal components by the parameters of the noise part or vice versa increases when the number of sensors decreases. When the array size is not very large, the probability of mis-modelling may be large.

5.2.2 Cross-covariance information and a new strategy

To give the detection problem in the presence of spatially correlated noise a more reliable solution, the most important thing is to build the new method on information which distinguishes the noise from signals. In the white noise environment, the success of information criteria and the ET method is built on a cornerstone: the determinable difference of the noise spectrum and the signal spectrum. White noise has a flat spectrum and the signals have line spectra. This usable information is *invariant* to changes of noise power which is assumed to be unknown in the white noise problem. However, this information is not invariant to changes in noise correlation. As we all know, the power spectrum is intimately connected with the covariance coefficients by the Fourier transform. Therefore, the autocovariance matrix may not be a good starting point for attacking the non-white noise problem, because the covariance matrix is not consistent with respect to changes in the noise spectrum.

To find a consistent source of information, we should mention that in most engineering problems, the noise is only correlated over a limited spatial range. This factor implies that there may be consistent information embedded in covariances of the outputs of array sensors which are properly separated in a spatial range.

An example of this kind is the reverberation noise in underwater target detection problem. Reverberation is the noise resulting from the scattering of energy from a propagating pulse as a result of inhomogeneities in the ocean and its boundaries. The background noise in an active sonar for detecting an underwater target is ambient noise and/or reverberation. Reverberation, especially, causes difficulties in sonar signal detection since the reverberation does not satisfy the white noise assumption. The statistical properties of reverberation were studied by Y. Omichi [47], and Q. T. Zhang, et. al. [72]. However, the banded structure of the noise covariance is well illustrated by figures in [47]. These figures are enclosed here as Figures 5.2 and 5.3.

The experimental data used to obtain Figures 5.2 and 5.3 were obtained from the wind driven surface of a fresh water lake. Two types of signals were transmitted to obtain

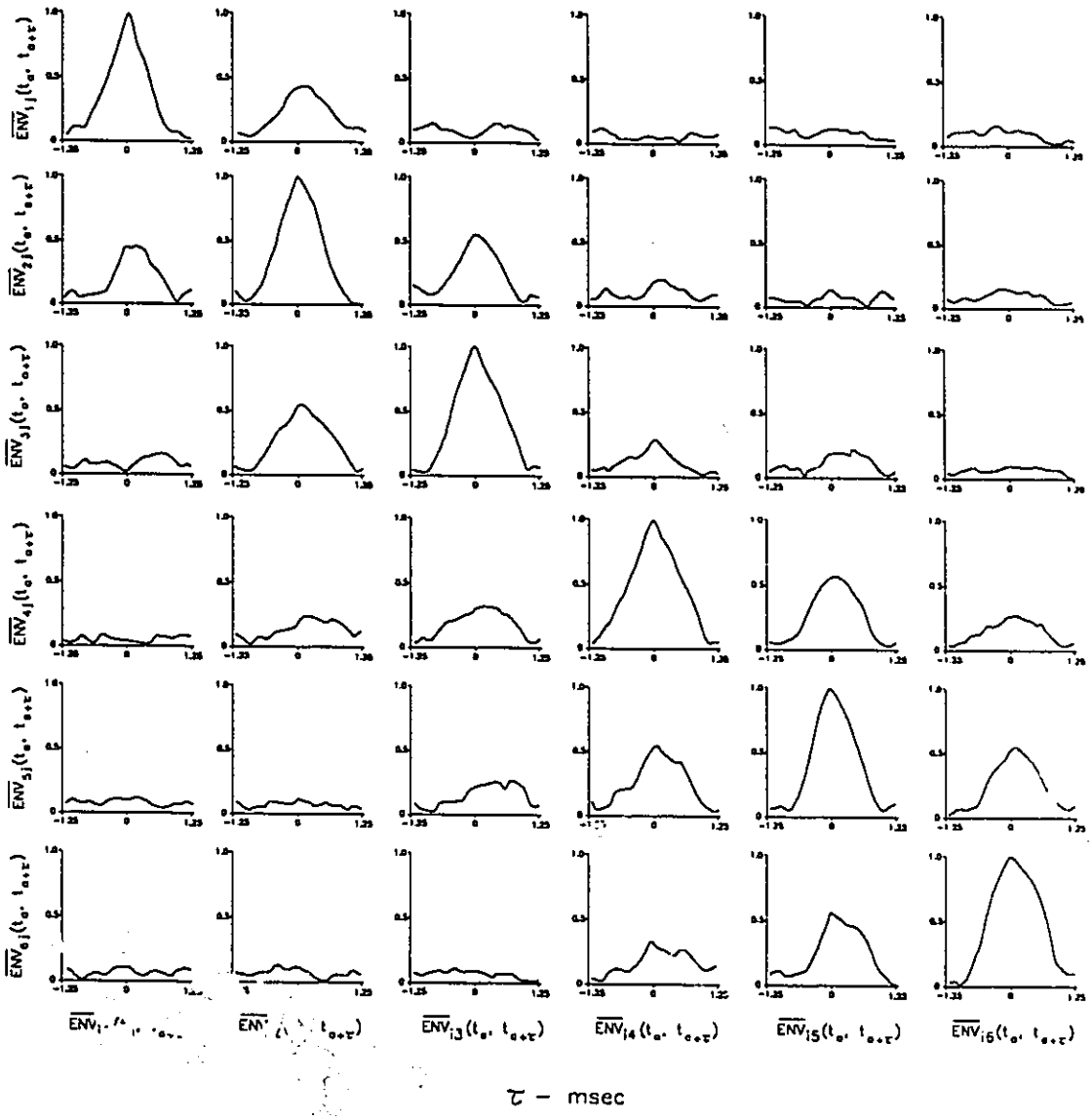

Figure 5.2: Envelope of the normalized covariance matrix of continuous wave reverberation at the observation time $t = 18.4$ msec after transmission. Maximum temporal separation $\tau = \pm 1.25$ msec. (This is the Fig. 15 of [47]

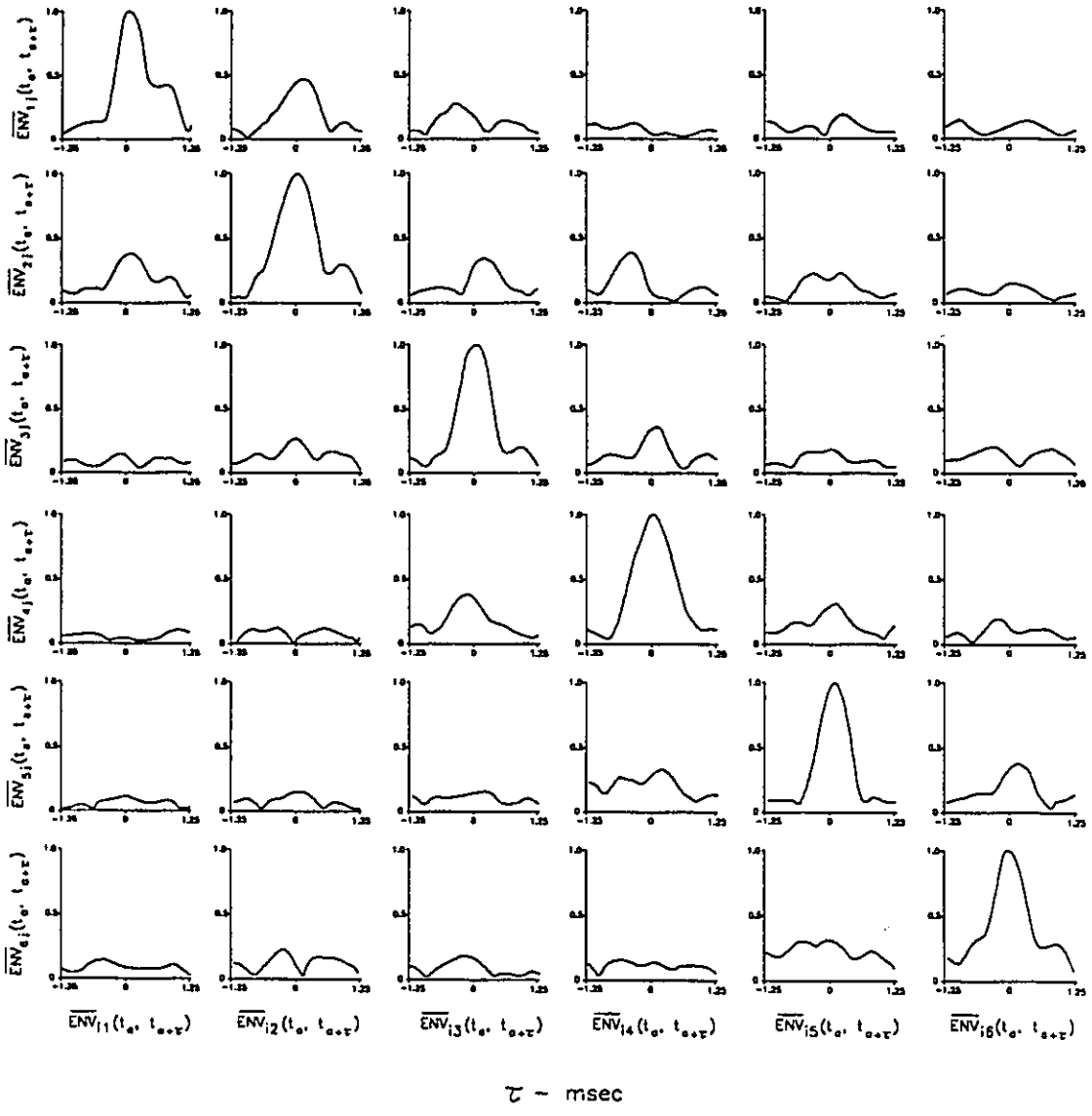

Figure 5.3: Envelope of the normalized covariance matrix of linear FM reverberation at the observation time $t = 18.4$ msec after transmission. Maximum temporal separation $\tau = \pm 0.3$ msec. (This is the Fig. 17 of [47]

the reverberation data: a pulsed continuous wave (CW) signal with a duration of 1.0 msec with a carrier frequency of 80 kHz, and a linear frequency modulated (LFM) signal with a duration of 1.0 msec and a sweep bandwidth of 10 kHz centered at 80 kHz. For each signal, 98 snapshots were sampled in quadrature form (mathematically expressed in complex data) from a linear array of six hydrophones. The data matrix can be written as

$$Z = \begin{bmatrix} z_1(t_a,1) & z_1(t_a,2) & \cdots & z_1(t_a,98) \\ z_2(t_a,1) & z_2(t_a,2) & \cdots & z_2(t_a,98) \\ \cdots & \cdots & \cdots & \cdots \\ z_6(t_a,1) & z_6(t_a,2) & \cdots & z_6(t_a,98) \end{bmatrix} \tag{5.1}$$

The envelope of the normalized covariance function is given by

$$\overline{ENV}_{ij}(t_a, t_a+\tau) = \frac{\widehat{ENV}_{ij}(t_a, t_a+\tau)}{\sqrt{\widehat{ENV}_{ii}(t_a,t_a)\,\widehat{ENV}_{jj}(t_a+\tau, t_a+\tau)}} \tag{5.2}$$

where the envelope of the covariance function is expressed as

$$\widehat{ENV}_{ij}(t_a, t_a+\tau) = [\{X_{ij}(t_a, t_a+\tau)\}^2 + \{Y_{ij}(t_a, t_a+\tau)\}^2]^{1/2} \tag{5.3}$$

where

$$X_{ij}(t_a, t_a+\tau) = \frac{1}{2N}\sum_{m=1}^{N}[x_i(t_a,m)x_j(t_a+\tau,m) + y_i(t_a,m)y_j(t_a+\tau,m)] \tag{5.4}$$

$$Y_{ij}(t_a, t_a+\tau) = \frac{1}{2N}\sum_{m=1}^{N}[x_i(t_a,m)y_j(t_a+\tau,m) - y_i(t_a,m)x_j(t_a+\tau,m)] \tag{5.5}$$

and $N = 98$, $x_i(t_a,m) = \mathrm{Re}(z(t_a,m))$, and $y_i(t_a,m) = \mathrm{Im}(z(t_a,m))$

It can be observed that:

1. The diagonal elements of the matrices have the largest power.

2. The power diminishes very quickly along the direction of element index away from the diagonal. The covariances of the elements separated by more than two index units are no longer significant.

This observation suggests that for many engineering problems, even when the noise is spatially correlated, the noise covariance of array elements separated beyond a certain spatial range can be insensitive to changes in the spatial correlation of the noise. For these engineering problems, a new detection strategy is suggested as:

1. Mathematically represent the covariance of the noise by a Hermitian matrix with a banded structure as shown in Figure 5.4. The parameter δ is the bandwidth of the non-zero elements of the matrix.

2. Apply two spatially separated arrays for detection. These two arrays should be sufficiently separated so that, although the noise of the elements in each array is spatially correlated, the noise between elements of different arrays is uncorrelated. This structure involving two arrays is called a bi-array structure[1]. As an example, Figure 5.5 shows a bi-array structure in which the two arrays have parallel normals. In general, we do not require parallel normals for the arrays in a bi-array structure.

3. Define the composite covariance of the two arrays as *cross-covariance*. The cross-covariance of all the elements in these two arrays form a matrix called the *cross-covariance matrix*.

4. Since the cross-covariance matrix is still not a consistent information source with respect to changes in noise correlation, a canonical transform can be used to normalize the cross-covariance to make the resulting criterion insensitive to the noise correlation. This technique, called canonical analysis, is introduced in the following chapter. The details of the application of this technique to the new method is discussed in Chapter 7.

To conclude this chapter, the relationships between the various detection methods, and the corresponding knowledge required from the noise components are summarized in Figure 5.6.

[1]Similar array structures have been used in a paper of Prasad and Chandna [50], and also in the ESPRIT algorithm due to Roy and Kailath [55] for direction of arrival estimation. Our new method can be viewed as a natural extension of this bi-array structure to the detection problem.

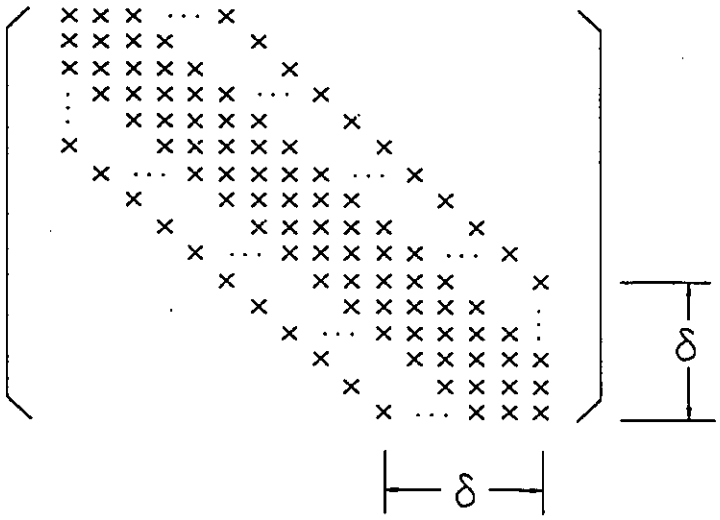

Figure 5.4: Banded structure of the covariance matrix

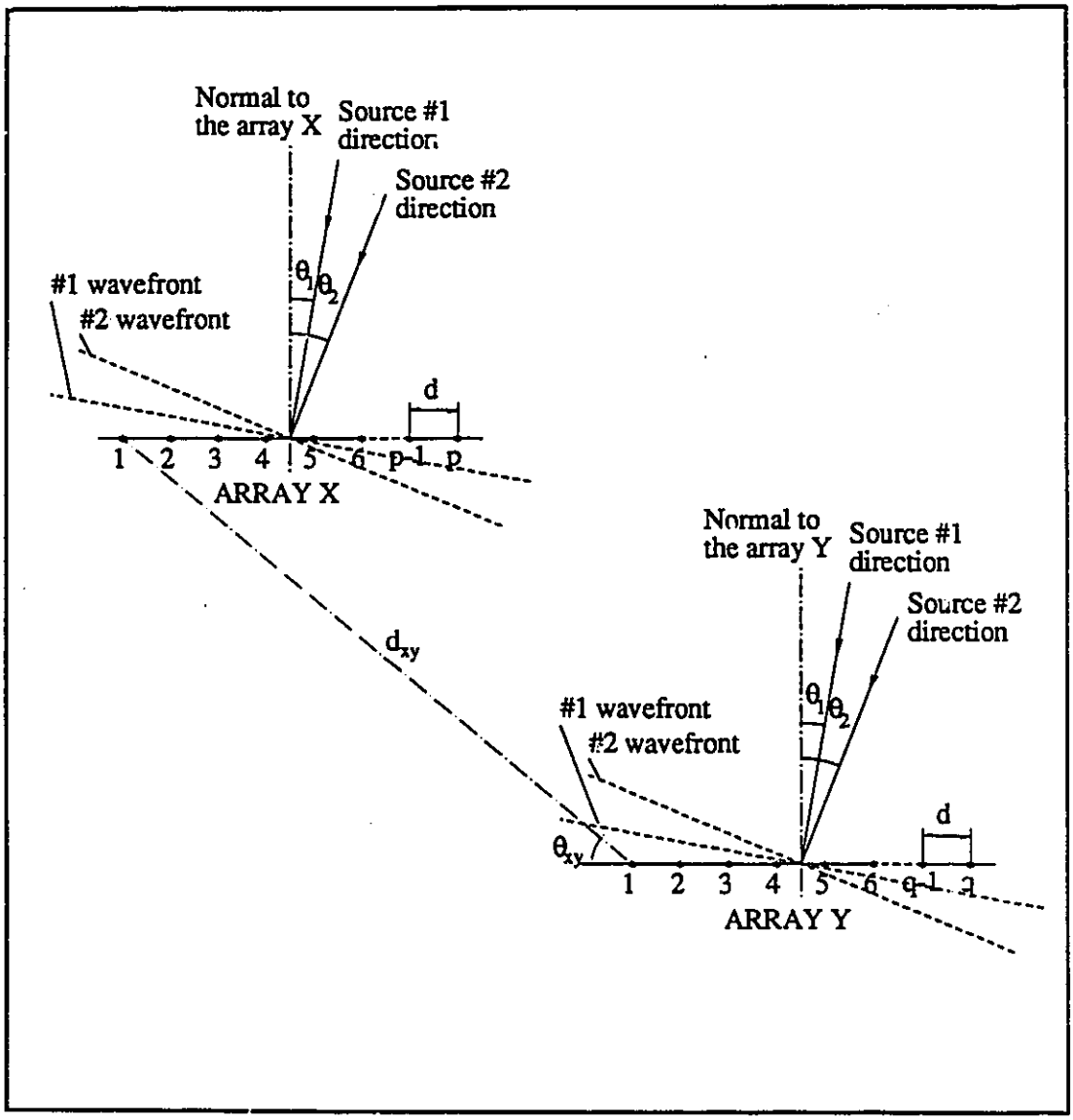

Figure 5.5: Illustration of the bi-array structure.

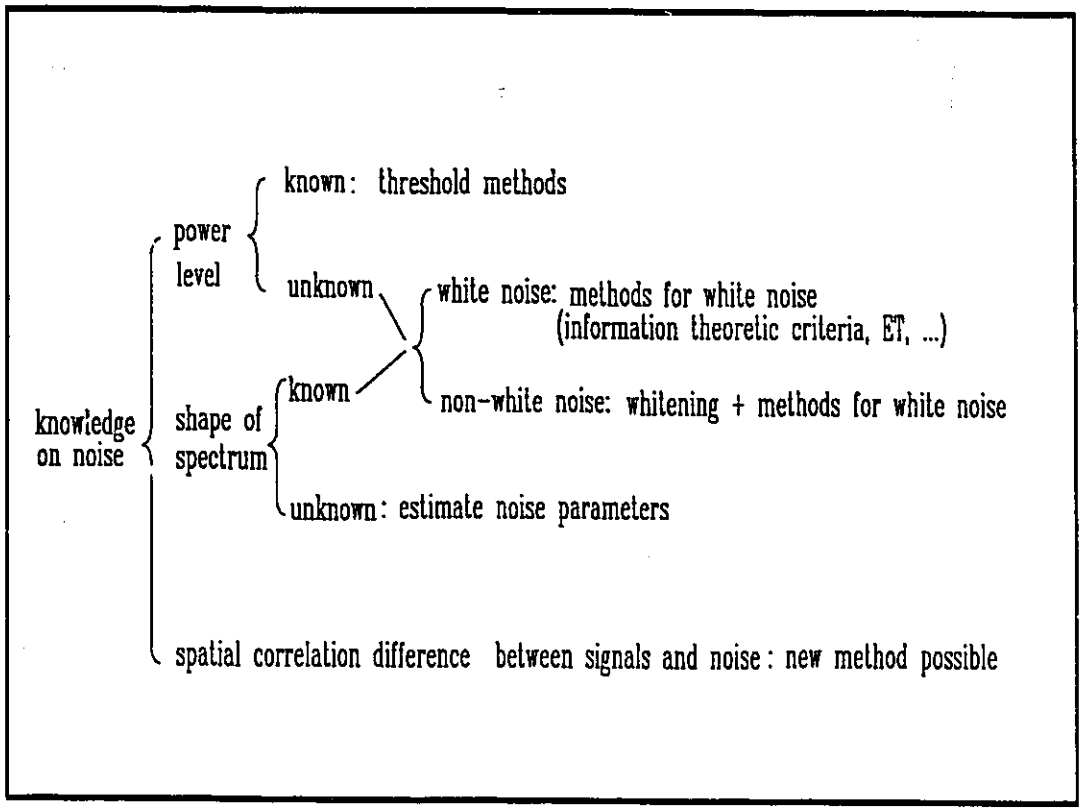

Figure 5.6: Detection methods relating to the required knowledge of the noise

Chapter 6

Canonical correlation and Canonical variables

This chapter introduces some important concepts and theorems of canonical correlation analysis. This technique was developed by Hotelling [34], and is the principal statistical tool used in the derivation of our new detection method for non-white noise environments. The new method is discussed in further detail in the next chapter.

In canonical correlation analysis, two sets of variates with a joint distribution are studied, and the correlations between these two sets of variates are analyzed under a normalized and orthogonal form (canonical form). This form is achieved by finding a canonical transformation, which can be interpreted geometrically as finding a coordinate system in the space of each set of variates so that the new coordinates display unambiguously the correlation of the two sets of variates.

From the practical viewpoint, canonical correlation analysis is concerned with characterizing the correlation structure between two sets of variables, without losing much information, by replacing them with new sets with smaller number of variables which are pairwise highly correlated. This can be shown by the following discussion on the canonical transformation.

6.1 Population Canonical Correlation Coefficients and Canonical Variables

Suppose that $x(t)$ and $y(t)$ are, respectively, $p \times 1$ and $q \times 1$ random vector processes which may be expressed in a composite form as

$$z(t) = \begin{bmatrix} x(t) \\ y(t) \end{bmatrix} \tag{6.1}$$

Assuming the means of both $x(t)$ and $y(t)$ are zero, the variance-covariance matrix Σ of $x(t)$ and $y(t)$ can be written as

$$\Sigma = E[z(t)z(t)^H] = \begin{matrix} \\ \\ \\ p \quad q \end{matrix} \begin{bmatrix} \Sigma_{11} & \Sigma_{12} \\ \Sigma_{21} & \Sigma_{22} \end{bmatrix} \begin{matrix} p \\ q \end{matrix} \tag{6.2}$$

Without loss of generality, in the following discussion, we will assume that $p \leq q$. For $x(t)$, $y(t)$ and Σ defined above, a transform, namely the *Canonical transform*, can be introduced as given by the following theorem.

Theorem 6.1 *If Σ is positive definite, and* $\text{rank}(\Sigma_{12}) = k$, *then there exist linear transformations L of order p and M of order q defined by [39, p249]*

$$u(t) = L\, x(t) \tag{6.3}$$

$$v(t) = M\, y(t) \tag{6.4}$$

such that the variance-covariance matrix of $u(t)$ and $v(t)$ has the form

$$E\left(\begin{bmatrix} u(t) \\ v(t) \end{bmatrix} \begin{bmatrix} u^H(t) & v^H(t) \end{bmatrix} \right) = \begin{matrix} \\ \\ \\ p \quad q \end{matrix} \begin{bmatrix} I_p & P \\ P^H & I_q \end{bmatrix} \begin{matrix} p \\ q \end{matrix} \tag{6.5}$$

where

$$P = [\tilde{P} \;\; O]\,, \tag{6.6}$$

and $\tilde{P}$ is a $p \times p$ diagonal matrix given by

$$\tilde{P} = \text{diag}(\rho_1, \rho_2, \ldots \rho_k, 0, \ldots, 0)\,. \tag{6.7}$$

Proof: Since Σ is a positive definite Hermitian matrix, Σ_{11} and Σ_{22} are positive definite and there exist full rank-matrices $\Sigma_{11}^{1/2}$ and $\Sigma_{22}^{1/2}$ and their inverses, which are defined as

$$\Sigma_{11} = \Sigma_{11}^{1/2} \left(\Sigma_{11}^{1/2}\right)^H \tag{6.8}$$

$$\Sigma_{22} = \Sigma_{22}^{1/2} \left(\Sigma_{22}^{1/2}\right)^H \tag{6.9}$$

$$\Sigma_{11}^{-1/2} = \left(\Sigma_{11}^{1/2}\right)^{-1} \tag{6.10}$$

$$\Sigma_{22}^{-1/2} = \left(\Sigma_{22}^{1/2}\right)^{-1}\,. \tag{6.11}$$

Using the inverses above to define a transformed matrix $\tilde{\Sigma}_{12}$

$$\tilde{\Sigma}_{12} = \Sigma_{11}^{-1/2}\, \Sigma_{12}\, \left(\Sigma_{22}^{-1/2}\right)^H \tag{6.12}$$

and applying the singular value decomposition on this matrix, we have

$$\tilde{\Sigma}_{12} = Q_1\, P\, Q_2^H \tag{6.13}$$

where Q_1 and Q_2 are unitary matrices. P has the form defined by Equations (6.6) (6.7) because

$$\text{rank}(\tilde{\Sigma}_{12}) = \text{rank}(\Sigma_{12}) = k \leq p \leq q \tag{6.14}$$

Now, we can define transformation matrices L and M by

$$L = Q_1^H\, \Sigma_{11}^{-1/2} \tag{6.15}$$

$$M = Q_2^H\, \Sigma_{22}^{-1/2}. \tag{6.16}$$

Applying these matrices to the transformation defined by Equations (6.3) (6.4), we have

$$E[u(t)u^H(t)] = L E[x(t)x^H(t)]L^H = L\, \Sigma_{11}\, L^H = I_p \tag{6.17}$$

$$E[v(t)v^H(t)] = M\, E[y(t)y^H(t)]M^H = M\, \Sigma_{22}\, M^H = I_q \tag{6.18}$$

$$E[u(t)v^H(t)] = L E[x(t)y^H(t)]M^H = L\, \Sigma_{12}\, M^H = P \tag{6.19}$$

Notice that Equations (6.17) to (6.19) are equivalent to the corresponding partition of Equation (6.5); hence, the theorem is proved. □

By applying the transformation defined in Theorem 6.1, the original variables $x(t)$, and $y(t)$ are replaced by new variables $u(t)$ and $v(t)$. Furthermore, the new variables have the following properties, whose proofs follow directly from the definitions:

$$\text{(i)} \quad \textit{normality}: \quad E[|u_i(t)|^2] = E[|v_j(t)|^2] = 1 \quad \forall \ 1 \le i \le p, \ 1 \le j \le q \tag{6.20}$$

$$\text{(ii)} \quad \textit{orthogonality}: \quad E[u_i(t)v_j^*(t)] = E[v_i(t)v_j^*(t)] = 0 \qquad \forall \ i \ne j \tag{6.21}$$

$$\text{(iii)} \quad \textit{correlation}: \quad E[u_i(t)v_j^*(t)] = \begin{cases} \rho_i & \forall \quad i = j \le k \\ 0 & \forall \quad i \ne j \text{ or } k < i = j \le p \end{cases} \tag{6.22}$$

where $0 < \rho_i \le 1, i = 1, \cdots, k$.

With these properties, the elements of the vector $u(t)$ defined by Equation (6.3) are called the *canonical variables* of the x-space, and those of $v(t)$ defined by Equation (6.4) are called the *canonical variables* of the y-space. The first k canonical variables actually carry the whole correlation information of the original variables, since the correlation of the remaining canonical variables equal zero. The quantities ρ_i $i = 1, \cdots, k$ are called *canonical correlation coefficients.* Each ρ_i is a measure of the correlation between $u_i(t)$ and $v_i(t)$. The columns of L^H and M^H are called *canonical vectors.* If the canonical correlation coefficients are so arranged that

$$\rho_1 \ge \rho_2 \ge \ldots \ge \rho_k \ge 0 \tag{6.23}$$

then, we define the following

$u_1(t)$ is the 1st canonical variable of x-space

$v_1(t)$ is the 1st canonical variable of y-space

$u_2(t)$ is the 2nd canonical variable of x-space

$v_2(t)$ is the 2nd canonical variable of y-space

...

and so on .

The canonical variables have the following optimality property. The first canonical variables $u_1(t)$, and $v_1(t)$ are linear combinations of the components of $x(t)$ and $y(t)$, respectively, with unit variance having the largest possible correlation, and this correlation is ρ_1; then out of all linear combinations of the components of $x(t)$ and $y(t)$ which are uncorrelated with both $u_1(t)$ and $v_1(t)$ and have unit variance, the second canonical variables $u_2(t)$ and $v_2(t)$ are most highly correlated, and their correlation is ρ_2, and so on. These characteristics and relations are mathematically described by Equations (6.3), (6.4), (6.7), and (6.20) to (6.22). Readers familiar with principal component analysis can immediately recognize that the canonical variables $u_i(t)$, $v_i(t)$ are the i-th principal canonical correlation components in x-space and y-space. Theorem 6.1 guarantees the existence of this canonical transformation.

6.2 Sample canonical correlations

Before introducing sample canonical correlations, we give a lemma which will be used in the proof of Theorem 6.2 in this section.

Lemma 6.1 *If on the basis of a given sample $\hat{\theta}_1, \cdots, \hat{\theta}_m$ are maximum likelihood estimators of the parameters $\theta_1, \cdots, \theta_m$ of a distribution, then $\phi_1(\hat{\theta}_1, \cdots, \hat{\theta}_m)$, $\cdots$, $\phi_m(\hat{\theta}_1, \cdots, \hat{\theta}_m)$, are maximum likelihood estimators of $\phi_1(\theta_1, \cdots, \theta_m)$, $\cdots$, $\phi_m(\theta_1, \cdots, \theta_m)$, if the transformation from $\theta_1, \cdots, \theta_m$ to $\phi_1, \cdots, \phi_m$ is one-to-one. If the estimators of $\theta_1, \cdots, \theta_m$ are unique, then the estimators of $\phi_1, \cdots, \phi_m$ are unique.*

Proof: See Corollary 3.2.1 of [5]. □

In practice, canonical correlations must be estimated from sampled data. Let $z_1, ..., z_N$ be N observations from a $p+q$ variate Gaussian distribution $G(\mathbf{0}, \Sigma)$. It is well known

[5] that the maximum likelihood estimate of Σ is

$$\hat{\Sigma} = \begin{bmatrix} \hat{\Sigma}_{11} & \hat{\Sigma}_{12} \\ \hat{\Sigma}_{21} & \hat{\Sigma}_{22} \end{bmatrix} = \frac{1}{N}\sum_{i=1}^{N} z_i z_i^H = \frac{1}{N}\begin{bmatrix} S_{11} & S_{12} \\ S_{21} & S_{22} \end{bmatrix} \triangleq \frac{1}{N} S \,. \tag{6.24}$$

The maximum likelihood estimates of $\{\rho_i\}$, which are the population canonical correlation coefficients, are given by the following theorem.

Theorem 6.2 *Let $z_1, \cdots, z_N$ be N observations from $z(t)$ which is defined in Equation (6.1) and follows the distribution $G(0, \Sigma)$. Let Σ be partitioned as Equation (6.2) (assuming $p \leq q$). The maximum likelihood estimators of the canonical correlations are the singular values of the matrix*

$$\tilde{S}_{12} \triangleq S_{11}^{-1/2} S_{12} \left(S_{22}^{-1/2}\right)^H = D_1 \Gamma D_2^H \tag{6.25}$$

where

$$\Gamma = [\tilde{\Gamma}_p \;\; O] \tag{6.26}$$

$$\tilde{\Gamma}_p = \text{diag}(\gamma_1, \gamma_2, \ldots \gamma_p) \tag{6.27}$$

where $1 \geq \gamma_1 \geq \gamma_2 \geq \ldots \geq \gamma_p \geq 0$.

Proof: Now, we have $\hat{\Sigma}$ which is the maximum likelihood estimate of Σ, and the transformation being considered here is

$$\Phi(\Sigma) = \text{SVD}\left(\Sigma_{11}^{-1/2} \Sigma_{12} \left(\Sigma_{22}^{-1/2}\right)^H\right) \tag{6.28}$$

which is one-to-one. Then, making use of Lemma 6.1, the conclusion of the theorem follows. □

The exact distribution of the sample canonical correlation coefficients for complex data has been derived by James [35] as

$$\prod_{i=1}^{p}(1-\rho_i^2)^N \, {}_2\tilde{F}_1(N, N; q; P^2, \Gamma^2) \cdot \frac{\tilde{\Gamma}_p(N)\pi^{p(p-1)}}{\tilde{\Gamma}_p(N-q)\tilde{\Gamma}_p(q)\tilde{\Gamma}_p(p)}$$
$$\cdot \prod_{i=1}^{p}(\gamma_i^2)^{(q-p)} \cdot \prod_{i=1}^{p}(1-\gamma_i^2)^{(N-p-q)} \cdot \prod_{i=1}^{p-1}\prod_{j=i+1}^{p}(\gamma_i^2 - \gamma_j^2)^2 \tag{6.29}$$

$$(1 > \gamma_1^2 > \ldots > \gamma_p^2 > 0)$$

where $\tilde{\Gamma} = \text{diag}(\gamma_i)$ and $\tilde{P} = \text{diag}(\rho_i)$. The quantity $\tilde{\Gamma}_p(\cdot)$ is defined in Equation (3.9). The function ${}_2\tilde{F}_1(N, N; q; \tilde{P}^2, \tilde{\Gamma}^2)$ is the Gaussian hypergeometric function. For details of the derivation of the distribution function and the definition of the Gaussian hypergeometric function, one may consult the work of James [35] and Constantine [20].

6.3 More Properties of Canonical Correlation

In this section we provide further theoretical insight into canonical correlation analysis by discussing other significant aspects of this methodology other than the normality, orthogonality, and the optimality property of the canonical variables mentioned in Section 6.1, and the maximum likelihood property of the sample canonical correlation mentioned in Section 6.2. These aspects are stated in the following theorems:

Theorem 6.3 *In a narrowband system in the absence of noise, the largest k sample canonical correlation coefficients equal unity, whereas the smallest $(p-k)$ coefficients are zero. We refer to these groups as the signal and noise coefficients, respectively.*

Proof:

Define the $p \times N$ and $q \times N$ sample matrices $\boldsymbol{X}$ and $\boldsymbol{Y}$ as

$$\boldsymbol{X} = [\boldsymbol{x}_1, \boldsymbol{x}_2, \ldots, \boldsymbol{x}_N] \tag{6.30}$$

$$\boldsymbol{Y} = [\boldsymbol{y}_1, \boldsymbol{y}_2, \ldots, \boldsymbol{y}_N]\,. \tag{6.31}$$

Then the $p \times p$, $q \times q$, and $p \times q$ covariance matrices of $\boldsymbol{X}$ and $\boldsymbol{Y}$ are

$$\boldsymbol{S}_{11} = \boldsymbol{X}\boldsymbol{X}^H\,;\;\; \boldsymbol{S}_{22} = \boldsymbol{Y}\boldsymbol{Y}^H\,;\;\; \boldsymbol{S}_{12} = \boldsymbol{X}\boldsymbol{Y}^H\,. \tag{6.32}$$

and

$$\tilde{\boldsymbol{S}}_{12} = \boldsymbol{S}_{11}^{-1/2}\boldsymbol{S}_{12}(\boldsymbol{S}_{22}^{-1/2})^H\;. \tag{6.33}$$

Let the singular value decomposition of $\boldsymbol{X}$ and $\boldsymbol{Y}$ be written as

$$\boldsymbol{X} = \boldsymbol{U}_x\boldsymbol{\Gamma}_x\boldsymbol{V}_x^H \tag{6.34}$$

$$\boldsymbol{Y} = \boldsymbol{U}_y\boldsymbol{\Gamma}_y\boldsymbol{V}_y^H \tag{6.35}$$

where Γ_x, a $p \times N$ matrix can be partitioned to $\tilde{\Gamma}_x$, a $p \times p$ diagonal matrix and a $p \times (N-p)$ null matrix as

$$\Gamma_x = \left[\tilde{\Gamma}_x \; 0\right] \tag{6.36}$$
$$\tilde{\Gamma}_x = \text{diag}(\sigma_1^{(x)}, \ldots, \sigma_k^{(x)}, 0, \ldots, 0),$$

and where $\sigma_i^{(x)}$ are the singular values of X. The matrix Γ_y is defined in a similar way.

In the absence of noise, for narrow band systems, the row spaces of X and Y are equivalent, because the temporal variation of the received signal on each array is identical. Hence, there exist V_x and V_y satisfying Equations (6.34), (6.35), and

$$V_x = V_y = V. \tag{6.37}$$

Using the generalized inverse, we can write

$$S_{11}^{-1/2} = (XX^H)^{-1/2} = U_x \Gamma_x^+ U_x{}^H \tag{6.38}$$
$$S_{22}^{-1/2} = (YY^H)^{-1/2} = U_y \Gamma_y^+ U_y{}^H \tag{6.39}$$
$$S_{12} = U_x \Gamma_x \Gamma_y^H U_y^H = U_x \Gamma_{xy} U_y^H \tag{6.40}$$

where $\Gamma_x^+ = \text{diag}(\frac{1}{\sigma_1^{(x)}}, \ldots, \frac{1}{\sigma_k^{(x)}}, 0, \ldots, 0)$; similarly for Γ_y^+. Γ_{xy} is a $p \times q$ matrix which can be partitioned as

$$\Gamma_{xy} = \left[\tilde{\Gamma}_{xy} \; 0\right] \tag{6.41}$$

where $\tilde{\Gamma}_{xy}$ is a diagonal matrix which has the form

$$\tilde{\Gamma}_{xy} = \text{diag}(\sigma_1^{(x)} \cdot \sigma_1^{(y)}, \sigma_2^{(x)} \cdot \sigma_2^{(y)}, \cdots, \sigma_k^{(x)} \cdot \sigma_k^{(y)}, 0, \cdots, 0) \tag{6.42}$$

By substituting (6.32), (6.34), (6.35), and (6.37) - (6.39) into Equation (6.33) and simplifying, we obtain

$$\begin{aligned} \tilde{S}_{12} &= S_{11}^{-1/2} S_{12} (S_{22}^{-1/2})^H \\ &= U_x \Gamma_x^+ \Gamma_{xy} \Gamma_y^+ U_y^H \\ &= U_x \begin{bmatrix} I_k & 0 \\ 0 & 0 \end{bmatrix} U_y^H \end{aligned} \tag{6.43}$$

where the matrix I_k is the $k \times k$ identity matrix. Equation (6.43) is in the form of the (unique) singular value decomposition of $\tilde{S}_{12}$. Hence, the largest k singular values of S_{12} are unity, and the remaining values are zero.

Since from (6.25) we have the singular values of $\tilde{S}_{12}$ are the sample canonical correlation coefficients, the proof is complete. □

It is noteworthy that this result is independent of N, the number of snapshots.

Another important property of canonical correlations is given by the following theorem:

Theorem 6.4 *The canonical correlation coefficients are* invariant *with respect to the transformation*

$$\tilde{x} = C\,x \tag{6.44}$$

$$\tilde{y} = B\,y \tag{6.45}$$

where C and B are nonsingular matrices.

Proof: Under the transformation defined by Equations (6.44) and (6.45), the covariance matrices of $\tilde{x}(t)$ and $\tilde{y}(t)$ can be expressed as

$$\tilde{\Sigma}_{11} = C\,\Sigma_{11}C^H = C\,\Sigma_{11}^{1/2}(\Sigma_{11}^{1/2})^H C^H = C\,\Sigma_{11}^{1/2}(C\,\Sigma_{11}^{1/2})^H = \tilde{\Sigma}_{11}^{1/2}(\tilde{\Sigma}_{11}^{1/2})^H \tag{6.46}$$

$$\tilde{\Sigma}_{22} = B\,\Sigma_{22}B^H = B\,\Sigma_{22}^{1/2}(\Sigma_{22}^{1/2})^H B^H = B\,\Sigma_{22}^{1/2}(B\,\Sigma_{22}^{1/2})^H = \tilde{\Sigma}_{22}^{1/2}(\tilde{\Sigma}_{22}^{1/2})^H \tag{6.47}$$

$$\tilde{\Sigma}_{12} = C\,\Sigma_{12}B^H \tag{6.48}$$

where

$$\begin{cases} \tilde{\Sigma}_{11}^{1/2} = C\,\Sigma_{11}^{1/2} \\ \tilde{\Sigma}_{22}^{1/2} = B\,\Sigma_{22}^{1/2} \end{cases} \tag{6.49}$$

are full rank matrices. Therefore, there exist inverses

$$\begin{cases} \tilde{\Sigma}_{11}^{-1/2} = \Sigma_{11}^{-1/2}C^{-1} \\ \tilde{\Sigma}_{22}^{-1/2} = \Sigma_{22}^{-1/2}B^{-1} \end{cases} \tag{6.50}$$

such that

$$\begin{aligned}\tilde{\Sigma}_{11}^{-1/2}\tilde{\Sigma}_{12}(\tilde{\Sigma}_{22}^{-1/2})^H &= \Sigma_{11}^{-1/2}C^{-1}C\,\Sigma_{12}B^H(B^{-1})^H(\Sigma_{22}^{-1/2})^H \\ &= \Sigma_{11}^{-1/2}\Sigma_{12}(\Sigma_{22}^{-1/2})^H \\ &= Q_1PQ_2^H \end{aligned} \tag{6.51}$$

now, define transformation matrices

$$\tilde{L} = Q_1^H\tilde{\Sigma}_{11}^{-1/2} \tag{6.52}$$

$$\tilde{M} = Q_2^H\tilde{\Sigma}_{22}^{-1/2} \tag{6.53}$$

the transformed covariance matrix of $\tilde{x}$ and $\tilde{y}$ becomes

$$\begin{aligned}\tilde{L}\tilde{\Sigma}_{12}\tilde{M}^H &= Q_1^H\tilde{\Sigma}_{11}^{-1/2}\tilde{\Sigma}_{12}(\tilde{\Sigma}_{22}^{-1/2})^HQ_2^H \\ &= Q_1^H\Sigma_{11}^{-1/2}C^{-1}C\,\Sigma_{12}B^H(B^{-1/2})^H(\Sigma_{22}^{-1/2})^HQ_2^H \\ &= Q_1^H\Sigma_{11}^{-1/2}\Sigma_{12}(\Sigma_{22}^{-1/2})^HQ_2^H \\ &= L\Sigma_{12}M^H \end{aligned} \tag{6.54}$$

That is,

$$\tilde{L}\tilde{\Sigma}_{12}\tilde{M}^H = L\Sigma_{12}M^H = P \tag{6.55}$$

where P is a matrix with the form defined by Equations (6.6) (6.7). Referring to the definition of the canonical correlation coefficients given in Section 3, we can immediately derive the conclusion that the canonical correlation coefficients for the transformed variables $\tilde{x}(t)$ and $\tilde{y}(t)$ are the same as that of $x(t)$

Theorem 6.5 *The sample canonical correlation coefficients γ_i are consistent estimates of the true coefficients ρ_i.*

Proof: The proof follows directly from the fact that $\hat{\Sigma} = \frac{1}{N}S \to \Sigma$ as $N \to \infty$. □

Chapter 7

Detection using canonical correlation analysis

In this chapter, the canonical correlation analysis discussed in the last chapter is used in developing a new method for detecting the number of signals in a class of unknown noise environments. The noise considered here may be spatially uncorrelated, or correlated over a limited spatial range. In other words, the covariance matrix of the noise has a banded structure (white noise can also be considered as a special case since its bandwidth is equal to one). For this class of noise, the bi-array structure proposed in Chapter 5 and the canonical correlation analysis discussed in Chapter 6 are applied to solve the detection problem. For applying the canonical correlation analysis technique, the array geometric structures and the relative spatial positions which may be used are quite broad. However, in this chapter, we use a bi-array structure with two linear, equally spaced arrays with parallel normals in our derivation since this simple geometry is not only suitable for clearly illustrating the basic principle of our new method, but is also a commonly used structure in theoretical derivations and in the engineering practice of array systems.

7.1 Formulation of the problem

Let us consider k independent narrow band signals arriving from k different directions at two spatially separated linear arrays as shown in Figure 5.5. These arrays are denoted by

X and Y with p and q sensors respectively. The outputs of these two arrays are denoted by vectors $\boldsymbol{x}(t)$, $\boldsymbol{y}(t)$ which can be expressed as

$$\boldsymbol{x}(t) = \boldsymbol{A}_x \boldsymbol{s}(t) + \boldsymbol{n}_x(t) \tag{7.1}$$

$$\boldsymbol{y}(t) = \boldsymbol{A}_y \boldsymbol{B} \boldsymbol{s}(t) + \boldsymbol{n}_y(t) \tag{7.2}$$

where $\boldsymbol{s}(t)$ is a $k \times 1$ vector, describing the complex envelopes of k narrow band signals. The elements of $\boldsymbol{s}(t)$ are assumed to be independent Gaussian distributed random variables with zero mean. $\boldsymbol{A}_x$ and $\boldsymbol{A}_y$ are $p \times k$ and $q \times k$ matrices, representing direction matrices of the k signals. For simplicity, we assume: (1) the elements of each of the two arrays are equally spaced by d, (d is less than or equal to the half-wavelength of the incident fields), and (2) the normal of the two arrays are parallel. The direction matrices can be expressed under these assumptions as,

$$\boldsymbol{A}_x = \begin{bmatrix} 1 & 1 & \dots & 1 \\ e^{j\phi_1} & e^{j\phi_2} & \dots & e^{j\phi_k} \\ e^{j2\phi_1} & e^{j2\phi_2} & \dots & e^{j2\phi_k} \\ \dots & \dots & & \dots \\ e^{j(p-1)\phi_1} & e^{j(p-1)\phi_2} & \dots & e^{j(p-1)\phi_k} \end{bmatrix} \tag{7.3}$$

$$\boldsymbol{A}_y = \begin{bmatrix} 1 & 1 & \dots & 1 \\ e^{j\phi_1} & e^{j\phi_2} & \dots & e^{j\phi_k} \\ e^{j2\phi_1} & e^{j2\phi_2} & \dots & e^{j2\phi_k} \\ \dots & \dots & & \dots \\ e^{j(q-1)\phi_1} & e^{j(q-1)\phi_2} & \dots & e^{j(q-1)\phi_k} \end{bmatrix} \tag{7.4}$$

where $\phi_1, \phi_2, \dots, \phi_k$ are unique functions of the angles of arrival of the k signals. $\boldsymbol{B}$ is a diagonal matrix of dimension $k \times k$, the diagonal elements of which are the relative phase shifts of the k signals between the two arrays,

$$\boldsymbol{B} = \mathrm{diag}(\, e^{j\Delta_1}, \dots, e^{j\Delta_k} \,) \tag{7.5}$$

where Δ_i is defined as

$$\Delta_i = \frac{\omega d_{xy}}{c} \sin(\theta_i - \theta_{xy}) \tag{7.6}$$

where d_{xy} and θ_{xy} are parameters specifying the relative position of array X and array Y as shown in Figure 5.5, and ω is the angular frequency of the narrow band signals, c is the velocity of propagation. The vectors $\boldsymbol{n}_x(t)$ and $\boldsymbol{n}_y(t)$ are p and q dimensional vectors respectively, representing noise components in the outputs of array X and array Y. The noise is assumed to be Gaussian, complex, zero mean, with cross-covariance matrix satisfying

$$\boldsymbol{\Sigma}_{nxy} = E[\boldsymbol{n}_x(t)\boldsymbol{n}_y^H(t)] = \boldsymbol{O}, \tag{7.7}$$

where $\boldsymbol{O}$ denotes a $p \times q$ null matrix. Equation (7.7) implies that we may consider array X and array Y as two non-overlapping parts of a larger non-contiguous array, the noise covariance elements of which satisfy

$$\sigma_n(i,j) = 0 \quad \forall \ |i-j| \geq \delta \tag{7.8}$$

where δ, a constant defined in Figure 5.4, represents the half band width of the variance-covariance matrix structure of the noise of the large array. The output of this large array can be expressed by a composite vector $\boldsymbol{z}(t)$ with $\boldsymbol{x}(t)$ and $\boldsymbol{y}(t)$ as its components,

$$\boldsymbol{z}(t) = \begin{bmatrix} \boldsymbol{x}(t) \\ \boldsymbol{y}(t) \end{bmatrix} \tag{7.9}$$

The covariance matrix $\boldsymbol{\Sigma}$ of $\boldsymbol{z}(t)$ can be written as

$$\boldsymbol{\Sigma} = E[\boldsymbol{z}(t)\boldsymbol{z}(t)^H] = \begin{matrix} \\ p \\ q \end{matrix} \begin{bmatrix} \boldsymbol{\Sigma}_{11} & \boldsymbol{\Sigma}_{12} \\ \boldsymbol{\Sigma}_{21} & \boldsymbol{\Sigma}_{22} \end{bmatrix} \begin{matrix} \\ p \\ q \end{matrix} \tag{7.10}$$

In Equation (7.10), we have partitioned $\boldsymbol{\Sigma}$ according to the dimensions of $\boldsymbol{x}(t)$ and $\boldsymbol{y}(t)$ respectively. Without loss of generality, in the following discussion, we assume that $p \leq q$.

Assuming there exist k signals, the covariance between $\boldsymbol{x}(t)$ and $\boldsymbol{y}(t)$ is represented by the upper right submatrix $\boldsymbol{\Sigma}_{12}$ of $\boldsymbol{\Sigma}$ which may be expressed as

$$\begin{aligned} \boldsymbol{\Sigma}_{12} &= E[\boldsymbol{x}(t)\boldsymbol{y}^H(t)] \\ &= E[\boldsymbol{A}_x \boldsymbol{s}(t)\boldsymbol{s}^H(t)\boldsymbol{B}^H\boldsymbol{A}_y^H] \\ &= \boldsymbol{A}_x E[\boldsymbol{s}(t)\boldsymbol{s}^H(t)]\boldsymbol{B}^H\boldsymbol{A}_y^H \\ &= \boldsymbol{A}_x\boldsymbol{\Sigma}_s\boldsymbol{B}^H\boldsymbol{A}_y^H. \end{aligned} \tag{7.11}$$

where Σ_s is the $k \times k$ covariance matrix of the signals. The matrix Σ_s is full rank because the k signals are assumed independent. The matrices A_x, A_y are full column rank because the angles of arrival are all distinct, and B is a $k \times k$ full rank matrix; therefore, rank $(\Sigma_{12}) = k$, the number of signals.

Our detection procedure is based on the sampled outputs of $x(t)$. If we denote the set of samples by $x_1, x_2, \cdots, x_N$, as given by Equation (6.24) in last chapter, the maximum likelihood estimate of Σ is

$$\hat{\Sigma} = \frac{1}{N} \sum_{i=1}^{N} x_i x_i^H \ . \tag{7.12}$$

Making use of the fact that rank$(\Sigma_{12}) = k$, in the presence of signal and noise, the number of signals may be determined by testing the rank of $\hat{\Sigma}_{12}$, the sample estimate of Σ_{12} or equivalently, by testing the rank of S_{12} since $S_{12} = \hat{\Sigma}_{12}/N$. One possible way to accomplish this is to test the significance of the singular values of S_{12}. However, due to the possible involvement of unknown spatially correlated noise, these singular values are still not invariant to changes in spatial spectra of the noise. To obtain an invariant detection method, instead of testing the singular values of S_{12} directly, we test the amplitude of the singular values of a matrix with a standard form $\tilde{S}_{12}$. This matrix is obtained by converting S_{12} through the canonical transform given in last chapter. The singular values of matrix $\tilde{S}_{12}$ are invariant to the changes in the noise spectra.

7.2 Detection by testing the sample canonical correlation coefficients

Assume the canonical correlation coefficients of the outputs of array X and array Y are arranged in descending order of magnitude,

$$1 \geq \rho_1 \geq \rho_2 \geq \ldots \geq \rho_k > \rho_{k+1} = \rho_{k+2} = \ldots = \rho_p = 0 \ , \tag{7.13}$$

and a similar relation is also applied to the sample canonical correlation coefficients γ_i which are defined by Equations (6.25) (6.26), and (6.27). We consider the following set of

hypotheses:

$$H_m: \ \rho_1 \neq 0, \ \rho_2 \neq 0, \ ..., \ \rho_m \neq 0, \ \rho_{m+1} = \rho_{m+2} = \ ... \ = \rho_p = 0 \qquad (7.14)$$

for $m = p, \ p-1, \ \ldots, \ 0$. The physical meaning of the index m is the assumed number of signals under test. The detection problem is thus equivalent to a multiple hypothesis test to determine which value of m is most likely.

The procedure of testing $\{H_m\}$ to find the most likely m value is a multiple hypothesis test [62] which needs to be decomposed to a sequence of structured binary hypothesis tests. A traditional way to obtain such a decomposition is to construct each elementary binary hypothesis by applying two adjacent members among $\{H_m\}$. In other words, the multiple hypothesis test is decomposed to p elementary binary hypothesis tests; in each elementary binary hypothesis test, a primary hypothesis H_m is tested against its adjacent hypothesis H_{m-1}, for $m = p, p-1, \ldots, 1$. The hypothesis testing procedure starts with $m = p$, that is, by testing H_p against H_{p-1}. If H_p is accepted, we declare $\hat{k} = p$ and stop. Otherwise, we accept the alternative H_{p-1} at the stage $m = p$, decrement m by one and use H_{p-1} as the primary hypothesis of the next stage. The procedure is continued until a primary hypothesis is accepted. (Note that if the test continues until $m = 1$ and if H_1 is rejected, then the alternative hypothesis H_0 is accepted. Hence, all hypotheses from $p, \ p-1, \ \ldots, \ 0$ are considered). The logical structure of this testing procedure is summarized in Figure 7.1.

The criterion used for each step of binary hypothesis testing in Figure 7.1 is the likelihood ratio of the primary hypothesis and the alternative hypothesis in that step of testing. Denote the observation matrix $Z = [z_1, \ \cdots, \ z_N]$ and let $L(Z|\Omega_m)$ be the likelihood function of the observation Z with parameters in Ω_m, the parameter space constrained by the hypothesis H_m. The likelihood ratio for testing H_m against H_{m-1} is defined by

$$\Lambda_m^{(1)}(Z) = \frac{\max_{\Omega_m} L(Z|\Omega_m)}{\max_{\Omega_{m-1}} L(Z|\Omega_{m-1})} \ , \qquad (7.15)$$

where the superscript of $\Lambda_m^{(1)}(Z)$ distinguishes this likelihood ratio from the likelihood ratios proposed later. It is shown in Appendix A of this chapter that the maximum value of

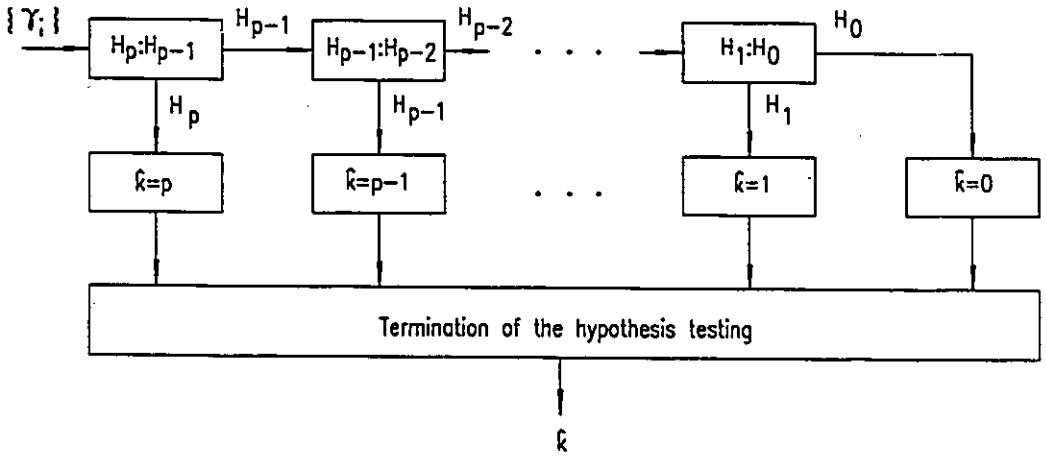

Figure 7.1: Testing Scheme 1: using traditional hypothesis decomposition.

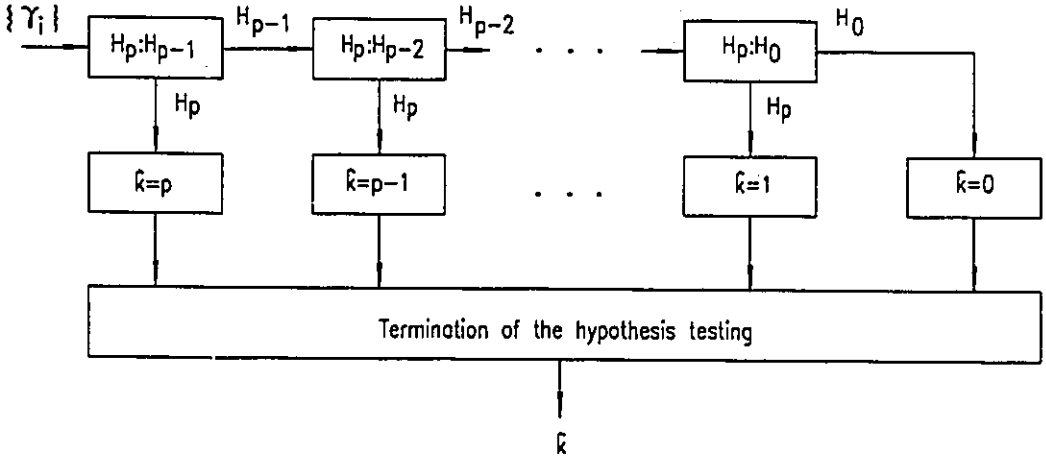

Figure 7.2: Testing Scheme 2: using a modified hypothesis decomposition.

$L(Z|\Omega_m)$ is

$$f_m^* = \max_{\Omega_m} L(Z|\Omega_m) = |\tilde{M}^{-1}|^2 \prod_{i=1}^{m}(1-\gamma_i^2) \,. \tag{7.16}$$

Therefore, the likelihood ratio defined by Equation (7.15) can be expressed by the sample canonical correlation coefficients as

$$\Lambda_m^{(1)}(Z) = \frac{\max_{\Omega_m} L(Z|\Omega_m)}{\max_{\Omega_{m-1}} L(Z|\Omega_{m-1})} = 1-\gamma_m^2 \,. \tag{7.17}$$

This likelihood ratio has a very simple formulation, in that only one sample canonical correlation coefficient is required in each step of the test. However, the price paid for this simplicity is the complexity of the effort required to determine the threshold values used in the hypothesis testing. The statistic support for determining the threshold value which is compared with this likelihood ratio in each elementary hypothesis test is unknown. The derivation of the distribution function of the likelihood ratio given by Equation (7.17) is quite complex. The complexity is caused by the fact that the marginal distributions of each sample canonical correlation coefficient can only be obtained through a $(p-k-1)$-fold integration which is a complicated procedure, and thus makes this scheme less attractive.

To find a better decomposition scheme, we note that canonical correlation analysis has a long history; there are previous results which give distribution rules related to sample canonical correlation coefficients. The χ^2 approximation given by Bartlett is one of these results. This approximation rule is given as follows.

Bartlett's approximation [1] [7][8]:

When the hypothesis

$$\mathrm{H}_{m-1}: \ \rho_1 \neq 0,\ \rho_2 \neq 0,\ \ldots,\ \rho_{m-1} \neq 0,\ \rho_m = \rho_{m+1} = \ \ldots\ = \rho_p = 0 \tag{7.18}$$

is true, the asymptotic distribution of the statistic

$$C(m) = -2\,[N - \frac{1}{2}(p+q+1)] \sum_{i=m}^{p} \log(1-\gamma_i^2) \tag{7.19}$$

is χ^2 with $2(p-m+1)(q-m+1)$ degrees of freedom. The factor $[N-\frac{1}{2}(p+q+1)]$ in Equation (7.19) is known as Bartlett's correction factor.

[1] The formula given here has beer modified for complex data

It is interesting to notice that the summation part in the statistic given by Equation (7.19) is the logarithm of the likelihood ratio of hypothesis H_p against $H_m - 1$. This likelihood ratio can be readily obtained using Equation (7.16) as

$$\Lambda_m^{(2)}(Z) = \frac{\max_{\Omega_p} L(Z|\Omega_p)}{\max_{\Omega_{m-1}} L(Z|\Omega_{m-1})} = \prod_{i=m}^{p}(1-\gamma_i^2) \ , \tag{7.20}$$

where the superscript of $\Lambda_m^{(2)}(Z)$ distinguishes this likelihood ratio from the one used in scheme 1. Therefore, a new decomposition scheme can be constructed by replacing $\Lambda_m^{(1)}(Z)$ in scheme 1 with $\Lambda_m^{(2)}(Z)$. This new scheme is illustrated by Figure 7.2.

In each step of the scheme shown by Figure 7.2, H_p is tested as the primary hypothesis against alternative hypothesis H_{m-1}, for $m = p, \cdots, 1$ respectively. With this testing strategy, as many noise subspace sample canonical correlation coefficients as possible are included in the testing criterion, so that Bartlett's result can be applied and the multi-fold integration required in the threshold setting for Scheme 1 can be avoided. Compared with the likelihood ratio used in Scheme 1, the only change in the new likelihood ratio is that the primary hypothesis H_m is replaced by H_p. This is a logical replacement because when the test reaches stage m, all the population canonical correlation coefficients with indices larger than m have already been accepted as zero. This new condition which is set up during the test procedure makes H_p convey the same meaning as H_m at stage m, although the threshold values for testing the resulting criteria may be different. This equivalence can also be shown by demonstrating the inter-connection between the thresholds applied in these two schemes.

From Equation (7.17), the criterion used for Scheme 1 is given by,

$$\Lambda_m^{(1)}(Z) = \frac{\max_{\Omega_m} L(Z|\Omega_m)}{\max_{\Omega_{m-1}} L(Z|\Omega_{m-1})} = 1-\gamma_m^2 \underset{H_{m-1}}{\overset{H_m}{\gtrless}} T_m^{(1)} \tag{7.21}$$

where $T_m^{(1)}$ denotes the threshold value in stage m of scheme 1.

For Scheme 2, in stage m, the likelihood ratio testing criterion be obtained using Equation (7.16) as

$$\Lambda_m^{(2)}(Z) = \frac{\max_{\Omega_p} L(Z|\Omega_p)}{\max_{\Omega_{m-1}} L(Z|\Omega_{m-1})} = \prod_{i=m}^{p}(1-\gamma_i^2) \underset{H_{m-1}}{\overset{H_m}{\gtrless}} T_m^{(2)} \ , \tag{7.22}$$

where the superscript of $\Lambda_m^{(2)}(Z)$ and $T_m^{(2)}$ indicates these likelihood ratio and threshold are for Scheme 2. Compared with the criterion used for Scheme 1, it can be found that $\Lambda_m^{(1)}(Z)$ and $\Lambda_m^{(2)}(Z)$ are related by

$$\Lambda_m^{(2)}(Z) = \prod_{i=m}^{p} \Lambda_i^{(1)}(Z) \ . \tag{7.23}$$

To show the relation between thresholds $T_m^{(1)}$ and $T_m^{(2)}$, we trace the testing procedures for both Scheme 1 and Scheme 2 comparatively. Starting with $m = p$, the criteria at this stage are the same for both schemes, so are the thresholds. If $\Lambda_p^{(1)}(Z) > T_p^{(1)}$ (or $\Lambda_p^{(2)}(Z) > T_p^{(2)}$ for Scheme 2), then H_p is accepted and the test is stopped, and the estimated number of signals is assigned as p. If $\Lambda_p^{(1)}(Z) \leq T_p^{(1)}$, or in other words, $\Lambda_p^{(1)}(Z) = \alpha_p T_p^{(1)}$, where $\alpha_p \leq 1$, then the test is continued with a reduced value of m. At stage m, for Scheme 1 we need to test

$$\Lambda_m^{(1)}(Z) \underset{H_{m-1}}{\overset{H_m}{\gtrless}} T_m^{(1)} \tag{7.24}$$

and for Scheme 2, the test is

$$\Lambda_m^{(2)}(Z) = \textstyle\prod_{i=m}^{p} \Lambda_m^{(1)}(Z) \underset{H_{m-1}}{\overset{H_m}{\gtrless}} T_m^{(2)} \tag{7.25}$$

Notice that when stage m is reached, from the previous binary hypothesis testing stages, we already have

$$\begin{aligned} \Lambda_p^{(1)}(Z) &= \alpha_p T_p^{(1)} \\ \Lambda_{p-1}^{(1)}(Z) &= \alpha_{p-1} T_{p-1}^{(1)} \\ &\vdots \\ \Lambda_{m+1}^{(1)}(Z) &= \alpha_{m+1} T_{m+1}^{(1)} \end{aligned} \tag{7.26}$$

where $\alpha_p \leq 1, \cdots, \alpha_{m+1} \leq 1$ are known numbers at this stage with given samples Z.

Therefore, the threshold value of Scheme 2 can be expressed by the threshold values of Scheme 1 at the current stage and previous stages as

$$T_m^{(2)} = \alpha_p T_p^{(1)} \alpha_{p-1} T_{p-1}^{(1)} \cdots \alpha_{m+1} T_{m+1}^{(1)} T_m^{(1)} \tag{7.27}$$

for $m = p, \cdots, 1$. This set of equations gives a one-to-one correspondence between the two sets of thresholds for a given set of samples Z. Thus, Scheme 1 and Scheme 2 are equivalent.

The reason why the two schemes are discussed is as follows. Scheme 1 is the most rigorous from a statistical perspective, whereas Scheme 2 is far easier to use. By establishing the equivalence of these two schemes, we have demonstrated the validity of using Scheme 2. Therefore, in the sequel, we consider only Scheme 2.

With scheme 2 the multiple hypothesis test is decomposed. By generating a set of thresholds T_m, $m = p, p-1, \ldots, 1$ according to the χ^2 distribution rule given by Bartlett's approximation, such that the probability of exceeding the threshold remains constant for each value of m, we may recursively test each hypothesis H_m in turn. The value of m where $C(m)$ first exceeds the threshold T_m corresponds to the most likely number of signals.

We now turn our attention to the performance of this detection algorithm. From the testing structure, we know that a correct detection happens when $\hat{k} = k$, otherwise we say an error has occurred. Furthermore, an error can be classified into two kinds; whenever $\hat{k} < k$, we say a missing error has occurred. Whenever $\hat{k} > k$, we say a false alarm error has occurred. A miss happens when $C(m)$ is below threshold for $m \leq k$. A false alarm happens when $C(m)$ exceeds the threshold for $m > k$. Accordingly, the probability of detection error can be expressed by

$$P_e = 1 - P_D = P_M + P_F \tag{7.28}$$

where P_e is the total probability of a detection error, and P_D is the probability of a correct detection. P_M is the probability of missing; P_F is the probability of false alarm.

In this analysis, we concentrate only on the probability of false alarm, because P_F is the dominant detection error mechanism at moderate and high SNR conditions. That P_F is dominant may be justified in the following way. First, according to (7.19), $C(m)$ is approximately χ^2-distributed for $m > k$, independent of SNR. On the other hand, we see from Theorem 6.3 that, for a specific N, the signal coefficients approach unity as the SNR becomes large. Hence, with fixed N and increasing SNR, the probability of $C(m)$ exceeding the threshold remains approximately constant for $m > k$ (false alarm), whereas the probability of $C(m)$ being smaller than the threshold for $m \leq k$ (missing) becomes small. Hence, P_F dominates at high SNR. Therefore, by considering only the medium/high SNR

case, the performance of the method may be quantified by considering only the probability of false alarm.

We further simplify the error analysis as follows. It has been verified [70] that since γ_{k+1} is the largest of the noise canonical correlation coefficients, $C(k+1)$ is more likely to exceed the threshold T_{k+1} than $C(k+2),\ldots,C(p)$ are likely to exceed their respective thresholds. Therefore, P_F, the composite probability of false alarm, is dominated by $P[C(k+1) > T_{k+1}]$, the probability of false alarming one signal given k signals are present. The latter symbol is denoted by $P_{F|k}(1)$.

If H_m is true, then $P_{F|m}(1)$ is related to the threshold value T_{m+1}, according to Bartlett's criterion by

$$P_{F|m}(1) = \int_{T_{m+1}}^{\infty} \frac{1}{2^{\frac{n}{2}}\Gamma(\frac{n}{2})} x^{\frac{n-2}{2}} e^{\frac{x}{2}} dx\,, \qquad m = 0,1,2,...,p-1 \tag{7.29}$$

where $n = 2(p-m)(q-m)$. Therefore, for a specified false alarm error rate, the required threshold values can be determined by solving this equation for T_{m+1} for $m = 0,\ 1,\cdots,p-1$. The details of this process are given in Appendix B of this chapter. The threshold values generated in this way maintain the false alarm rate at approximately the specified level for $k = 0,1,...,p-1$. Therefore, the performance of the new criterion is *quantitatively controllable.*

The proposed detection procedure, with a means of controlling the moderate to high SNR performance, is now complete. The steps involved in the execution of the method are outlined below:

1. Use the sample outputs x_1, x_2, ..., x_N of array X and y_1, y_2, ..., y_N of array Y to form the sample product matrices S_{11}, S_{22}, and S_{12} by

$$S_{11} = \sum_{i=1}^{N} x_i x_i^H \tag{7.30}$$

$$S_{22} = \sum_{i=1}^{N} y_i y_i^H \tag{7.31}$$

$$S_{12} = \sum_{i=1}^{N} x_i y_i^H\,. \tag{7.32}$$

2. Calculate the singular values $\gamma_1, \gamma_2, \ldots, \gamma_p$, of the transformed matrix

$$\tilde{S}_{12} = S_{11}^{-1/2} S_{12} (S_{22}^{-1/2})^H . \tag{7.33}$$

3. For a specified false alarm rate P_F a set of threshold values $\{T_m\}$ can be pre-calculated according to χ^2 distributions with $2(p-m+1)(q-m+1)$, $m = p, \ldots, 1$, degrees of freedom, where m is the assumed number of signals under test. The details of the method for obtaining the thresholds can be found in Appendix B of this chapter.

4. Hypothesis testing: Denote the hypothesis that there are m signals by H_m. The testing starts from $m = p$. For each m, the criterion

$$C(m) = -2\,[N - \frac{1}{2}(p+q+1)] \sum_{i=m}^{p} \log(1-\gamma_i^2) \tag{7.34}$$

is compared with threshold value T_m. If the criterion is larger than the threshold, we accept H_m, stop the testing, and assign the value of $\hat{k} = m$. Otherwise we reject the hypothesis, decrease m by one, and continue the testing until a H_m is accepted, or m becomes 1. At this stage, if the criterion exceeds the threshold, then H_1 is accepted; otherwise, the alternative H_0 is chosen.

There are other criteria for hypothesis testing using canonical correlation coefficients [67] [45]. However, here we concentrate exclusively on Bartlett's criterion.

7.3 Simulations and Discussion

7.3.1 Design of the computer simulations

To examine the detection method we proposed above, a group of computer simulations are designed to check the performance of the new method, and to compare it with the existing detection methods, namely, AIC and MDL.

The new method is examined using computer generated data which simulates the signals polluted by spatially correlated noise. The noise data are generated by a group

Table 7.1: MA COEFFICIENTS FOR THE NOISE MODEL

Model No.	b_0	b_1	b_2
1	1.00	$0.90i$	-0.81
2	1.00	$0.40i$	-0.16
3	1.00	$0.10i$	-0.01

of Moving Average (MA) models. The reason for using an MA model is the correlation coefficients of a moving average process are "tail cut". In other words, the covariance matrix of a moving average process is of banded structure, which coincides with the basic assumption of the new method.

The theoretical covariance matrix of the MA noise is generated in following way. Assuming the MA coefficients are given by b_0, b_1, $\cdots$, b_m, the covariance matrix of the MA process can be formed by [24]

$$\boldsymbol{R}_n = \left(\sum_{i=0}^{p} b_i Y_i\right)\left(\sum_{i=0}^{p} b_i Y_i\right)^H \tag{7.35}$$

where $\{Y_i\}$ are rectangular $p_n \times 2p_n$ (p_n is the dimension of the noise covariance matrix) matrices defined by

$$Y_i(j,k) = \begin{cases} 1 & \text{if } k-j=i \\ 0 & \text{otherwise} \end{cases} \tag{7.36}$$

Once the noise covariance matrix is constructed, it can be used to convert white noise (such as pseudo white noise generated by computers) into noise with a specified covariance matrix through the following transformation,

$$\boldsymbol{V} = \boldsymbol{R}_n^{1/2}\boldsymbol{W} \tag{7.37}$$

where $\boldsymbol{W}$ is the white noise data matrix, and $\boldsymbol{V}$ is the noise data matrix with covariance matrix $\boldsymbol{R}_n$.

To give the new method a more complete performance picture, three different noise matrices, which correspond to different levels of severity of noise correlation, are used. The

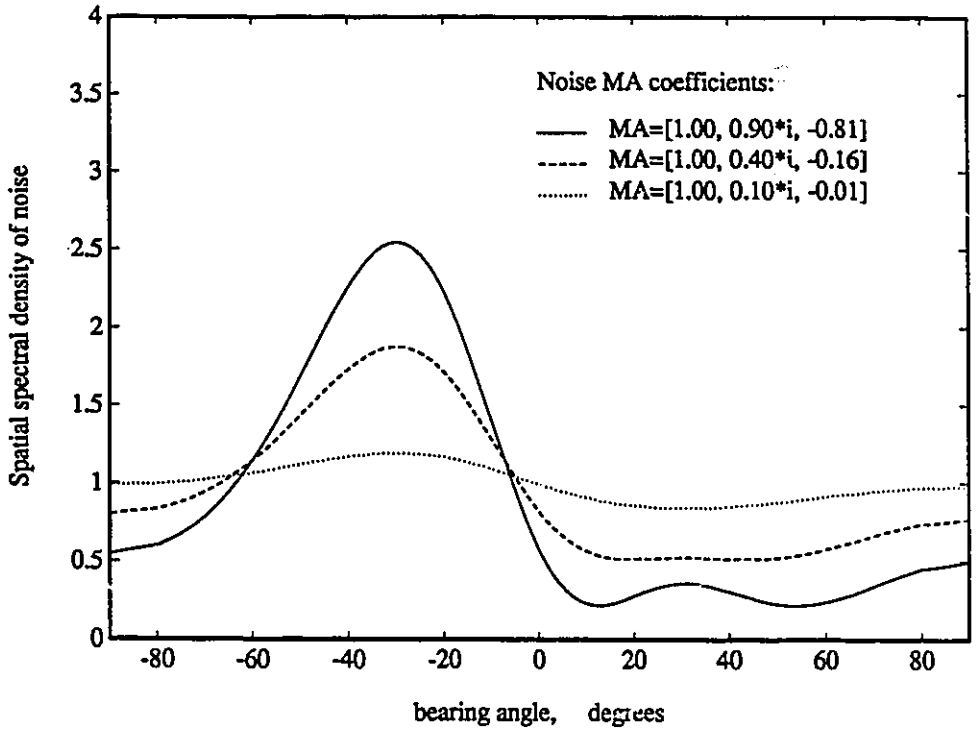

Figure 7.3: Spectra of the coloured noise used in the simulations

Table 7.2: THRESHOLD VALUES FOR $p = 8$, $q = 8$

Theoretical P_F	10^{-1}	10^{-2}	10^{-3}	10^{-4}	10^{-5}
$s = 8$	4.6052	9.2103	13.8155	18.4207	23.0259
$s = 7$	13.3616	20.0902	26.1245	31.8276	37.3316
$s = 6$	25.9894	34.8053	42.3124	49.1894	55.6829
$s = 5$	42.5847	53.4858	62.4872	70.5712	78.0942
$s = 4$	63.1671	76.1539	86.6608	95.9687	104.5417
$s = 3$	87.7430	102.8163	114.8351	125.3766	135.0114
$s = 2$	116.3153	133.4757	147.0104	158.7915	169.4956
$s = 1$	148.8853	168.1332	183.1864	196.2112	207.9896

MA coefficients for these three noise matrices are given in Table 7.1. The bandwidth of the noise covariance matrix used in the simulations is three. The spatial spectra of the noise generated by each MA model are plotted in Figure 7.3. Two closely located signals are used in the simulation. The separation of these two signals is 0.5 standard beamwidths of an 8-element array. The simulations use four different directions of arrival with fixed signal separations. By doing so, the performance of the new method for different relative locations of the signals and the noise peaks can be checked. The number of sensors of array X and array Y each equal eight. The two arrays are assumed to be linear, and the two arrays are oriented along the same line. The sensors of the arrays are equally spaced with separation equal to a half wavelength.

To check the accuracy of the theoretical false alarm given by Equation (7.29), five groups of thresholds corresponding to theoretical false alarm rates (TFR) of $P_F = 10^{-1}, \ldots, 10^{-5}$ are generated and used in the simulations. These threshold values are listed in Table 7.2. The MATLAB program for generating these threshold is enclosed as Appendix B of this chapter.

In all the simulations the SNR is defined as the ratio of total signal power to total noise power of the arrays.

Table 7.3: COMPARISON OF TFR WITH SIMULATION RESULTS

Theoretical P_F	10^{-1}	10^{-2}	10^{-3}	10^{-4}
Simulation $\hat{P}_F$	0.93×10^{-1}	0.87×10^{-2}	0.83×10^{-3}	0.87×10^{-4}

* 195,000 trials are averaged over SNR range 6 to 15 dB.

7.3.2 Simulation results and discussion

The results of the simulation are given in one table and five figures. In Table 7.3, the average false alarm rates of the simulations for the CCT method are compared with the theoretic values. These results were obtained using a wide range of coloured noise models and different signal locations. In total 195,000 trials are averaged. From these results, we see that the false alarm rates obtained from simulations are in close agreement with the specified P_F values.

The error performance of the CCT method with respect to SNR is illustrated by the simulation results given in Figure 7.4 to Figure 7.8, each corresponding to a specific theoretic false alarm rate. The parameters of the noise model (MA coefficients) are labeled on the bottom of each figure.

Figure 7.4 gives simulation results for TFR=10^{-1}. It can be observed that that in the moderate and high SNR range (in which the detection error is dominated by false alarms), the detection error rate is close to the theoretic value of 10^{-1}, and is invariant to changes in noise spectrum and the position of the signals. This shows the robustness of the new method with respect to coloured noise, and this characteristic is a result of the invariant property of the canonical correlation coefficients given by Theorem 6.3. In the lower SNR portion of the curve, however, the P_e–SNR threshold changes its position when the signal position is changed. This is understandable, since as we mentioned before, missing errors are SNR dependent. When the signals are located around the peaks of the noise spectrum, the noise has more effect on the signal, which results in a lower effective SNR. Therefore, a higher SNR value than what is required for the white noise case is required to reach the

point beyond which a missing error can be eliminated. In contrast, if the signals are located in the valley of the noise spectrum, the effective SNR is higher, so the threshold appears at a lower value of SNR. The three plots of Figure 7.4 also demonstrate the trend that when the noise spectrum becomes flat, the effect of signal position on effective SNR diminishes, and the threshold SNR values for different signal positions converge to the same value of SNR. When the SNR value increases beyond a certain value, missing errors are almost eliminated.

The four figures following Figure 7.4 confirm the robustness of our new method for different TFR values (TFR=10^{-2}, 10^{-3}, 10^{-4}, 10^{-5} respectively for these four figures). Comparing Figure 7.4 to Figure 7.8, the tradeoff between TFR and P_e-SNR threshold caused mainly by missing errors, can be observed.

To compare our new CCT method with other existing methods, the widely accepted AIC and MDL criteria are also tested in the same noise environment. The results are shown in Figure 7.9 to Figure 7.12.

The plots in Figures 7.9 and Figure 7.11 are the simulation results for AIC and MDL respectively, from an 8-sensor array (the same number of sensors used by array X of the CCT method). For the results in Figure 7.11 and Figure 7.12, the number of sensors is 16 (the sum of the sensors used by both array X and array Y of the CCT method).

Comparing Figures 7.9 and 7.10 to Figures 7.4- 7.8, (also with reference to Figure 7.3), we see that, even under very mildly coloured noise (MA=[1.00, 0.10i, -0.01]), the performance of AIC experiences severe degradation. On the other hand, we see that the performance of the CCT method is relatively robust to changes in the shape of the noise spectrum, and continues to maintain its controllable high-SNR performance. Also it is observed that MDL no longer exhibits continuously diminishing P_e with increasing SNR as it does under white noise, and starts to show slight false alarm errors in the high SNR range.

For an intermediate degree of noise colour (MA=[1.00, 0.40i, -0.16]), $P_e \rightarrow 100\%$ for AIC. This is because AIC requires the noise to have a flat spectral shape. For the same reason, MDL has also degraded substantially, whereas the performance of the CCT has remained relatively unchanged. Comparing the performance of MDL and AIC, we see that

Table 7.4: COMPARISON OF COMPUTATIONAL INTENSITY*

Method,Size	AIC,MDL, $p = 8$	CCT, $p = q = 8$	AIC,MDL, $p = 16$
Flops/trial	60319	126675	262189

* This comparison is done by using the FLOP function of MATLAB; N=100; one flop is defined as one multiplication and one addition

MDL shows somewhat more tolerance than AIC, because MDL is over-penalized, as has been mentioned in several papers [70] [73].

For a relatively large degree of colour (MA=[1.0, 0.90i, -0.81]), the performance of the CCT method again remains relatively constant. In this case, both MDL and AIC fail completely ($P_e \rightarrow 100\%$).

The results using a 16-sensor array show basically the same comparison, except for lower SNR thresholds. This is because the 16-sensor array gives a larger sample size. However, this advantage contributes little to improve the coloured noise performance of MDL and AIC.

The comparison of the computational intensity for the CCT method, and AIC, MDL with 8, and 16 sensors is listed in Table 7.4.

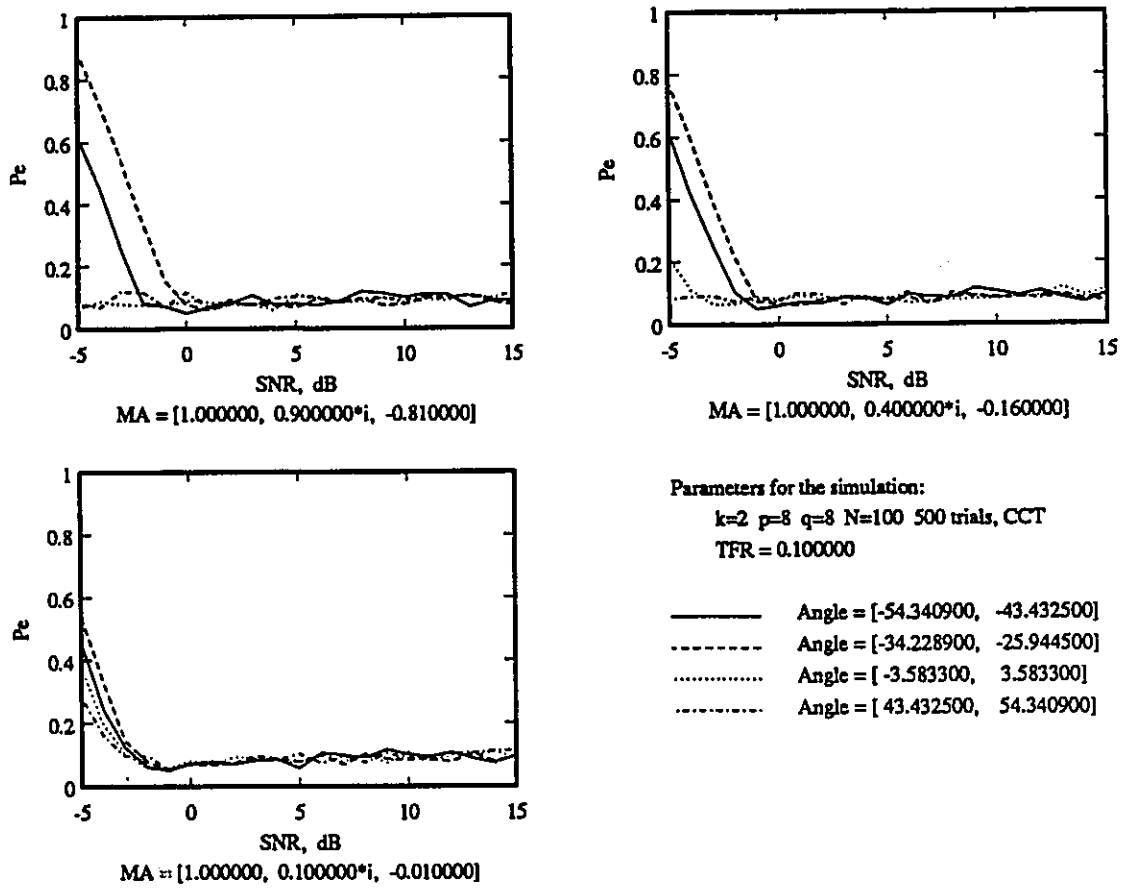

Figure 7.4: Simulation results of CCT method for TFR=10^{-1}

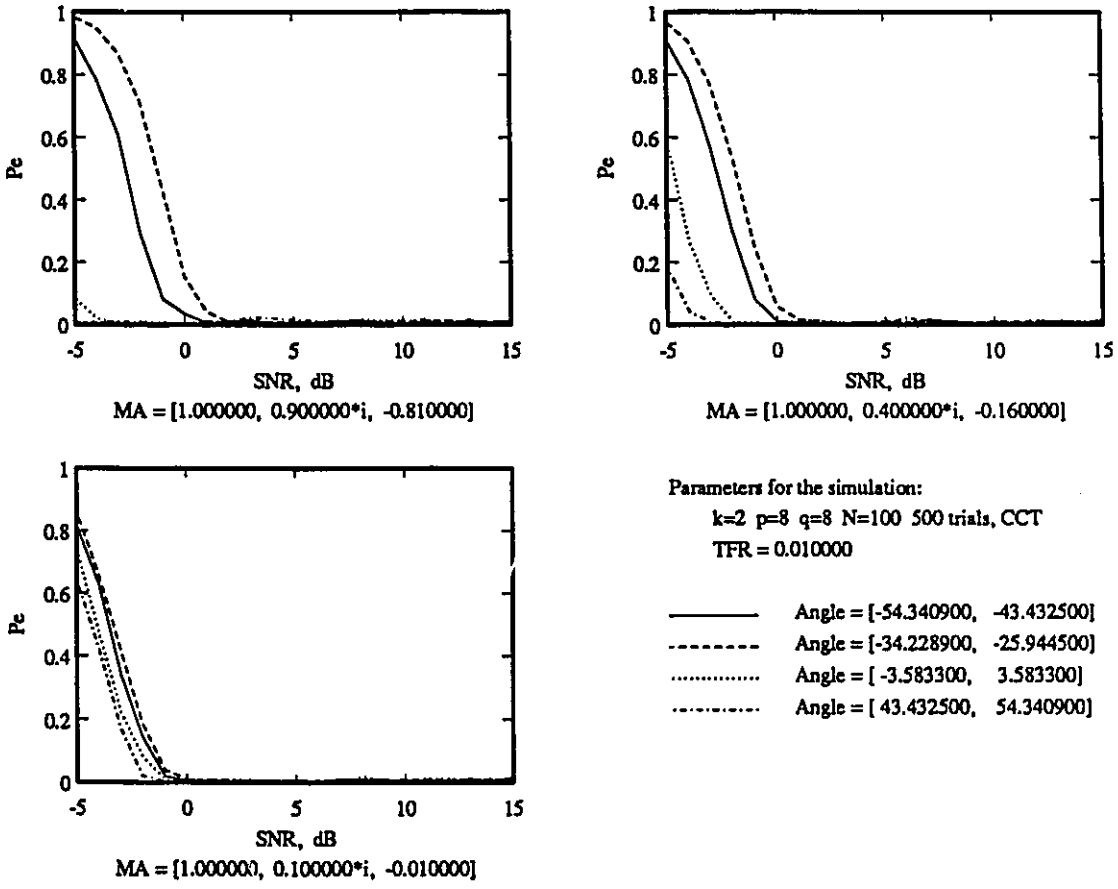

Figure 7.5: Simulation results of CCT method for TFR=10^{-2}

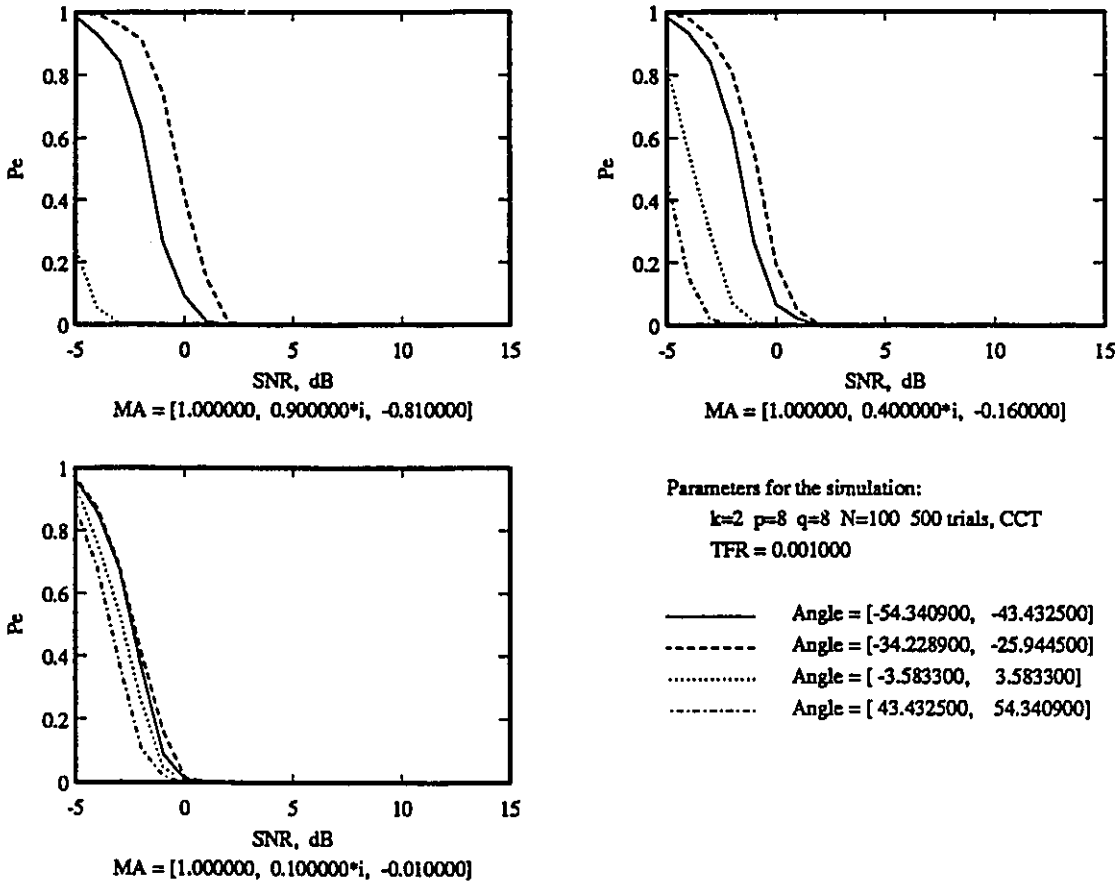

Figure 7.6: Simulation results of CCT method for TFR=10^{-3}

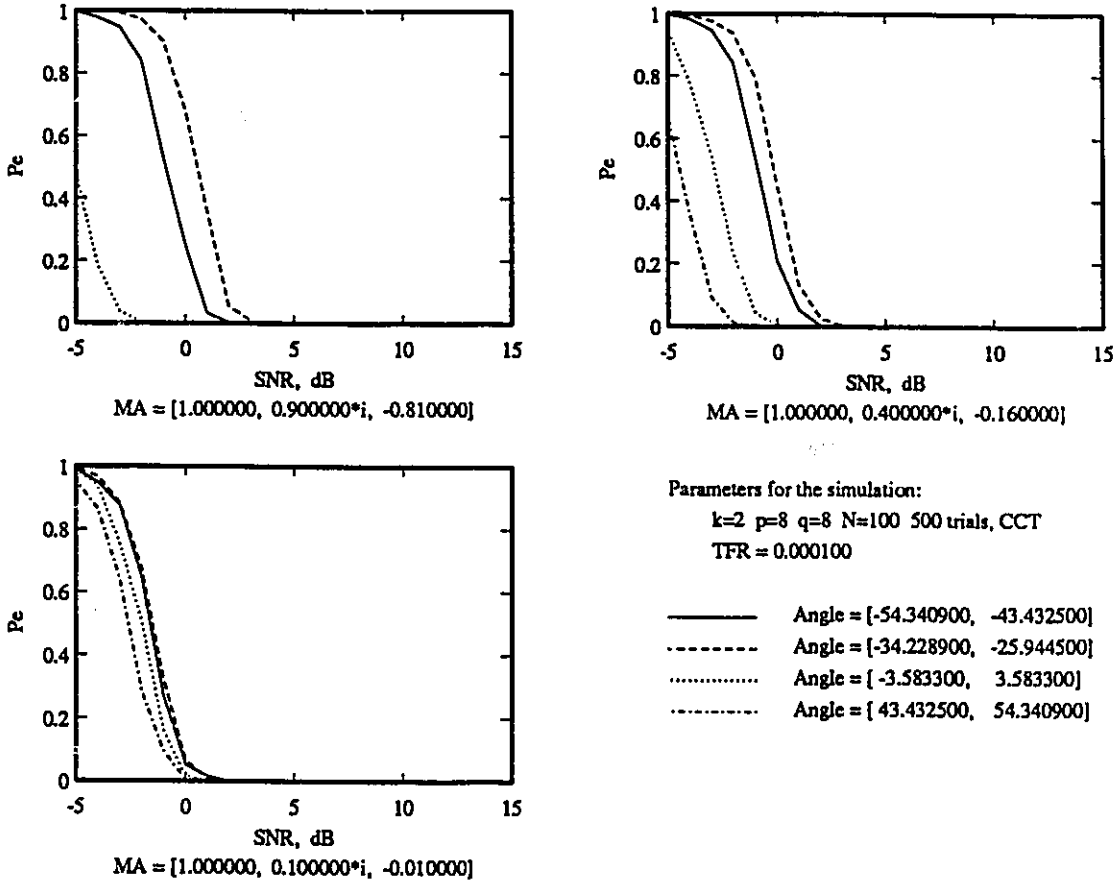

Figure 7.7: Simulation results of CCT method for TFR=10^{-4}

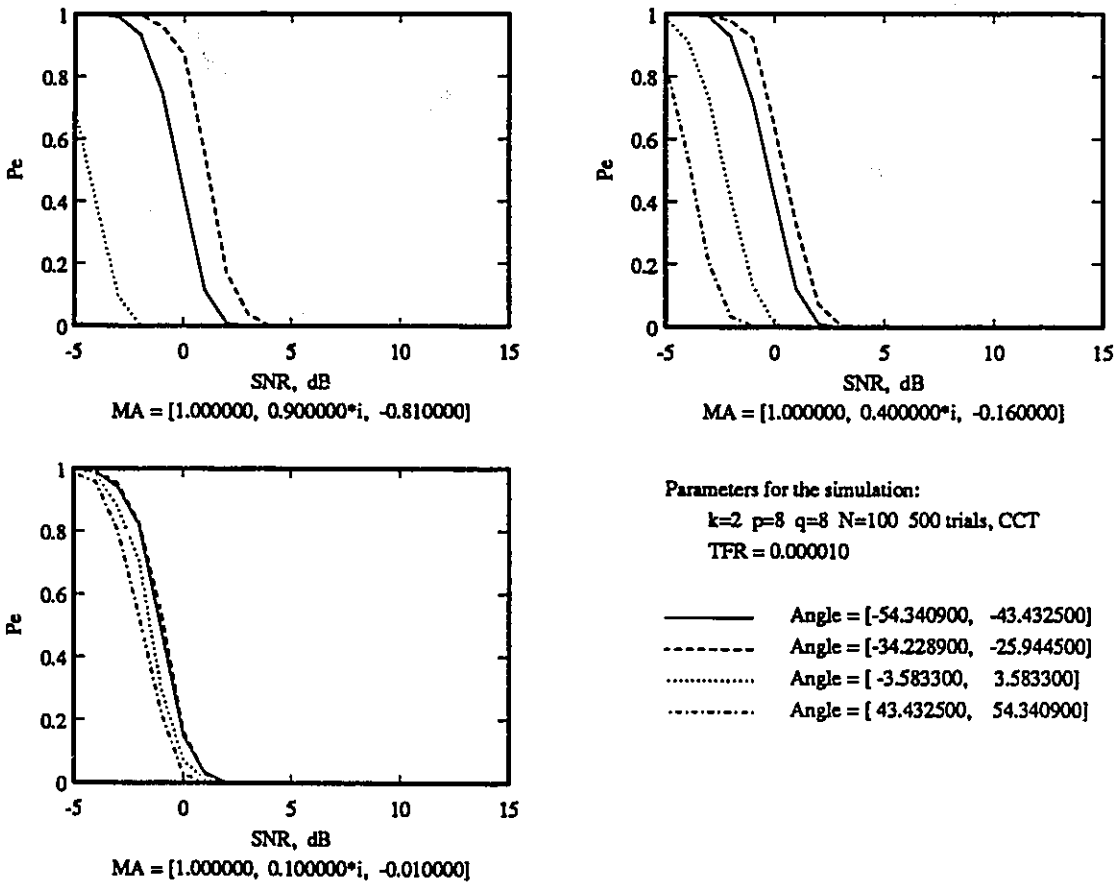

Figure 7.8: Simulation results of CCT method for TFR=10^{-5}

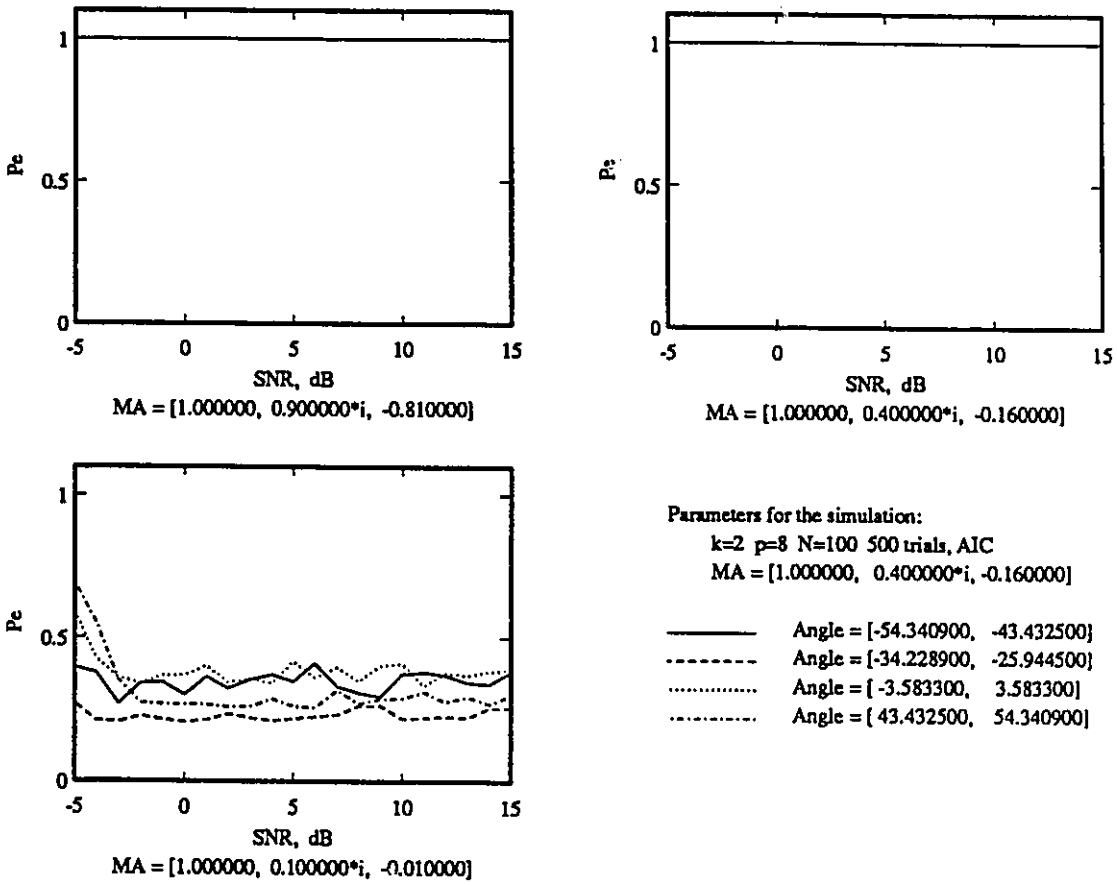

Figure 7.9: Simulation results of AIC using eight sensors

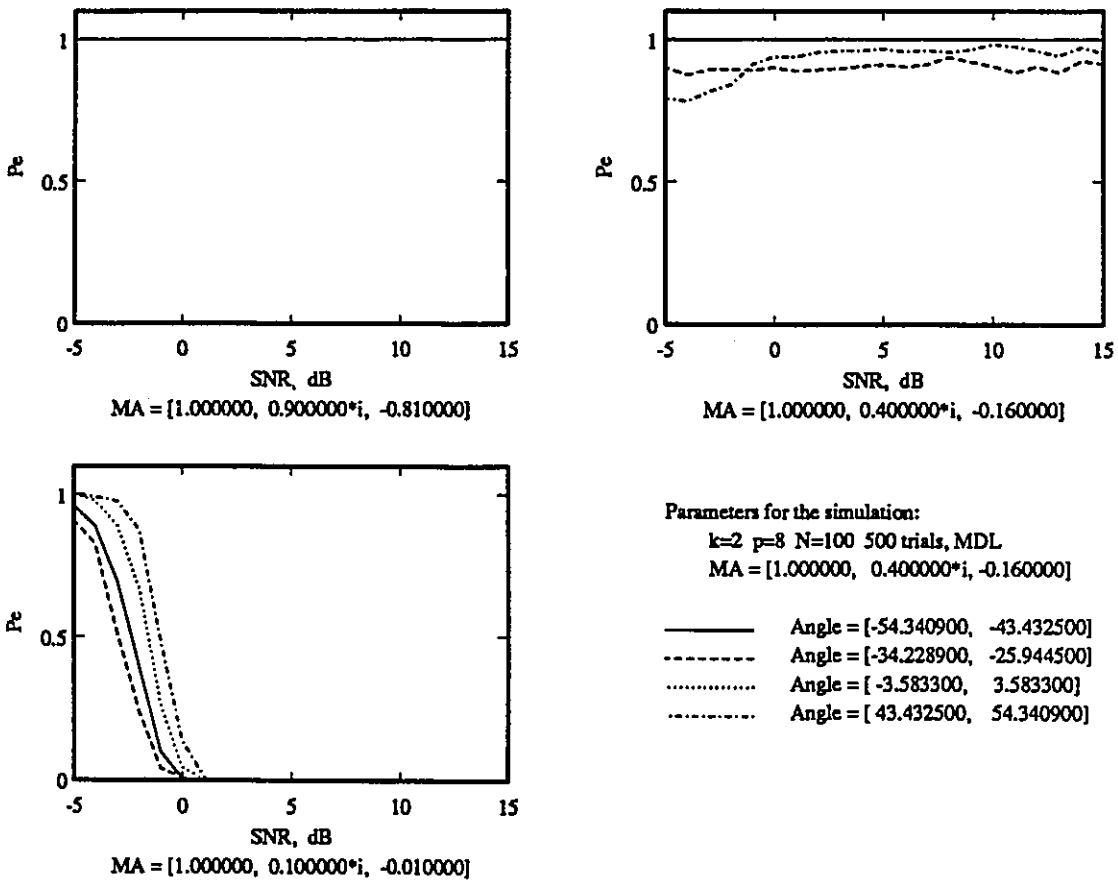

Figure 7.10: Simulation results of MDL using eight sensors

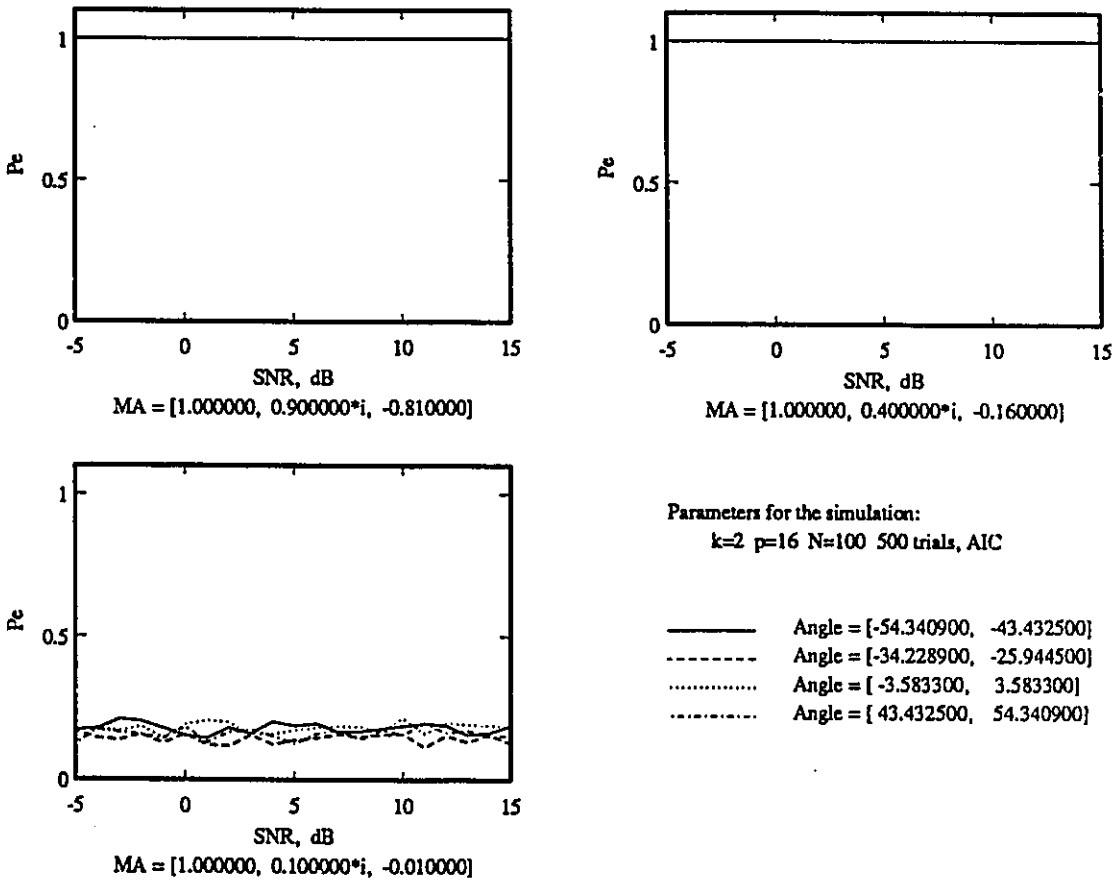

Figure 7.11: Simulation results of AIC using sixteen sensors

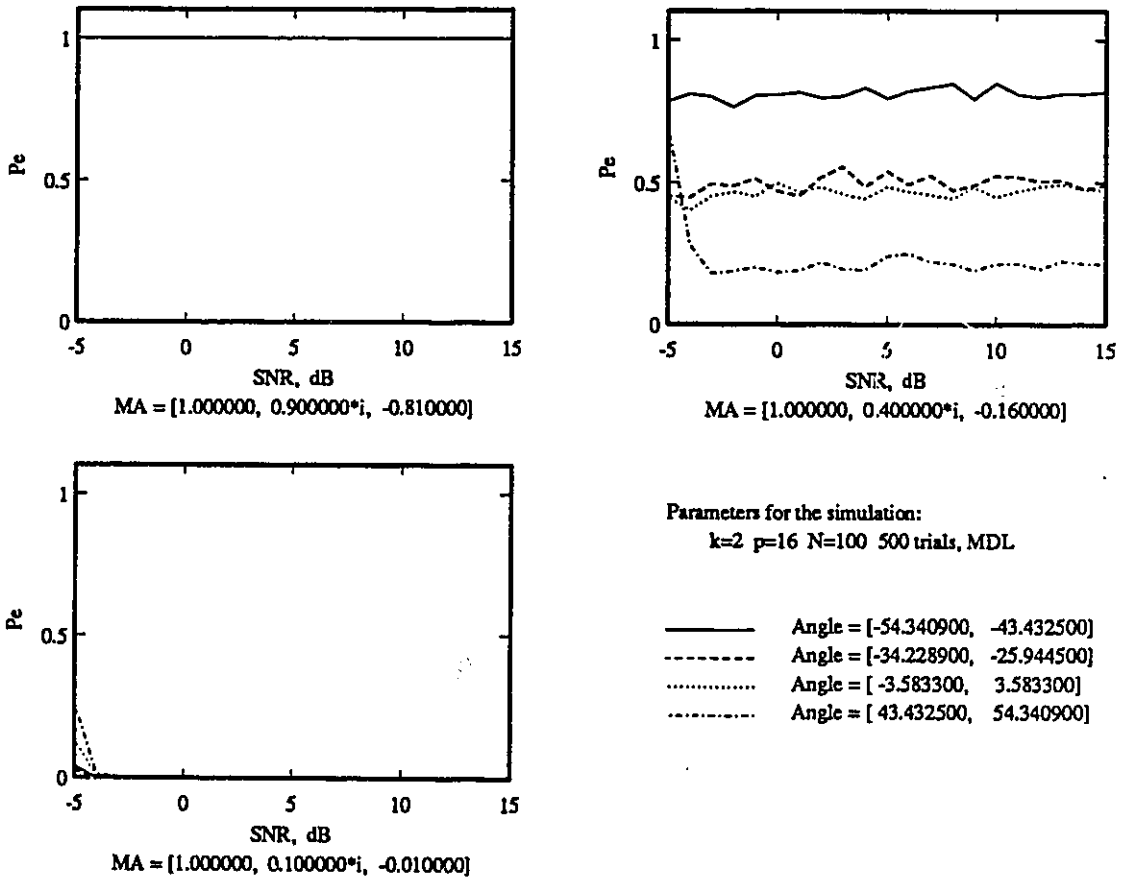

Figure 7.12: Simulation results of MDL using sixteen sensors

7.3.3 Further discussion on the CCT method

Now, let us briefly discuss several potential aspects of the CCT method.

In the previous discussion, the canonical correlation coefficients of the signal components are assumed to be unity, because for narrow band signals, the signal components at the outputs of the different sensors are highly correlated. However, with little modification, the CCT method can also be applied to the case when the canonical correlation coefficients of the signal components are not equal to unity (this situation may happen in wide band array processing, and in the presence of array calibration errors, etc.). For this class of problems, we may use the Lawley-Glynn-Muirhead criterion in which the influence of non-unity principle canonical correlation coefficients is considered, to replace Bartlett's criterion. The Lawley-Glynn-Muirhead criterion can be considered as a further refinement made to Bartlett's correction factor, by Lawley (1959)[41], and Glynn and Muirhead (1978)[29]. This criterion is given as:

Lawley's approximation [41]:

When the hypothesis

$$\mathrm{H}_m: \ \rho_1 \neq 0,\ \rho_2 \neq 0,\ \ldots,\ \rho_m \neq 0,\ \rho_{m+1} = \rho_{m+2} = \ \ldots\ = \rho_p = 0 \tag{7.38}$$

is true, the asymptotic distribution of the statistic

$$-2\,[N - m - \frac{1}{2}(p+q+1) + \sum_{i=1}^{m} \rho_i^{-2}] \sum_{i=m+1}^{p} \log(1-\gamma_i^2) \tag{7.39}$$

is χ^2 with $2(p-m)(q-m)$ degrees of freedom. This result is correct to terms of order of N^{-2}.

It is interesting to note that if the magnitude of the first m canonical correlations $\rho_1, \ldots, \rho_m$ are all unity or at least near to it, Bartlett's test will agree with Lawley's result.

If the values of $\rho_1, \rho_2, \cdots, \rho_m$ are known, the criterion above can be directly applied in the CCT method; otherwise, $\gamma_1, \gamma_2, \cdots, \gamma_m$, the maximum likelihood estimates of $\rho_1, \rho_2, \cdots, \rho_m$, may be used to obtain an approximation.

Another difficult situation which may occur in array processing is the presence of fully correlated incident signals. Once the signals are fully correlated, $\text{rank}(\Sigma_{12}) < k$. Hence, spatial smoothing [60] must be used to generate a rank k matrix under these conditions. Provided the number of subarrays v generated in array X and array Y are identical, it is easy to verify that all the preceding algebraic results are valid in the spatial smoothing case.

However, statistically, the effective value of N to be used with (7.19) is difficult to determine. This is a consequence of the fact that the samples from each subarray under the same snapshot are not independent. This implies that the effective value of N lies between N, the number of snapshots, and $N \times v$, where v is the number of subarrays used in spatial smoothing. An inexact estimate of this quantity will cause the actual P_F to differ from the value specified. However, by choosing the effective N to be equal to N, we can at least say that the actual P_F will bounded above by the specified value, under the spatial smoothing case.

7.4 Appendix A

The content of this section is the derivation of the likelihood ratio under H_s. The major reference is a paper by Tso [61].

The hypothesis H_m is defined as

$$H_m : \ \rho_i \neq 0, \quad for\ i = 1, ..., m \ \text{ and } \ \rho_i = 0, \quad for\ i = m+1, ..., p \tag{7.40}$$

where ρ_i is the ith largest singular value of Σ_{12}, the $p \times q$ cross-correlation matrix defined in Section 3. Without loss generality we assume here $p \leq q$.

This hypothesis serves as a constraint on the rank of Σ_{12} in our derivation.

We use the following steps to derive the likelihood ratio we need. We first convert the signal model to a equivalent model in a regression form, which makes the expression of the derivation more compact. Then, the maximum likelihood with constraint H_m is derived.

We start with the signal model of arrays X and Y with p and q sensors,

$$\boldsymbol{x}(t) = \boldsymbol{A}_x \boldsymbol{s}(t) + \boldsymbol{n}_x(t) \tag{7.41}$$

$$\boldsymbol{y}(t) = \boldsymbol{A}_y \boldsymbol{B}\, \boldsymbol{s}(t) + \boldsymbol{n}_y(t) \tag{7.42}$$

and convert these to regression form by pre-multiplying Equation (7.41) by $\boldsymbol{A}_x^H$, solving the signal vector $\boldsymbol{s}(t)$ as

$$\boldsymbol{s}(t) = (\boldsymbol{A}_x^H \boldsymbol{A}_x)^{-1} \boldsymbol{A}_x^H (\boldsymbol{x}(t) - \boldsymbol{n}_x(t)) \tag{7.43}$$

defining $\boldsymbol{\Sigma}_A^{-1} = (\boldsymbol{A}_x^H \boldsymbol{A}_x)^{-1} \boldsymbol{A}_x^H$ and substituting the result into Equation (7.42), we get the equivalent regression model

$$\boldsymbol{y}(t) = \boldsymbol{A}_y \boldsymbol{B}\, \boldsymbol{\Sigma}_A^{-1} (\boldsymbol{x}(t) - \boldsymbol{n}_x(t)) + \boldsymbol{n}_y(t) \quad . \tag{7.44}$$

Denote the samples of $\boldsymbol{x}(t)$ and $\boldsymbol{y}(t)$ by matrices $\boldsymbol{X}$ of $p \times N$ dimension and $\boldsymbol{Y}$ of $q \times N$ dimension. According to the signal model, we can write

$$\boldsymbol{Y} = \boldsymbol{D}\boldsymbol{X} + \boldsymbol{n} \tag{7.45}$$

where

$$\boldsymbol{D} = \boldsymbol{A}_y \boldsymbol{B}\, \boldsymbol{\Sigma}_A^{-1} \tag{7.46}$$

is of dimension $q \times p$, and

$$\boldsymbol{n} = \boldsymbol{D}\boldsymbol{n}_x + \boldsymbol{n}_y \tag{7.47}$$

which follows the normal distribution

$$\boldsymbol{n} \sim \mathrm{G}(\boldsymbol{O}, \boldsymbol{\Sigma}_n). \tag{7.48}$$

According to Equations (7.45)(7.48), we seek to maximize the likelihood function

$$\log_e L = const. + N \log_e |\boldsymbol{\Sigma}_n^{-1}| - \mathrm{tr}\{(\boldsymbol{Y} - \boldsymbol{D}\boldsymbol{X})^H) \boldsymbol{\Sigma}_n^{-1} (\boldsymbol{Y} - \boldsymbol{D}\boldsymbol{X})\} \tag{7.49}$$

with respect to $\boldsymbol{D}$ and $\boldsymbol{\Sigma}_n$ subject to the constraint H_m. We may eliminate $\boldsymbol{\Sigma}_n$ by noticing that the maximum likelihood estimate of $\boldsymbol{\Sigma}_n$ conditional on $\boldsymbol{D}$ is

$$\boldsymbol{\Sigma}_{n|D}^{*} = \frac{1}{N} \sum_{i=1}^{N} (\boldsymbol{Y} - \boldsymbol{D}\boldsymbol{X})(\boldsymbol{Y} - \boldsymbol{D}\boldsymbol{X})^H \tag{7.50}$$

Inserting $\Sigma^*_{n|D}$ into the likelihood function (7.49), the third term of the right side of (7.49) becomes a constant, and maximizing the likelihood function is equivalent to minimizing

$$f(D) = |(Y - DX)(Y - DX)^H| \tag{7.51}$$

subject to the constraint H_m.

When H_m is true, the rank of D equals m. That means the matrix D can be decomposed in the form of

$$D = GF \tag{7.52}$$

where G is a $q \times m$ matrix with full column rank, and F is a $m \times p$ matrix with full row rank, and F satisfies

$$FX = W \tag{7.53}$$

where W satisfies

$$WW^H = I_m \ . \tag{7.54}$$

Using this decomposition, we can express (7.51) as

$$f(W, G) = |(Y - GW)(Y - GW)^H| \tag{7.55}$$

Applying the identity

$$Y - GW = Y(I_N - W^H W) + (YW^H - G)W \tag{7.56}$$

the form of Equation (7.55) can be changed to

$$f(W, G) = |Y(I_N - W^H W)Y^H + (YW^H - G)(YW^H - G)^H| \tag{7.57}$$

Noticing that Equation (7.57) has the form of $|A_1 + A_2|$, we apply the inequality

$$|A_1| \leq |A_1 + A_2| \tag{7.58}$$

where A_1 and A_2 are positive semi-definite Hermitian matrices. Therefore, (7.57) is minimized with respect to G as

$$f^* = f(W, G^*) = |Y(I_N - W^H W)Y^H| \tag{7.59}$$

when G takes the value

$$G^* = YW^H \ . \tag{7.60}$$

Now we apply the canonical transform

$$X = \hat{L}^{-1}U \tag{7.61}$$

$$Y = \hat{M}^{-1}V \tag{7.62}$$

where

$$UU^H = I_p \tag{7.63}$$

$$VV^H = I_q \tag{7.64}$$

and $\hat{L}^{-1}$ and $\hat{M}^{-1}$ are the sample version of the transform matrices defined by Equation (6.3)(6.4) calculated from S defined by Equation (6.24). The matrix W can be expressed accordingly as

$$W = FX = F\hat{L}^{-1}U \ . \tag{7.65}$$

Define

$$T = F\hat{L}^{-1} \tag{7.66}$$

we have

$$W = TU \tag{7.67}$$

$$TT^H = I_m \ . \tag{7.68}$$

Furthermore, define

$$R = UV^H \tag{7.69}$$

so the form of Equation (7.59) can be further changed to

$$\begin{aligned} f(TU) &= |\hat{M}^{-1}V(I_N - U^HT^HTU)V^H(\hat{M}^{-1})^H| \\ &= |\hat{M}^{-1}|^2|I_q - VU^HT^HTUV^H| \\ &= |\hat{M}^{-1}|^2|I_q - R^HT^HTR| \\ &= |\hat{M}^{-1}|^2|I_m - TRR^HT^H| \\ &= |\hat{M}^{-1}|^2|T(I_p - RR^H)T^H| \end{aligned} \tag{7.70}$$

Here, we introduce a theorem without prove. For the proof of the theorem, readers may refer Theorem 10 of [9] and [26].

Theorem 7.1 *If Φ is an arbitrary positive semi-definite Hermitian matrix of order p, the minimum of $|Z^H \Phi Z|$ over all matrices Z of order $p \times m$ consisting of $m < p$ orthonormal columns is the product of the m smallest eigenvalues $\phi_{p-m+1}, ..., \phi_{p-1}, \phi_p$ of Φ. This minimum is attained when the columns of Z are the corresponding eigenvectors.*

By applying this theorem, the minimum value of Equation (7.59) can be found as

$$f_m^* = |\hat{M}^{-1}|^2 \prod_{i=1}^{m} (1 - \gamma_i^2) \tag{7.71}$$

where γ_i, $i = 1, ..., m$ are the m largest singular values of $\boldsymbol{R}$, the sample canonical correlation coefficients of $\boldsymbol{X}$ and $\boldsymbol{Y}$.

7.5 Appendix B

The content of this section is the details for calculation of the threshold values T_i's.

Suppose that the probability of a threshold χ_t^2 being exceeded is specified. Let us denote this probability by $P_{\chi_t^2}$. Using the definition of the χ^2 distribution we can write

$$P_{\chi_t^2} = 1.0 - \int_0^{\chi_t^2} \frac{1}{2^{\frac{n}{2}} \Gamma(\frac{n}{2})} x^{\frac{n-2}{2}} e^{-\frac{x}{2}} dx \tag{7.72}$$

where n is the degrees of freedom. Replacing variables $n/2$, $x/2$ and χ^2 in Equation (7.72) by a, y, and $2x$, Equation (7.72) becomes

$$P_{\chi_t^2} = 1.0 - \int_0^{x} \frac{1}{\Gamma(a)} e^{-y} y^{a-1} dy. \tag{7.73}$$

Recognizing that the second term in Equation (7.73) is the incomplete Gamma function $\Gamma(a, x)$, Equation (7.72) can be written as

$$P_{\chi_t^2} = 1.0 - \Gamma(\frac{n}{2}, \frac{\chi_t^2}{2}) \tag{7.74}$$

the incomplete Gamma function can be evaluated by many well developed application software packages; e.g., MATLAB [27].

To determine the χ_t^2 value according to $P_{\chi_t^2}$, an equation is defined by changing the form of Equation (7.74) to

$$f(\chi_t^2, n) = 1.0 - P_{\chi_t^2} - \Gamma(\frac{n}{2}, \frac{\chi_t^2}{2}) \tag{7.75}$$

the desired threshold value χ_t^2 equals the root of this nonlinear equation. A convenient way to solve this equation is to use the built-in MATLAB function FSOLVE. For the convenience of readers who may wish to calculate thresholds, the MATLAB programs for their evaluation are enclosed.

```
% chi_th.m
% this program used for determine the threshold values of
% chi-squire
% distribution such that
%
%                1.0 - error = chi(dof,ta).
% where
%  dof:    input vector, degrees of freedom of the chi-square
%          distribution.
%  error:  input vector, probability of the threshold values be
%          exceeded.
%
% The output threshold values are in matrix ta.
% The number of columns of ta equals to the dimension of vector
% error,
% each column is
% dof, error, idex1, idex2 should be declared as global variables.
%
```

```
global dof error idex1 idex2

dof=input('input degrees of freedom vector:  ');
error=input('error rate vector:  ');
nn=length(dof);
ne=length(error);
ta=zeros(nn,ne);
for idex1=1:nn
  for idex2=1:ne
    ta(idex1,idex2)=fsolve('fchi', 1.1*dof(idex1));
  end
end
disp('check the accuracy of the results ...')
a=diag(dof)*ones(nn,ne);
b=ones(nn,ne)-gamma(a/2,ta/2);
%
% end of program chi_th.m
%


function y=fchi(x)
% Function called by chi_th.m to evaluate the value of function
%
%      fchi = C*(1-chi(x, dof(idex1))-error(idex2))
%
% the meaning of dof and error are the same as stated in chi_th.m,
% C is a scale factor to achieve the accuracy required.
%
% where dof, error, idex1, idex2 are global variables
%
```

```
a=gamma(dof(idex1)/2.0,x/2.0);
y=1.e5*dof(idex1)*dof(idex1)*(1.0-a-error(idex2));
%
% end of function fchi.m
%
```

Chapter 8

Conclusions

This thesis addresses two important aspects of the detection problem in array signal processing:

1. Detection in white noise environments.

2. Detection in the presence of unknown coloured (spatially correlated) noise.

Novel approaches, namely the Eigen-Threshold (ET) method for the white noise environment, the Canonical Correlation Testing (CCT) method for unknown coloured noise environments, are developed in this thesis. Theoretical analysis for both these two methods are provided. Computer simulation results demonstrate and confirm the effect and the controllable performance of our new approaches.

For array outputs which contain signals polluted by white noise, our new Eigen-Threshold method offers an attractive alternative to the existing methods applicable to the white noise problem. Using predicted thresholds of the eigenvalues of the sample covariance matrix, the new Eigen-Threshold method does not require a *subjective* threshold setting which causes essential difficulties with the traditional threshold methods. Compared with the information theoretic criteria, the ET method solves the white noise detection problem through a different approach. The information theoretic criteria are based on certain information measures which are used to trade off the information loss and the complexity of the

resulting model in terms of the modelling order (i.e. number of signals in detection problems). Both the ET method and the information theoretic criteria can be formulated by the eigenvalues of the sample covariance matrix, but the ET method involves a more direct exploitation of the statistical characteristics of these eigenvalues. The ET method is also distinct from information theoretic criteria by its *controllable performance*. The information criteria emphasize the asymptotic consistency of the criteria for infinitely large sample sizes. This argument leaves the finite sample performance of information theoretic criteria rigid and uncontrollable. For example, the AIC suffers persistent residual false alarm errors even when the SNR is high and/or the sample size is large, and the MDL is over-penalized. In contrast, the ET method is based on an "equal false alarm rate" concept for a finite sample size. Although the asymptotic consistency argument used by information theoretic criteria has important theoretic significance, a *controllable* performance is more useful for solving practical problems since in practice only samples of limited size are available. The results of computer simulations using the ET method show close agreement between the theoretic predicted performance and the simulation results. In addition to the development of new ET method, this thesis also provides a deeper insight into the statistical performance of the eigenvalues of sample covariance matrices (especially for the eigenvalues of complex data). Many concepts and theories in this thesis are also valuable tools for solving other eigenvalue related problems.

Detection in unknown spatially correlated noise environments is a difficult problem. It is challenge not only because of its complicated nature, but also because of the lack of some fundamental work. The most important issue may be how to classify coloured noise. In the space of parameters which specify various noise models, white noise is only a specific point but the term "coloured noise" includes infinitely many noise realizations! There might not exist a general method suitable for all forms of coloured noise. To develop effective methods for specific kinds of noise, the classification of noise is as necessary as naming the colors in our daily life. In this thesis, a class of coloured noise is defined by the banded structure of its covariance matrix. The practical support for this assumption is from the fact that the spatial correlation of most noise decays much faster than that of signals, as we discussed

in Chapter 5.

There has not been a satisfactory detection method for detection in the presence of unknown noise so far. The existing detection methods fail to provide satisfactory performance due to their dependence on the noise spectrum. This thesis successfully contributes to this difficult problem by introducing a new approach. The derivation of this new method is characterized by

1. assuming a banded structure for the covariance matrix of the unknown noise, and
2. applying two spatially separated arrays (bi-array structure) combined with
3. employing the invariance property of the canonical correlation coefficients of the outputs of the two arrays to changes in SNR and noise spectrum.

The resulting method, namely the CCT method, provides a simple, reliable, statistically solid way to solve the detection problem in unknown noise environments. This new method is also characterized with quantitatively controllable performance, so that the false alarm rate is controllable and predictable.

A number of other problems are also worth further research and development:

1. The discussion of this thesis is concentrated on the detection problem with narrow band signals and linear equally spaced arrays, although at certain points we have given a brief indication of the possible extension of our new methods to wide band signals and correlated signals. Further research is needed to give more detail into these potential applications.
2. In this thesis, the concept of an eigen-threshold is introduced. To approximate the true eigen-threshold, a prediction formula is derived by division of inequalities. However, other approaches for approximation are possible, and may be used to develop new detection methods.
3. In our CCT method, the bi-array structure is used in a specific form; i.e., linear equally spaced arrays with parallel normals, to illustrate the principle of the CCT

method. This by no means limits the application of the CCT method to this specific array structure. The canonical correlation analysis technique can be used over a broad range of array geometric structures. Further research should be conducted to apply the canonical analysis to other array structures.

4. In the CCT method, we have only discussed the application of the Bartlett's criterion in detail. Canonical correlation is a well-developed field, and there are many other good criteria which may be used for detection purpose. Further research is needed.

5. For all coloured noise problems, the classification of the coloured noise is a essential requirement. We have not seen any standard classification procedure for this purpose. In this thesis, we only defined the noise set relevant to our method. Further work in this direction will benefit a wide class of research work involving coloured noise problems.

Bibliography

[1] *Proceedings of the Symposium on Signal Processing in Radar and Sonar Directional Systems (with Special Reference to Systems common to Radar, Sonar, Radio Astronomy, Ultrasonics, and Seismology),* July 6-9, 1964, published by The Institution of Electronics and Radio Engineers, 8-9 Bedford Square, London, W.C. 1.

[2] H. Akaike, "A new look at the statistical model identification," *IEEE Trans. Automatic Control*, vol.19, No.6, pp.716-723, 1974.

[3] G. A. Anderson, "An asymptotic expansion for the distribution of the roots of the estimated covariance matrix," *Ann. Math. Stat.*, vol.36, pp.1153-1173, 1965.

[4] T. W. Anderson, "Asymptotic theory for principal component analysis," *Ann. J. Math. Stat.*, vol.34, pp.122-148, 1963.

[5] T. W. Anderson, *An Introduction to Multivariate Statistical Analysis* Second edition, John Wiley & Sons, New York, 1984.

[6] M. S. Bartlett, "The effect of standardization on a χ^2-approximation in factor analysis," *Biometrika* vol.38, p.337, 1951.

[7] M. S. Bartlett, "A note on multiplying factors for various χ^2 approximation," *j. R. Statist. Soc. Ser. B* vol.16, pp.296-298, 1954.

[8] M. S. Bartlett, "Further aspects of the theory of multiple regression", *Proc. Camb. Phil. Soc.*, vol.34, p.33, 1938.

[9] R. Bellman, *An Introduction to Matrix Analysis*, McGraw Hill, New York, 1960.

[10] G. E. P. Box and G. M. Jenkins, *Time Series Analysis: Forecasting and Control*, San Francisco, CA:Holden-Day, 1970.

[11] W. G. Bruner, W. N. Case, and R. C. Leedom, "digital Control in Modern Radar," *EASCON 1971 Record, IEEE Electronics and Aerospace Systems Convention*, October 6-8, 1971, Washington, DC, pp.200-207.

[12] H. P. Bucker, "Comparison of FFT and Prony algorithms for bearing estimation narrow-band signals in a realistic ocean environment," *J. Acoust. Soc. Amer.*, vol.61, pp.756-762, March 1977.

[13] K. M. Buckley, L. J. Griffiths, "Broad-band signal-subspace spatial-spectrum (BASS-ALE) Estimation," *IEEE Trans. ASSP*, vol.36, no.7, July 1988.

[14] J. P. Burg, *Maximum entropy spectral analysis*, Ph.D. dissertation, Dept. Geophysics, Stanford Univ., Stanford, CA, May 1975.

[15] A. K. Chattopadhyay, "An asymptotic distribution theory and applications in multivariate analysis," Dept. Statistics, Purdue Univ., Mimeograph Series no.256, 1971.

[16] W. G. Chen, K. M. Wong, J. P. Reilly, "Detection of number of signals: a predicted eigen-threshold approach," *IEEE Trans. ASSP*, May, 1991.

[17] W. G. Chen, K. M. Wong, J. P. Reilly, "Detection of number of signals by eigen-threshold method," *Advanced algorithm and architectures for signal processing IV*, Proc. SPIE 1152, pp346-357, 1989.

[18] W. G. Chen, J. P. Reilly, K. M. Wong "Detection of number of signals when noise has an unknown covariance matrix with banded structure," submitted to *IEEE Trans. Signal Processing.*

[19] W. G. Chen, J. P. Reilly, K. M. Wong "Detection of number of signals in the presence of noise with an unknown, banded structured covariance matrix," Proc. of *IEEE Pacific Rim Conference* Victoria, B.C., Canada, paper number 243.

[20] A. G. Constantine, "Some noncentral distribution problem in multivariate analysis," *Ann. Math. Statist.* vol.34, pp.1270-1285, 1963.

[21] H. V. Cottony, and A. C. Wilson, "a high-resolution rapid-scan antenna," *Nat. Bur. Stand. J. Res.* vol.65, pp.101-110.

[22] D. E. Dudgeon, "Fundamentals of digital array processing," *Proc. IEEE,* vol.65, pp.898-904, June 1977.

[23] J. E. Evans, J. R. Johnson, and D. F. Sun, "Applications of advanced signal processing techniques to angle of arrival estimation in ATC navigation and surveillance system," Lincoln Lab., Lexington, MA, Rep.582, June 1982.

[24] B. Friedlander, "On the computation of the Cramer-Rao bound for ARMA estimation," *IEEE Trans. ASSP*, vol. 32, pp.721-727, Aug. 1984.

[25] M. A. Girshick, "On the sampling theory of roots of determinantal equations," *Ann. Math. Stat.*, vol.10, pp.203-224, 1939.

[26] H. Marcus and H. Mink, *An Introduction to Linear Algebra*, MacMillan, New York, 1965.

[27] *MATLAB user's Guide*, The Math Works, Inc., 1989.

[28] Robert A. Monzingo, and Thomas W. Miller, *Introduction to Adaptive Arrays*, John Wiley & Sons, New York, 1980.

[29] W. J. Glynn and R. J. Muirhead, "Inference in canonical correlation analysis," *J. Multivariate Analysis*, vol.8, pp.468-478, 1979.

[30] E. J. Hannan, and B. G. Quinn, "The determination of the order of an autoregression," *J. Royal Stat. Soc., Series B*, vol.41, no.2, pp.190-195, 1979.

[31] H. G. Hayes, "Detection of submarines," *Proc. Am. Phil. Soc.,* vol.59, no.1, 1920.

[32] S. Haykin, and J. P. Reilly, "Mixed autoregressive-moving average modeling of the response of a linear array antenna to incident plane waves," *Proc. IEEE,* vol.68, pp.622-623, May 1980.

[33] S. Haykin, Editor, *Array signal processing*, Prentice-Hall, Inc., 1985.

[34] H. Hotelling, "Relations between two sets of variates," *Biometrica*, vol.28, pp.321-377, 1936.

[35] A. T. James, "Distributions of matrix variates and latent roots derived from normal samples," *Ann. Math. Stat.*, vol.35, pp.475-501, 1964.

[36] S. M. Kay, and S. L. Marple, Jr., "Spectrum analysis–A modern perspective" *Proc. IEEE*, vol.69, no.11, pp.1380-1419, Nov. 1981.

[37] M. G. Kendall and A. Stuart, *The Advanced Theory of Statistics*, vol.1, Fourth edition, MacMillan Publishing Co., Inc, 1977.

[38] J. Krolik, D. Swingler, "Focused wide-band array processing by spatial resampling," *IEEE Trans. ASSP*, vol.38, no.2, Feb. 1990.

[39] A. M. Kshirsagar, *Multivariate Analysis* Marcel Dekker, Inc. New York, 1972.

[40] D. N. Lawley, "Tests of significance of the latent roots of the covariance and correlation matrices," *Biometrica*, vol.43, pp.128-136, 1956.

[41] D. N. Lawley, "Tests of significance in canonical analysis," *Biometrica*, vol.46, pp.59-66, 1959.

[42] J. P. Le Cadre, "Parametric methods for spatial signal processing in the presence of unknown coloured noise fields," *IEEE Trans. ASSP*, vol.37, No.7, pp.965-983, 1989.

[43] H. C. Li, C. S. Pillai, and T. C. Chang, "Asymptotic expansions for distribution of the roots of two matrices from classical and complex Gaussian populations," *Ann. Math. Stat.*, vol.41, no.5, pp.1541-1556, 1970.

[44] R. J. Muirhead, *Aspects of Multivariate Statistical Theory*, John Wiley and Sons, 1982.

[45] Hisao Nagao, "On some test criteria for covariance matrix," *Ann. Stat.*, vol.1, pp.700-709, 1973.

[46] J. Neyman, and E. Pearson, "On the problem of the most efficient tests of statistical hypotheses," *Phil. Trans. Roy. Soc.* A 231, p289, 1933.

[47] Y. Omichi, "An experimental study of covariance functions of reverberation from a lake surface," *ARL Tech. Report,* ARL-TR-75-25, ARL, University of Texas at Austin, May 1975.

[48] Athanasios Papoulis, *Probability, Random Variables, and Stochastic Processes,* McGraw-Hill, Inc. New York, 1965.

[49] A. Paulraj, and T. Kailath, "Eigenstructure methods for DOA estimation in the presence of unknown noise fields," *IEEE Trans. ASSP,* vol.34, no.1, pp.13-20, Feb., 1986.

[50] S. Prasad, and B. Chandna, "Signal subspace algorithms for direction of arrival estimation in the presence of a class of unknown noise field," in *Proc. ICASSP,* 1988, pp.2913-2916.

[51] V. U. Reddy, A. Paulraj, and T. Kailath, "Performance analysis of the optimum beamformer in the presence of correlated sources and its behavior under spatial smoothing," *IEEE Trans. ASSP,* vol.35, no.7, July 1987.

[52] J. P. Reilly, and S. Haykin, "Maximum likelihood receiver for low-angle tracking radar Part 2: the nonsymmetric case," *IEE Proc.,* vol.129, Pt. F, no.5, Oct. 1982, pp.331-340.

[53] J. P. Reilly, K. M. Wong, and P. M. Reilly, "Direction of arrival estimation in the presence of noise with unknown, arbitrary covariance matrices," *Advanced Algorithms and Architectures for Signal Processing IV,* Franklin T. Luk, Editor, Proc. SPIE 1152, pp.313-325, 1989.

[54] J. Rissanen, "Modeling by shortest data description," *Automatica,* vol.14, pp.465-471, 1978.

[55] R. Roy, and T. Kailath, "ESPRIT-Estimation of Signal Parameters Via Rotational Invariance Techniques," *IEEE Trans. ASSP,* vol.37, no.7, July 1989.

[56] E. H. Satorius and J. R. Zeidler, "Maximum entropy spectrum analysis of multiple sinusoids in noise," *Geophysics*, vol.43, pp.1111-1118, Oct. 1978.

[57] R. O. Schmidt, "Multiple Emitter Location and Signal Parameter Estimation", *IEEE Trans. ASSP*, vol.34, no.3, pp.276-280, March, 1986.

[58] G. Schwartz, "Estimating the dimension of a model," *Ann. Stat.*, vol.6, pp.461-464, 1978.

[59] T. J. Shan, M. Wax, and T. Kailath, "Spatial smoothing approach for location estimate of coherent sources," in *Proc. 17th Asilomar Conf. Circuits Syst. Comput.*, pp.367-371, Nov. 1983.

[60] T. J. Shan, and T. Kailath, "On spatial smoothing for direction of arrival estimation of coherent signals," *IEEE Trans. ASSP*, vol.33, no.4, pp.806-811, 1985.

[61] M. K. Tso, "Reduced rank regression and canonical analysis," *J. R. Statist. Soc.* B, vol.43, no.2, pp.183-189, 1981.

[62] Harry L. Van Trees, *Detection, Estimation, and Modulation Theory*, Part I Detection, Estimation, and Linear Modulation Theory, John Wiley & Sons, Inc., New York, 1968.

[63] A. Wald, "Contributions to the theory of statistical estimation and testing of hypotheses," *Ann. Math. Stat.* Vol. 10, p.299, 1939.

[64] H. Wang, M. Kaveh, "Coherent Signal-subspace processing for the detection and estimation of angles of arrival of multiple wide-band sources," *IEEE Trans. ASSP*, vol.33, no.4, August 1985.

[65] H. Wang, M. Kaveh, "On the performance of signal subspace processing Part I: Narrow-band systems," *IEEE Trans. ASSP*, vol34, np.5, pp.1201-1209, 1986.

[66] M. Wax and T. Kailath, "Detection of signals by information theoretic criteria," *IEEE Trans. ASSP*, vol.33, No.2, pp.387-392, 1985.

[67] S. S. Wilks, "Certain generalizations in the analysis of variance," *Biometrica*, vol.24, p.471, 1932.

[68] K. M. Wong, Q. T. Zhang, J. P. Reilly, and P. C. Yip, "On information theoretic criteria for determining the number of signals in high resolution array processing," *IEEE Trans. ASSP,* vol.38, no.11, pp.1959-1971, 1990.

[69] Y. Q. Yin, and P. R. Krishnaiah, "Some nonparametric methods for detection of the number of signals," *IEEE Trans. ASSP,* vol.35, no.11, Nov. 1987.

[70] Q. T. Zhang, K. M. Wong, P. C. Yip, and J. P. Reilly, "Statistical analysis of the performance of information theoretic criteria in the detection of the number of signals in array processing," *IEEE Trans. ASSP*, vol.37, no.10, pp.1557-1567, 1989.

[71] Q. T. Zhang, K. M. Wong, "The asymptotic distribution of eigenvalues of a complex covariance matrix," CRL, McMaster University, CRL Rep. no.181, June 1987.

[72] Q. T. Zhang, S. Haykin, and K. M. Wong, "Echo structures of ocean reverberation and target returns" CRL, McMaster University, Internal Rep., December 1989.

[73] L. C. Zhao, P. P. Krishnaiah, and Z. D. Bai, "On detection of the number of signals in presence of white noise," *J. Multivariate Anal.,* vol.20, pp.1-25, 1986.

[74] L. C. Zhao, and Z. D. Bai, "On detection of number of signals when the covariance matrix is arbitrary," *J. Multivariate Anal.,* vol.20, pp.26-49, 1986.

[75] L. C. Zhao, P. P. Krishnaiah, and Z. D. Bai, "Remarks on certain criteria for detection of the number of signals," *IEEE Trans. ASSP,* vol.35, no.2, pp.129-132, Feb., 1987.